DEVELOPMENT OF NANOCOMPOSITE HYDROGELS FOR CONTROLLED RELEASE OF PROTEINS

A THESIS SUBMITTED TO
THE GRADUATE SCHOOL OF NATURE AND APPLIED SCIENCES
OF
MIDDLE EAST TECHNICAL UNIVERSITY

BY

SEDA SİVRİ

IN PARTIAL FULFILLMENT OF THE REQUIREMENTS
FOR
THE DEGREE OF MASTER OF SCIENCE
IN
THE DEPARTMENT OF CHEMICAL ENGINEERING

SEPTEMBER 2016

Approval of the thesis:

DEVELOPMENT OF NANOCOMPOSITE HYDROGELS FOR CONTROLLED RELEASE OF PROTEINS

submitted by **SEDA SİVRİ** in partial fulfillment of the requirements for the degree of **Master of Science in Chemical Engineering Department, Middle East Technical University** by,

Prof. Dr. Gülbin Dural Ünver
Director, Graduate School of **Natural and Applied Sciences** _____

Prof. Dr. Halil Kalıpçılar
Head of Department, **Chemical Engineering** _____

Asst. Prof. Dr. Erhan Bat
Supervisor, **Chemical Engineering Dept., METU** _____

Prof. Dr. Ülkü Yılmazer
Co-Supervisor, **Chemical Engineering Dept., METU** _____

Examining Committee Members:

Prof. Dr. Pınar Çalık
Chemical Engineering Dept., METU _____

Asst. Prof. Dr. Erhan Bat
Chemical Engineering Dept., METU _____

Assoc. Prof. Dr. Bora Maviş
Mechanical Engineering Dept., Hacettepe University _____

Asst. Prof. Dr. Salih Özçubukçu
Chemistry Dept., METU _____

Asst. Prof. Dr. Harun Koku
Chemical Engineering Dept., METU _____

Date: 08.09.2016

I hereby declare that all information in this document has been obtained and presented in accordance with academic rules and ethical conduct. I also declare that, as required by these rules and conduct, I have fully cited and referenced all material and results that are not original to this work.

Name, Last name : Seda Sivri

Signature :

ABSTRACT

DEVELOPMENT OF NANOCOMPOSITE HYDROGELS FOR CONTROLLED RELEASE OF PROTEINS

Sivri, Seda
M.S., Department of Chemical Engineering
Supervisor: Asst. Prof. Dr. Erhan Bat
Co-Supervisor: Prof. Dr. Ülkü Yılmazer

September 2016, 145 Pages

Owing to the fact that a vast number of biological functions are performed via proteins in living tissues, many human diseases are resulted from the malfunction or deficiency of particular proteins. Hence, there has been extensive work on industrial production of therapeutic proteins for the treatment of diseases in recent years. However, proteins could be denatured or degraded *in vivo* in a short time before reaching target site due to their fragile nature. Additionally, owing to the renal clearance and short half-lives of proteins, frequent injection or excessive protein loading is required to reach a therapeutically effective dose *in vivo*. Therefore, there has been necessity of controlled release systems which effectively deliver proteins in a targeted, controlled manner while preserving their structure and function.

In this study, alginate based injectable nanocomposite hydrogels with hydrazone bonds were prepared. Due to the incorporation of Laponite XLG, a synthetic clay, these hydrogels were presumed to have higher drug loading capacity and provide a better control of protein release.

Adsorption studies were conducted for Bovine Serum Albumin (BSA) and Laponite XLG in the weight ratio ranging from 0.33 to 10 for various pH and molarity values. The maximum adsorption percentage of BSA was found to be 99.2±0.57 % while the highest adsorption capacity was attained as 1.1±0.01 mg BSA for per mg Laponite XLG. BSA-Laponite XLG complexes were evaluated via Fourier Transform Infrared Spectroscopy (FTIR) and X-Ray Diffraction technique (XRD). It was found from FTIR analysis that secondary structure of BSA in the complexes was conserved. The results of XRD analysis showed that BSA molecules formed intercalated structure with Laponite XLG.

Alginate based injectable hydrogels were produced with hydrazone chemistry and polymer concentrations ranging from 1.7% to 5.75% (w/v). Stability of hydrazone bond at neutral medium and degradation of hydrogels were investigated via swelling test for pure hydrogels and Laponite XLG containing nanocomposite hydrogels. Hydrogels containing 3.2% (w/v) polymer concentration conserved hydrogel morphology in the period of 3 months and demonstrated a stable swelling profile. Laponite XLG incorporation with 0.1% (w/v) into hydrogels contributed to increased degradation time and a controlled release profile.

Protein containing hydrogels were produced with 2.55% (w/v) polymer concentration and 0.2% (w/v) BSA addition. Protein containing nanocomposite hydrogels were generated with 2.55% (w/v) polymer concentration and the addition of BSA-Laponite XLG complexes, in which 59% (w/w) of the protein was in adsorbed to Laponite XLG, with 0.2% (w/v) BSA, 0.2% (w/v) Laponite XLG. Influence of Laponite XLG and adsorption mechanism on release of BSA from hydrogels were evaluated with Bradford Assay. Burst release was minimized via addition of BSA-Laponite XLG complexes. After 3 days, protein entrapped in the hydrogel matrix for protein containing hydrogel. However, release of BSA was continued for protein containing nanocomposite hydrogels. BSA release was comparably higher but more stable in the protein containing nanocomposite hydrogels.

Keywords: Protein Release, Injectable Hydrogels, clay, Alginate, Hydrazone

ÖZ

KONTROLLÜ PROTEİN SALIMI İÇİN NANOKOMPOZİT HİDROJEL GELİŞTİRİLMESİ

Sivri, Seda
Yüksek Lisans, Kimya Mühendisliği Bölümü
Tez Yöneticisi: Yrd. Doç. Dr. Erhan Bat
Ortak Tez Yöneticisi: Prof. Dr. Ülkü Yılmazer

Eylül 2016, 145 Sayfa

Canlı hücrelerde çok sayıda biyolojik işlev proteinler aracılığıyla gerçekleştiğinden, pek çok rahatsızlık belirli proteinlerin işlevini yerine getirememesinden ya da eksikliğinden kaynaklanmaktadır. Bundan dolayı son yıllarda hastalıkların tedavisi için terapötik proteinlerin endüstriyel olarak üretimi üzerine yoğun çalışmalar bulunmaktadır. Ancak proteinler hassas yapılarından dolayı vücut içerisinde hedef dokuya ulaşmadan kısa süre içerisinde denature olabilmekte yada bozulabilmektedir. Ayrıca böbrekten atılım ve kısa yarı ömürlerinden dolayı sık enjeksiyon ya da fazla protein yüklemesi gerekmektedir. Bu nedenle proteinlerin yapısının ve işlevinin korunarak hedef dokuya etkili ve kontrollü bir şekilde iletiminin sağlandığı kontrollü salım sistemlerine ihtiyaç bulunmaktadır.

Bu çalışmada hidrazon kimyasına sahip enjekte edilebilen nanokompozit aljinat bazlı hidrojeller geliştirilmiştir. Bu hidrojellerin sentetik bir kil olan Laponit XLG takviyesiyle daha yüksek ilaç depolama kapasitesine sahip olacağı ve protein salımının daha iyi kontrol edilmesinin sağlanacağı öne sürülmüştür. BSA ve Laponit

XLG arasındaki adsorpsiyon çalışmaları 0.33 ile 10 arasında değişen kütlesel oranlarda çeşitli pH ve molarite değerlerinde gerçekleştirilmiştir. BSA'nın maksimum adsorplama yüzdesi %99.2±0.57 olarak bulunurken, en yüksek adsorplama kapasitesi ise mg Laponit XLG kili başına 1.1±0.01 mg BSA olarak elde edilmiştir. BSA-Laponit XLG kompleksleri Fourier Dönüşümlü Kızılötesi Spektroskopisi (FTIR) ve X-Ray Difraksiyon (XRD) tekniğiyle değerlendirilmiştir. Komplekslerde bulunan BSA'nın ikincil yapısının korunduğu bulunmuştur. XRD analizi sonuçları BSA moleküllerinin Laponit XLG ile araya katılan yapı oluşturduğunu göstermiştir.

%1.7 ile %5.75 (a/h) arasında değişen konsantrasyonlarda hidrazon kimyasına sahip aljinat bazlı enjekte edilebilen hidrojeller üretilmiştir. Nötr ortamda hidrazon bağının stabilitesi ve hidrojellerin bozunumu saf hidrojeller ve Laponit XLG içeren nanokompozit hidrojeller için şişme testi ile incelenmiştir. %3.2 (a/h) konsantrasyonunda polimer içeren hidrojeller 3 aylık bir sürede hidrojel morfolojisini korumuş ve kararlı bir şişme profile sergilemiştir. Hidrojellere yapılan %0.1 (a/h) oranında Laponit XLG ilavesi bozunma süresinin artışına ve daha iyi bir profil elde edilmesine katkı sağlamıştır.

Protein içeren hidrojeller, %2.55 (a/h) polimer konsantrasyonunda ve %0.2 (a/h) oranında BSA ilavesi üretilmiştir. Protein içeren nanokompozit hidrojeller, %2.55 (a/h) polimer konsantrasyonunda proteinin %59 (a/a) 'u Laponit XLG üzerine adsorbe edilmiş olan BSA-Laponit XLG kompleksinin ilavesiyle %0.2 (a/h) BSA ve %0.2 (a/h) Laponit XLG oranında geliştirilmiştir. BSA salımı üzerinde Laponit XLG ve adsorpsiyon mekanizmasının etkisi Bradford tayiniyle değerlendirilmiştir. Ani salımlar BSA-Laponit XLG kompleksleriyle azalmıştır. Protein içeren hidrojellerde 3 gün sonunda protein matriks içine hapsolmuştur. Ancak protein içeren nanokompozit hidrojellerde BSA salımı devam etmiştir. BSA salımı protein içeren nanokompozit hidrojellerde göreceli olarak daha yüksek olmasına rağmen daha kararlıdır.

Anahtar Kelime: Protein Salımı, Enjekte Edilebilen Hidrojel, kil, Aljinat, Hidrazon

To my beloved parents&Alp and Serra

and the memory of Chen …

ACKNOWLEDGEMENT

I had turned a new leaf by starting master studies and now it is a good pleasure for me to finalize this chapter which presents a chance to spread my wings. There were many people by my side during the whole thesis studies. I would not be able to complete this work without their help and effort.

Firstly, I am greatly appreciated to my supervisor Asst. Prof. Dr. Erhan Bat for his positive attitude towards me from the beginning of the project. It is such an honour to be his first graduate student. His guidance, support and tolerance provided a significant contribution to my studies. Thanks to him, I have gained an exceptional academic perspective about polymers, hydrogels and drug delivery studies. Secondly, I would like to thank my co-supervisor Prof. Dr. Ülkü Yılmazer for kindly accepting me as a master student.

I would like to express my special thanks to Prof. Dr. Göknur Bayram for her kindness and permission to work in her laboratory for research purposes at the beginning of the work.

I am thankful to Asst. Prof. Dr. Salih Özçubukçu and his research group especially to Dr. Aytül Saylam, Gökçil Bilir and Güzide Aykent for their kind permission and help to use Freeze Dry System in the long period.

I am also appreciated to all my committee members Prof. Dr. Pınar Çalık, Assoc. Prof. Dr. Bora Maviş and Asst. Prof. Dr. Harun Koku for their help about suggestions and thesis corrections.

I would like to express my thanks to my friends-colleagues Berrak Erkmen, Merve Özkutlu, Arzu Arslan, Hande Güneş and my favourite couple Zeynep Karakaş and Veysi Halvacı for cheering me up and motivating me in the never ending days. I also want to thank all C Block residents.

I owe a sincere appreciation to my office mate Ezgi Yavuzyılmaz for being with me in both good days and tough moments. Even if our routes change, I believe that our friendship will remain.

Many thanks to TUBITAK (The Scientific and Technological Research Council of Turkey) for the financial support attained to the project with the number 114C068. I also want to thank Bat Lab research group members-Cemre Avşar, Öznur Doğan, Gözde Şahin, Ayşe Elif Kıratlı, Cansu Çaylan, Sevil Demirci and Zeynep Cansu Özçınar-for their help and accompaniment.

Finally, I want to express my gratitude to the most significant people for me who are in my family. Presence of each one gives me happiness, strength and peace.

I want to acknowledge many thanks to my bighearted aunt Serpil who has provided a great influence on my personality. Many thanks to my helpful, calm and patient cousin Serra for her strong impression on my thesis, all her support and hope she gave me in the home stretch. I am grateful to Duru and Ela, who fill my life with endless joy. And last but not the least, many thanks to my cousin, Berra for her distinctive humour which had never failed to cheer me up when I needed.

I am most thankful for my parents and my brother Alp. My dear mom, I cannot express my gratitude enough for you, for being the most positive person I have ever known, for being so caring all the time and for showing me unconditional love which lets me make my own mistakes and learn from them. My lovely father, thank you for always staying besides me and giving me confidence to stand on my own feet. My beloved brother Alp for helping me not only in this thesis but also all the stages of my life.

Thanks to you I smile more, I love more and I challenge myself more. I am so grateful to have you…

TABLE OF CONTENTS

LIST OF TABLES

TABLES

LIST OF FIGURES

FIGURES

NOMENCLATURE

A	Alginate
A-A	Alginate aldehyde
A-H	Alginate hydrazide
AA	Pure hydrogel
AAN	Nanocomposite hydrogel
AAP	Protein containing hydrogel
AANP	Protein containing nanocomposite hydrogel
BSA	Bovine serum albumin
ADH	Adipic acid dihydrazide
EDC	1-ethyl-3-(3-dimethylaminopropyl) carbodiimide hydrochloride
NHS	N-hydroxysuccinimide
TNBS	2,4,6-trinitrobenzene sulfonic acid
tBC	tert-Butyl carbazate
PB	Phosphate buffer
DS	Degree of substitution
DS_A	Degree of substitution of modified polymer have aldehyde group
DS_H	Degree of substitution of modified polymer have hydrazide group

$M_{waverage}$	Average molecular weight of a monomer in the polymer
$M_{wmodified}$	Average molecular weight of a monomer in the modified polymer
$M_{wunmodified}$	Average molecular weight of a monomer in the unmodified polymer
m_A	Mass of modified polymer have aldehyde group
m_H	Mass of modified polymer have hydrazide group
M_A	Molecular weight of a repeating unit in modified polymer have aldehyde group
M_H	Molecular weight of a repeating unit in modified polymer have hydrazide group
W_t	Hydrogel weight at selected time
W_o	Hydrogel weight at formation

CHAPTER I

INTRODUCTION

Proteins are comprised of combinations of amino acids. A vast number of proteins are formed through different sequences of varied amino acids, and they gain ability to fulfill a wide range of biological tasks both functionally and structurally. These tasks include, among these, featuring in biochemical reactions as enzymes and hormones, transmitting of substances to target cell or organs via carrier molecules, generation of intracellular and extracellular scaffolding tissues, presenting storage proteins, creation of oncotic pressure, and conducting biocontrol operations such as DNA-RNA replication, cell reproduction, and repair.(1)

Since proteins are crucial for vital activities in body, many human diseases are related to malfunction of particular proteins. The most known example is insulin hormone, which provides a mechanism to regulate glucose level in blood. Diabetes patients must take insulin drugs through their lives. Hence, there has been extensive work on industrial production of therapeutic proteins by means of recombinant DNA technology and genetic engineering via yeast, bacteria and mammalian cells.(1) However, protein delivery to the target tissue may become a tough process due to their tendency to denaturation and degradation, short half-life and poor bioavailability.(2) Therefore, both industrial production of therapeutic agents and their successful delivery to the target organ is required.

Administration route is influential on protection of these fragile biomacromolecules. Preservation of the three dimensional structures of proteins from external factors (pH, temperature, desiccation, proteolysis etc.) is essential for a successful protein

therapy. Oral delivery induces fast degradation and protein bioactivity loss in the stomach by proteolytic enzymes and in gastrointestinal tract. Although it is known that most therapeutic proteins are delivered parenterally, frequent injection or excessive protein loading is required due to the renal clearance and short half-lives of proteins.(1,3) Consequently, short half-life of proteins *in vivo* sparks off inefficient drug loading and low patient compliance. Thus, it is apparent that the design of controlled release systems to effectively deliver proteins in a targeted controlled manner while preserving their structure and function is highly desired. At this point, it has been known that hydrogels offer a solution for drug delivery applications including protein therapy.

Hydrogels are generally defined as hydrophilic materials with the ability of absorbing a great deal of water or other biological fluids. Tailored properties of hydrogels and its capability to mimic tissues enable the usage in a diverse range of biomedical applications. Yet, many hydrogels have insufficient elastic modulus which obstructs the utilization *in vivo* via operative surgical procedures.(4) Thus, injectable or in situ gelling hydrogel concept has arisen, which delivers therapeutics *in vivo* via injection and then rapidly forms gel inside the body.(5) There have been prominent works on drug delivery involving protein applications through injectable hydrogels. Nevertheless, the ultimate problem encountered with these injectable systems is the release of active substances to the plasma within a short period of time, which is known as burst release.(6) This situation leads to the failure of therapy and side effects due to over dosage. Therefore, to maintain an effective therapy, every drug system has to demonstrate controlled release characteristics which hold the drug levels in the therapeutic dose range and avoid reaching below minimum effective concentration and above maximum tolerated concentration.

It was propounded that major factors causing rapid and instantaneous release are the weak interaction between active substances and matrix components, slow gelation and large pore size of the structure. To prevent rapid release, drug carrier formulation must be designed with the aim of improved attraction between the drug and the hydrogel. In this work, enhanced interaction between protein and clay

minerals via adsorption mechanisms was suggested for the enhancement of sustained release of proteins.

Clay minerals are presented in micro or nanometer sized particles composed of silicate layers. Nanocomposite hydrogels are produced to improve mechanical, thermal and permeability properties in pharmaceutical formulations.(7–9) Polymer-clay nanocomposites are frequently used in tissue engineering and controlled release applications.(10) Clay minerals are effective for stabilizing of DNA and proteins.(11) The complex electrostatic interaction and conformational entropies of proteins provide a large variety of interaction with clays.

On the other hand, fast gelation restrains diffusion of protein out of hydrogel matrix for controlled release. The hydrazone bond is known as a type of Schiff base, which has biodegradable linkages. Aldehyde or ketone groups react with hydrazide groups to form a hydrazone bond. The bond formation is realized in a short period of time. Hydrazone chemistry also exhibits biodegradable properties, which is generally biocompatible for the utilization *in vivo*. Bond is stable under physiological conditions whereas it hydrolyses under acidic conditions. Moreover, the by-products of the reaction are safe and toxic crosslinking agents are not needed for the bond formation. Thus, the chemistry is promising for *in vivo* applications.(12)

Carbohydrate based materials are biocompatible with tissues and show low immunogenicity in drug release applications. Hydrogels which are composed of alginate, dextran, chitosan and hyaluronic acid have been used for injectable hydrogel formulations with diverse cross linking chemistries.

In this study, alginate based injectable hydrogels were produced with hydrazone chemistry for protein delivery studies. Due to the absence of reactive groups for hydrazone bond formation in the alginate backbone, aldehyde and hydrazide modification were applied with several modification degrees. Oxidation was done through the reaction between sodium periodate and alginate with 10%, 25% and 50% theoretical substitution degree. Secondly, alginate was reacted with adipic acid dihydrazide in the presence of 1-ethyl-3-(3-dimethylaminopropyl) carbodiimide/N-hydroxysuccinimide to obtain hydrazide modification. Modification degrees of the

polymers were obtained via FTIR analysis and carbazate-TNBS assay. It was aimed that adjusting hydrolytic degradation with the alteration of polymer concentration and degree of substitution of alginate components. A biodegradable system was attained by means of the components of the system, which are carbohydrate material, hydrazone crosslinking chemistry.

Produced hydrogels were divided into four classes, which are alginate based hydrogel, protein containing alginate based hydrogel, alginate based nanocomposite hydrogel and protein containing alginate based nanocomposite hydrogel. Hydrogels were produced by mixing of precursors in several modification degrees with various hydrazide to aldehyde ratio and polymer concentration. Minimum polymer concentration, which requires for gel formation, were found for hydrogels with hydrazone bond chemistry.

In the generation of protein containing alginate based injectable nanocomposite hydrogels, Bovine Serum Albumin (BSA) was used as model protein whereas Laponite XLG was incorporated into system as synthetic clay and nano drug carrier due to its relatively small dimensions and biocompatibility in *in vivo* studies. A nanostructured design was assured with the addition of synthetic clay into matrix. Protein containing nanocomposite hydrogel was produced by adding BSA-Laponite XLG complexes. For this reason, model protein BSA was loaded onto Laponite XLG with an adsorption mechanism for several conditions. Produced complexes were then incorporated into hydrogel matrix. Enhanced interaction between protein and polymer was aimed to minimize burst release of protein.

Adsorption data was examined in terms of percentage adsorption and adsorption capacity for various weight ratio, pH and molarity values. The structure of BSA-Laponite XLG complexes was investigated with FTIR and XRD analysis.

Lastly swelling test was done for alginate based hydrogels and Laponite XLG containing alginate nanocomposite hydrogels. Protein release tests were done for protein containing alginate based hydrogel and protein containing nanocomposite hydrogel.

CHAPTER II

BACKGROUND INFORMATION

2.1 Protein Delivery and Therapy

Proteins, which are composed of amino acid residues and vary by different sequences of amino acids, have an important role in human life. It is known that protein deficiency causes disorders in vital functions. Especially, enzyme and hormone deficiency cause chronic diseases such as diabetes, growth hormone deficiency. Moreover, genes are determined via coded in DNA and failures observed in DNA can result in diseases. Since many diseases such as cancer and immune system disorders are related with the genetic background, protein drug developments are accelerated with recombinant DNA technology. Recombinant blood factors and hormones, vaccines, cytokines, antibodies and enzymes are produced commonly as protein and peptide drugs.(13,14) Insulin or recombinant human insulin (Humulin) was the first industrial protein for the treatment of diabetes, which is produced via recombinant DNA technology and approved by the U.S. Food and Drug Administration (FDA) in 1982. It is reported that over 100 million diabetes patients need therapy and the market value of the product is about $6 billion in U.S.A.(15) There are many analogues of human insulin produced by several drug companies. In a similar way, hormone deficiency is treated with the recombinant growth hormone while Gaucher's disease is cured with Ceredase and Cerezyme. Factor VIII and its equivalent forms are used for hemophilia therapy. It should be noted that there is a growing interest in treating cancer, immune disorders

and infectious diseases with therapeutic proteins.(15) Most therapeutic agents have relatively low molecular weight whereas protein drugs have high molecular weight along with complex chemical structure.(16)

Protein nature is comprised of primary, secondary, tertiary and quaternary structures. Primary structure is determined by the sequence of the amino acids connected with amide or peptide bonds. Secondary structure consists of α-helices and β-sheets. Tertiary structure is formed via folding of secondary structures, which are held together by the physical interactions between side chains and covalent disulfide bonds of cysteine residues. Combination of polypeptides with non-covalent bonds is named as quaternary structure of proteins.(17)

Ensuring same protein properties in each drug formula is challenging due to the low physical and chemical stability of proteins. High molecular weight and three dimensional structure of proteins compel the delivery of macromolecules *in vivo*. Therefore, stability of proteins must be enhanced for achieving a successful and reliable drug formula. The principal requirement to achieve a successful protein therapy is to preserve protein activity in various surroundings (18) – potential application area. In other words, the successful delivery of therapeutic proteins into target tissue by preserving their structure and stability is required.

The covalent and non-covalent interactions present in proteins are highly effective on their stability. Non-covalent interactions are the charge interactions in the ionic side chains and dipole-dipole interaction of neutral residues. Hydrogen bonding has significant effect on secondary structures whereas stability of tertiary structure is not highly affected by hydrogen bonding. However, hydrogen bonding in solution such as with water provides stability for tertiary structure. Hydrophobic interactions lead to folding into three dimensional structures.(17)

The inactivation of protein drug can be actualized in an instant when delivering the drug into tissue. Macromolecules can even be degraded in a non-enzyme containing medium.(18) It is relatively hard to change primary structures of proteins. Primary structure can be altered by chemical reactions. Three dimensional structure can be

destroyed due to physical interactions, which cause physical degradation or denaturation.(17)

Degradation of proteins can occur by chemical and physical routes. Hydrolysis, racemization of amino acids, oxidation, photo degradation, chain cleavage lead to alteration of primary structure of proteins.(17,19) The deformations observed in secondary, tertiary and quaternary structures result from physical instability. Denaturation, adsorption, aggregation and precipitation trigger instability. Temperature, pH, presence of ionic particles, organic solvents, solutes-detergents and mechanical applications can affect physical stability.(17) Aggregation occurs due to hydrophobic interactions.(20) When aggregates become large, precipitation occurs in solution. This process is irreversible and causes loss of activity in proteins(15). Physical degradation tends to loss of biological activity rapidly than chemical degradation.

Stability of proteins is concerned with conservation of structure. Structural deformations may lead to toxic effects.(17) Therapeutic efficiency of protein drug depend not only on its primary structure but also on spatial structure forms. Minor changes in secondary, tertiary and quaternary structure result in therapeutic protein destruction.(17) It is known that maximum thermodynamic stability is attained near isoelectric point, net charge is zero. Electrostatic repulsion and protein denaturation occurs when there is remarkable pH changes from pI point.(17) Some salts cause increased hydrophobic interactions and this leads to instability. However, monopotassium phosphate salt (KH_2PO_4) mainly increases stability of proteins.(17) In addition, shaking and stirring of protein solution cause foaming due to increased air-water interface and hydrophobic interactions.(17)

Proteins are conserved in specific sites of the extracellular matrix in natural surroundings to protect against degrading enzymes and hydrolysis.(21,22) After release of proteins in targeted area, they are degraded by enzymes and eliminated from the body.(18,23)

The most favorable administration route is oral ingestion for drugs.(13) However, protein delivery by oral administration is difficult due to great variation in terms of

pH, enzymes, electrolytes, fluidity and surface properties along the GI tract. Since their large molecular size and fragile nature cause proteins to be highly vulnerable to proteolytic degradation in GI tract and rapid degradation by digestive enzymes, low bioavailability and instability are observed for oral delivery of proteins.(23) Although intravenous or subcutaneous administration are common routes for protein delivery, frequent injection or high dosages are needed due to proteolytic degradation, renal clearance and short plasma circulation times, hindering a successful therapy. Excess dosage leads to toxic effects and evokes immune responses. Absorption of proteins are relatively slow compared to small drugs via subcutaneous route due to molecular size.(13) Parenteral administration is applied via injection or infusion. Many of the injectable drugs are in solution. However, suspensions can also be used even potential instability in some cases.(23) On the other hand, frequent injections reduce patient compliance and effectiveness of therapy. Thus, prolonged release of therapeutic proteins is highly desired to increase patient compliance and efficacy of the therapy.

2.2 Drug Delivery

Drug delivery can be basically defined as the control of the location and delivery rate of drug molecules *in vivo*.(24) A great portion of the drug is wasted before reaching the site of action due to drug intake at irrelevant tissues and devastation of drugs during the route of administration.(24) A limited portion of drug, therefore, arrives in target tissue. Transmittance of drugs into target tissue effectively directly increases the quality of therapy.

The conventional drugs provide immediate release of substances following administration. When the release rate of active substances is not controlled, a dramatic increase in concentration in plasma within a short period is observed and which is called burst release or rapid release. Burst release leads to the failure of therapy and over dosage. Thus, every drug system requires a controlled release mechanism which maintains the drug levels in the therapeutic region between

minimum effective concentration and toxic concentration. The solid line in the Figure 2.1 shows a drug that has controlled release mechanism to avoid sudden releases reaching adverse or no effect zones.

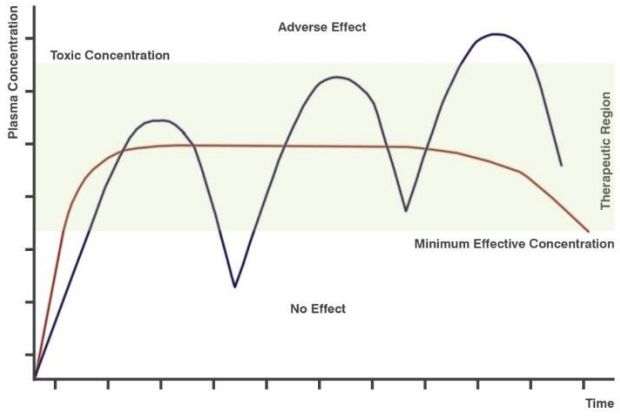

Figure 2.1. Comparison of drug concentration in plasma versus time for controlled release and conventional release profiles.(25)

It is clear that all drug formulations have a release mechanism without noticing the delivery type. Modified release formulations are generated to enhance therapeutic performance. Modified release ensures alterations on both release time and rate of the active substances. In addition, release location of the drug can be adjusted. Different types of release formulations have been presented with various aims-zero order, binary, quick-slow, slow-quick, positioned, accelerated, delayed and multiple pulse.(24) Extended release, delayed release and targeted release are the most common mechanisms. Figure 2.2 shows release mechanisms for pulsed, sustained and delayed release formulation drugs.

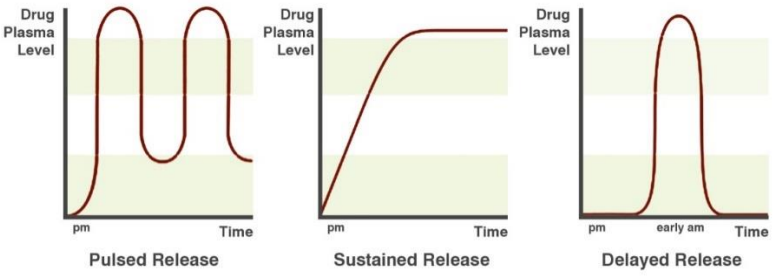

Figure 2.2. Drug concentration in plasma versus time for pulsed, sustained and delayed release mechanisms.(26)

Extended release can be described as the presentation of drug into plasma in a longer period by decreasing dosage frequency. Drugs that have extended dosage formulations provide increased half-life.(24) Side effects are observed if toxic concentrations are reached. Extended release formulations are generally designed to achieve zero-order release.(24)

Extended release can be expressed as controlled release, sustained release, slow release, programmed release and long acted performance drugs. Controlled release refers to the presentation of compounds in response to stimuli or time. For instance, glucose level in plasma fluctuates considerably due to exercise, sleep, infections and food intake for diabetes patients. Moreover, excessive insulin intake results in damage to eyes, kidneys, heart and the cardiovascular system. Blood glucose level must be maintained in the therapeutic region between 4 and 6 millimoles per litre. Therefore, there has been a growing interest in developing an insulin drug which assures slower and controlled release.(27) The comparison between sustained and conventional release can be seen from Figure 2.3.

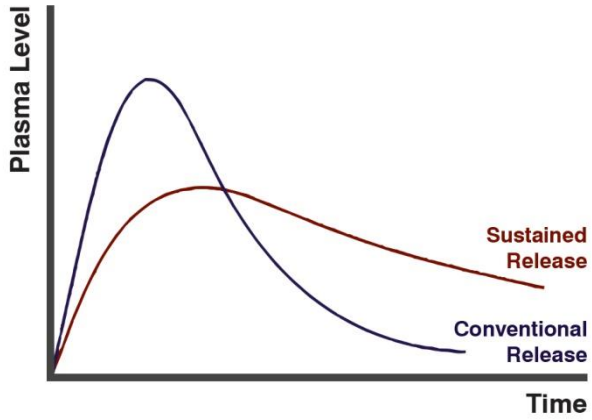

Figure 2.3. Comparison of drug level in plasma versus time for sustained and conventional release profiles.(28)

Delayed release is a kind of modified release formulation which delivers drug in discrete parts in a period of time. Timed release has several distinct variants. For instance, active substances do not immediately disintegrate in body for delayed release formulations. Pulsed type intends to release the drug rapidly within a short

period of time. Enteric coated drugs can be described as delayed release formulation drugs.

Targeted release is the delivery of the active substances to the site of action by reducing systematic damage or harm to neighbour tissues. For instance, most toxic chemotherapeutic agents cannot be delivered in a site specific manner to cancer tissues.(29) Excess chemotherapeutic agent is administered to provide minimum effective dosage at target cancer tissues. Targeted drug formulations reduce systematic damage of therapeutics. Drug delivery system can be designed as responsive to environmental factors such as pH and temperature.(30–32)

2.3 Hydrogels: An Overview

Hydrogels are generally defined as hydrophilic polymers that have three dimensional structure.(33,34) These materials are distinguished with the ability of absorbing a great deal of water or other biological fluids. The absorbing tendency is resulted from the functional groups present in the polymers such as –OH, -$CONH_2$, -CONH and –SO_3H.(33) There has been a considerable interest in hydrogels since their discovery in the early 1960s by Wichterle and Lim due to their superior properties.(35) Hydrogel materials are seen from the Figure 2.4.

Figure 2.4. Hydrogel materials.

Hydrogels are used in many fields for a myriad of purposes.(34,36–43) Easy processing of hydrogels enables their use as a film, coating or in micro- and nano-structured material design. One of the most promising areas is biomedical industry

for hydrogel materials. Hydrophobic polymers have low water absorption ability which limits their applications *in vivo*.(34,44,45) The outstanding property of hydrogels is to mimic tissues due to its high water content, soft and rubbery consistency, and low interfacial tension with water or biological fluids. Fluid absorbing capacity is influential on characteristic features of the hydrogel. Capability to mimic tissues and their tailored properties increase the usage in a great range of biomedical applications. Hydrogel materials gain acceptance in many biomedical applications such as drug delivery, implants, encapsulation of cells, regeneration of tissues.(39)

Hydrogels can be formed with physical or chemical cross-linking of the chains in the polymer and become insoluble in the solution by virtue of cross-linking. Hydrogels that are formed as a result of electrostatic interactions, hydrophobic interactions or by hydrogen bonding are cross-linked physically.(46) Hydrogels formed with physical interactions show weak mechanical properties when injected into body and disperse into medium in a shorter period.(4) Moreover, gel formation with physical attraction does not require toxic linking agents or initiators.

There have been mainly two types reaction classes for creating in situ gelling chemistry. The first one describes as redox/photo polymerization whereas the second type comprised of organic reactions. The most common organic reactions are Michael addition, Schiff base formation and click reactions. Mechanical properties of the chemically cross-linked hydrogels are better for long term applications *in vivo*.(46)

Thermodynamic compatibility with solution leads to swelling of hydrogels in aqueous solutions.(34) From another point of view, cross linking type along with concentration is critical on the hydrogel properties.

Hydrogels can be synthesized from synthetic and natural polymers. Both kind of polymers have significant advantages and disadvantages. For instance natural polymer based hydrogels present enhanced biological properties such as biocompatibility, biodegradability whereas they generally exhibit lower mechanical properties. A pivotal feature of natural based hydrogels composed of such as

alginate, hyaluronic acid, dextran and chitosan is to resemble extracellular matrix properties. Yet, it is difficult to attain the same material properties for each batches and sources on natural based hydrogels.(47) On the other side, since synthetic based hydrogels have insufficient biological properties, these properties need to be enhanced with modification.(34) The combination of natural and synthetic polymer attracts considerable attention. It gains positive sides of both natural polymers such as biodegradability and biocompatibility, and of synthetic polymers which provide controlling the material properties easier such mechanical and degradation properties.(48–50) Hydrogels have properties similar to living tissues such as their porous and aqueous network(51), which permit the transfer of oxygen and nutrients.(34,52) In addition, it is possible to prepare hydrogels in various shape and size for drug applications.(51)

2.4 Injectable Hydrogels

Injectable hydrogels belong to a special class among biomaterials due to their exceptional features. Invasive operations are required to implant classical hydrogels in body, which lead to low patient comfort and also contain risk of inflammation.

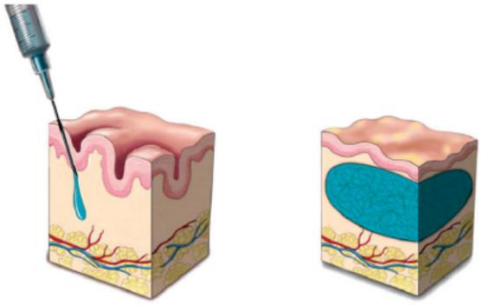

Figure 2.5. Application of injectable hydrogel to the tissues.(53)

Injectable materials form a gel *in situ* following injection to target site, which provides advantage in *in vivo* applications due to minimized surgical operations.(46) In addition, administration of the drugs is easier into hard to reach zones via injection than surgical operations and the material has capability to fill tissue defects

entirely as shown in the Figure 2.5.(46) Drug agents (protein, peptide, gene and cells) are integrated into gel precursors via uncomplicated mixing procedure.(46,54) In addition, hydrogels are used as therapeutics on their own and as cell repairing agents. A salient example of this is Osteoarthritis (OA). OA is a joint disorder, which is resulted with cartilage deformation of joints mostly in hips, spine, knees and hands. OA leads to joint damage, limited mobility and pain. There are numerous studies for cartilage tissue engineering via biodegradable injectable hydrogels.(55–58) Osteoarthritis theraphy is demonstrated in the Figure 2.6 with injectable hydrogel branded Synvisc-One. Moreover, there are commonly used injectable hydrogel formulations such as Synvisc-One® Sinovial®, Hyalgan to reduce friction and pain. Thus, there have been a growth attention on in situ hydrogel systems due to stated properties.

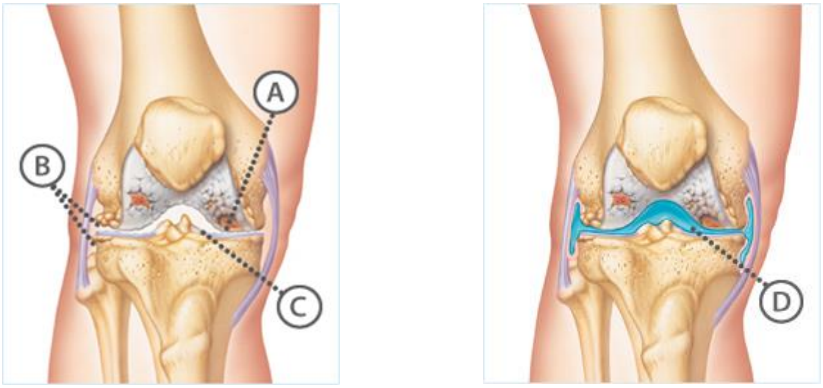

Figure 2.6. An example of osteoarthritis therapy with injectable hydrogel, which is branded Synvisc-One: A. Cartilage deformation B. Bone damage C. Joint fluid reduction down D. Hydrogel injection to reduce friction.(59)

Injectable hydrogels can be produced with physical and chemical interactions. Physical hydrogels are formed via non-covalent interactions. Gel formation occurs at gentle conditions via physical cross linking without the necessity of toxic cross linking agents. Mild conditions are favorable for protein delivery applications. However, hydrogels are weak in terms of mechanical properties and resistance to environmental factors. Covalently bonded injectable hydrogels can be designed via various chemistries such as Michael type addition(60), disulfide formation(61),

imine bond formation(37), hydrazone bond formation(49,62), oxime formation(63). Chemically crosslinked hydrogels provide fast gelation in general.(64) Hydrogel network are more stable to alterations in pH, temperature and ionic strength. Hydrogels can also be designed to respond to chemical or physical stimuli. However, in such a case, the stimuli should not harm the hydrogel network.(65)

2.5 Nanocomposite Hydrogels

Hybrid structure definition is proper for nanocomposite hydrogels.(51) Nanocomposite reinforced hydrogels contains organic/inorganic nanofillers in the polymer network, which have enhanced properties over conventional hydrogels.(66) Incorporated particles can be comprised of carbon based, inorganic, metallic and polymeric.(51) Tailor made nanocomposite hydrogels constitute a well-designed hydrogel structure for *in vivo* applications. High surface interaction between nanoparticles and polymers provide enhanced properties for biomedical applications.(51) Nanofillers are used as both reinforcing agent in the polymer network and as cross-linkers to form a hydrogel.(67)

Clay containing materials are widely used in tissue engineering, and demonstrate great performance in terms of physical, chemical and biological properties. Drug and gene delivery, biosensors, soft and hard tissue regeneration are main application areas of such materials(68). Smectitic clay minerals are widely used for nanocomposite hydrogel production.

Clay containing nanocomposite hydrogels are accelerated biomedical researches such as regenerative engineering and controlled drug delivery.(25) Main issue related with drug delivery is burst release of substances.(6) Drug release kinetics can be adjusted with clay addition.(69,70) Biocompatibility of clay should be considered such as clearence of nanoparticles from the body. In other terms, the nanoparticle should be eliminated from the body by depending on natural mechanisms or has biodegradable properties.

2.6 Drug Release from Hydrogels

A drug release system should be reliable in terms of biological, chemical and physical properties. In other words, drug system should be compatible with living cells, have mechanically desired properties, and have low affinity to interact with tissues, tolerate unintentional dosage release and respond the patient needs. Drug loading capacity should be high for the efficacy.(29,49,71)

Hydrogels are suitable materials for drug release applications due to their biocompatibility and diverse cross-linking chemistries available. Structure of the hydrogels determines drug release kinetics. Chemistry and possible interactions must be well defined to predict the physical and chemical properties of a hydrogel. A logically arranged hydrogel network is necessary for obtaining consistent release profiles. In addition, material properties and the interaction type have influence on release mechanism. Release of a drug from a hydrogel matrix can be tuned by adjusting parameters such as swelling ratio and polymer concentration.(72)

Fickian diffusion model is seen predominantly in swollen hydrogels.(73,74) However, zero order release model is preferred.(75)

2.6.1 Protein Release from Hydrogels

It is evident that there have been promising hydrogel formulations for protein release.(76–78) Some strategies have been applied for protein loading into hydrogels. Physical entrapment, adsorption of substances onto matrix via surface interaction, covalent and non-covalent linkers are commonly used techniques for protein loading. In the same way, release mechanism of these biomacromolecules dominates diffusion, swelling, erosion, degradation and environmental scissors (pH, Temperature etc.).(79) In addition, a synergistic effect can be obtained by the combination of various release mechanisms.(79) Enhanced prolonged release of proteins can be provided via increased attraction with polymers. Enzymatic degradation is involved in release mechanism along with diffusion and release rate can be adjusted with crosslinking density.(80) Since protein release shows burst release for many hydrogel designs due to weak interaction between protein and

polymer, controlled release of proteins has significant importance on drug studies.(81,82) Thus, hybrid hydrogels are offered for controlled release studies.

Targeted delivery and local delivery have improved release properties of proteins. Local delivery of antibodies leads to high efficacy due to local bioavailability. Systematic exposure is minimized by means of local treatment and lowering of the required drug dose.(83) A critical situation of local administration is related with possible interactions or reactions with injected area. If possible interactions occurred, invasive administration would be inconvenient. (84)

Particle containing polymers can be formulated as injectable for moderate solid content (85) whereas polymers that have high solid component can be troublesome considering their injectability. In a similar manner, high polymer concentration and high viscosities limit injectability.(86) Moreover, the interactions between polymer and polymer, polymer and protein can also increase viscosity.(87,88)

Drug carriers can be designed as biodegradable, biocompatible, targeted and stimuli responsive.(89) Injectable drugs can be delivered either parenterally or via local injection to the target site. Matrix material properties, substance characteristic highly determines release kinetics of drug.(90)

2.7 Drug Delivery System Design

A few points must be taken into consideration when designing a drug delivery system. Performance and biosafety of drug must be evaluated comprehensively. Hydrogel chemistry, tissue interaction and clearance are the main factors to be considered when developing a hydrogel system. In addition, gel network structure, release mechanism and biodegradability are key points to specify drug delivery system characteristics.

It is known that an ideal drug agent should be inert and or at least should not adversely interact with living tissues. Drug delivery system components must be safe for *in vivo* usage. Both main constituents with linkers and by products should

be non-toxic to prevent potential risks. More importantly, it should be cleared from body by depending on a natural mechanism.

Backbone chemistry can be composed of synthetic and natural polymers. Hydrogels should degrade into nontoxic parts and cleared from the body. It is known that carbohydrates have advantage on synthetic based polymers in terms of biodegradability. Functional groups are effective on characteristic properties and cross linking formation. Cross linking density, pore size, degree of swelling are adjusted via the reactive functional group density in polymer.(91) Tissue interactions with drug should not evoke host immune responses in body.

As injectable hydrogels precursors are introduced with needle, the precursors should have relatively low viscosity to allow injection. Standard 25G needle can be used for the delivery of injectable hydrogels.(92)

Separate barrels are used for loading gel precursors to prevent earlier gelation. Double barrel syringe is known as most common apparatus used. After precursors are loaded into separate barrels, both solutions are injected simultaneously to form a gel in situ.(93,94) Double barrel syringe is found in the Figure 2.7. Other apparatus can also be used such as micropipettes and syringes. However, precursors must be mixed effectively to obtain a homogenous solution.

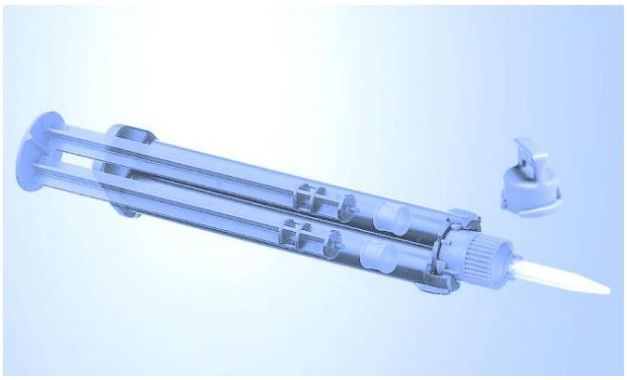

Figure 2.7. Double barrel syringe for mixing precursor solutions.(95)

The precursors should form a gel in a short period of time following injection under physiological conditions (aqueous, 37 °C, 0.15 M ionic strength, pH 7.4).(92) Fast

gelation provides prevention of therapeutic agent diffusion out of matrix in a short period of time. Therefore, burst release and toxic effect of therapeutic agent to adjacent tissues are minimized.(92)

2.8 Protein Adsorption onto Clay

Adsorption is defined as accumulation of ions, molecules and atoms at liquid or solid surfaces. The accumulated particles are named as adsorbate whereas the adsorption surface is known as adsorbent. The driving force of the adsorption process arises from unbalanced forces on the adsorbent surface. Molecules are bonded to surface based on two main mechanisms-physical adsorption (physisorption) and chemical adsorption (chemisorpton). Weak bonds such as Van Der Waals bond are presented in physisorption whereas strong chemical bonds are found in the chemisorption. On the other hand, there is not found a significant electron density distribution for adsorbate or adsorbent in physical adsorption in contrast to chemical adsorption. There have been many methods to characterize adsorption application. The most known isotherm is known as Langmuir which is based on rate equilibrium of adsorption-desorption.

Protein adsorption onto solid surfaces includes a complex process with various mechanisms. Surface and adsorbate properties, pH and ionic strength determine adsorption characteristics.(96) The most significant point is to provide stability of protein in the adsorption process. Protein molecules can be immobilized via physical adsorption or entrapment and chemical adsorption.(97) There are many parameters which determine adsorption of proteins onto clay minerals. Solution pH, temperature, interaction time, ionic strength and dielectric constant of medium and solvent are most effective parameters.(98)

Proteins can have different charges depending on pH. Carboxyl (COOH) and amino groups (NH_2) in the protein structure become charged as a result of deprotonation or protonation at solution. When the pH value of the solution is lower than the isoelectric (pI) point, protein gains net positive charge due to an excess of NH_3^+ ions. If the pH value of the solution equals to pI point, protein has no net charge, the

number of $NH3^{+}$ and COO^{-} groups are equal. There are minimum repulsive forces for protein solutions at pI value. Finally, at a pH value higher than the pI value, protein has net negative charge due to an excess of COO^{-} ions. In a similar way, pH value of solution affects electrical charges of clay minerals.(98)

Clays are strong adsorbents especially for proteins. There are several studies on determining the interaction of proteins, amino acids and also drugs with clays minerals.(99–104)

Clays are substantially used materials in biopharmaceutical industry as excipients or active substances.(99) Clays can be formulated in a wide range to adjust release and for targeting of substances. Clays are used to decrease oral absorption of drugs, which is the beginning step for use of clays in drug release studies.(99) Drug delivery systems containing clays in their formulations can be classified as natural clay minerals, commercial clays, synthetic clay, composites – films, nanocomposite hydrogels, nanocomposite polymers.(105) Clays are used to immobilize organic molecules for drug delivery, tissue engineering applications. There are many applications in which clay minerals are used as drug carriers.

2.9 Characterization Techniques

2.9.1 Fourier Transform Infrared Spectroscopy

Fourier transform infrared spectroscopy is commonly used for determination of functional groups in the materials. The technique is based on absorption or transmission of infrared radiation by the sample material. Mid wavelength infrared is located between 200 cm^{-1} and 4000 cm^{-1}. It is known that most applications are carried out in the mid infrared region.

Infrared radiation is not capable of inducing electronic transitions and breaking bonds in molecules. However, vibrational and rotational states of the molecules can be stimulated via IR. The atoms are not stable in the molecules which perform

vibrational movements and the dipole moment of the molecule undergoes a change with absorbing infrared radiation.

The vibrational movements are divided into two classes as stretching and bending. Stretching vibration occurs on a bond between two atoms by changing bond length. Streching vibrations are classified as asymmetric and symmetric. On the other hand, change of angle between two bonds is known as bending vibration. Rocking, scissoring, wagging and twisting are bending vibrations. In addition, coupling of vibrations can take place when the vibrational bonds are attached to a center atom.

Vibrational motion is depended on bond strength in the structure. The vibrational frequencies of the bonds are determined with infrared spectroscopy. The information about functional groups is identified in the material. Covalent bonds vibrate in certain frequencies with IR. This is detected and transformed into a spectrum. Bond intensities can be described as strong, medium, and weak. Since the intensity of the bonds is related to the dipole moment, strong polar bonds result in high intensities. The peaks observed in the spectrum are also identified as narrow and broad shapes.

Most polar bonds are IR active while apolar bonds are inactive. FTIR analysis gives information about the presence of functional groups. The most useful range is in between 600 cm^{-1} and 4000 cm^{-1}. Functional group region is from 1500 cm^{-1} to 4000 cm^{-1}. The range between 400 cm^{-1} and 1500 cm^{-1} is defined as fingerprint region – highly complex area including many peaks. Although FTIR spectrum provides insight into the structure, other techniques are needed for exact determination of the compound, since, signals could be inadequate or some structures presented cannot be identified.(106–109)

2.9.2 Thermal Gravimetric Analysis (TGA)

Thermal gravimetric analysis is done to measure weight change in a specified time or temperature range. Composition of the substances and thermal stability of the material are determined. Chemical and physical alterations are observed versus temperature or time functions.

TGA gives an insight about physical changes in the material such as phase transitions, adsorption, absorption and desorption applications, It also presents information about chemical changes occurring-decomposition, dehydration or oxidation. Mostly, thermal and oxidative stability, moisture present in the sample, volatile components, decomposition kinetics are determined via TGA.(110)

Both weight loss and weight gain based on chemical or physical changes occurring during the analysis may be observed. . The measurements may be carried out under air, N_2, or He atmosphere.

2.9.3 XRD

X-ray powder diffraction (XRD) is a powerful and rapid analytical technique mainly used for identification of atomic structure and spacings in crystalline planes, which also provides information about unknown inorganic samples, minerals and clays. XRD analysis presents change in intensities (I) with respect to diffraction angle (2θ). The diffraction pattern is plotted based on Braggs Law:

$$2d\ sin\ \theta\ =\ n\lambda \text{ (1.5)} \qquad (1)$$

where λ is radiation wavelength, θ is the scattering angle, d is the interplanar spacing. Diffraction peaks are converted to d-spacings to identify material. Each mineral has a specific d-spacing. Modification applications and alterations in the structure are examined with comparison of d-spacings of reference materials.

Amorphous materials do not show sharp peaks in the XRD analysis plot due to absence of translational symmetry. However, crystalline structure determination of materials can be examined with this technique. XRD is the common tool for evaluation of clay-polymer nanocomposites such as intercalated, exfoliated and immiscible. Figure 2.8 presents a demonstration of XRD patterns of nanocomposite materials, which are originated from reference.(6)

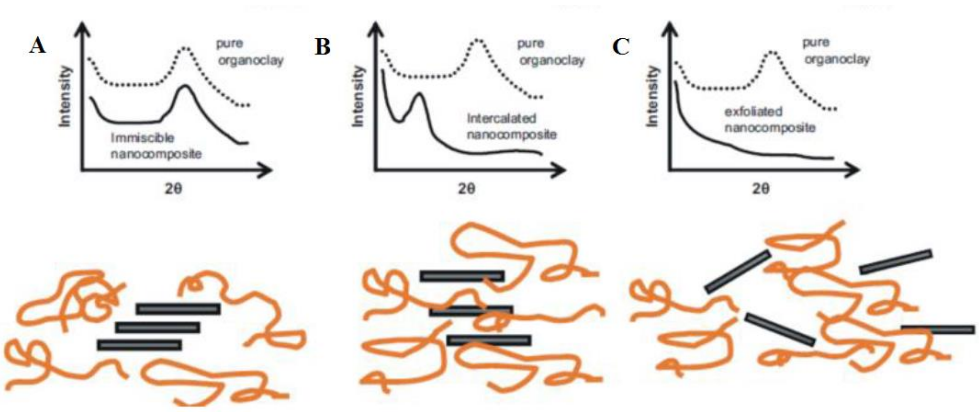

Figure 2.8. XRD patterns of nanocomposite materials: A. Immiscible nanocomposite B. Intercalated nanocomposite C. Exfoliated nanocomposite. (6)

2.9.4 UV-Visible Spectrophotomer (UV-VIS Spectrophotometer)

UV region is in the electromagnetic spectrum. Electrons level up to higher energy state with ultraviolet and visible radiation. UV-VIS spectrophotometer is used in near UV and near infrared region. The measurement is based on intensity of absorption or reflectance of passing light through the sample.(111)

The UV-VIS spectrophotometry is a photometric method in which measuring the absorbance at a given wavelength is used for determination of concentration of substances in a solution. This technique is widely used in bioanalytical applications.

Many protein detection methods are based on the interaction between the reagent and proteins and measuring the absorbance of the formed complex at a selected wavelength using UV-VIS spectrophometer. Carbazate assay and Bradford assay are defined as colorimetric methods.

2.9.4.1 Carbazate Assay

TNBS Assay or carbazate assay is based on UV-VIS Spectrophometric method for estimation of aldehyde and hydrazide groups in materials. 2,4,6-trinitrobenzene sulfonic acid (TNBS) is a chemical for quantification of free amino groups.(112,113)

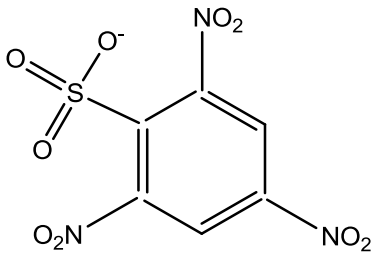

Figure 2.9. Structure of TNBS (2,4,6-trinitrobenzene sulfonic acid).

TNBS is reacted with primary amines, peptides and proteins at alkaline pH media to form a colored derivative.(114) Absorbance of the complex is measured at 335 nm.

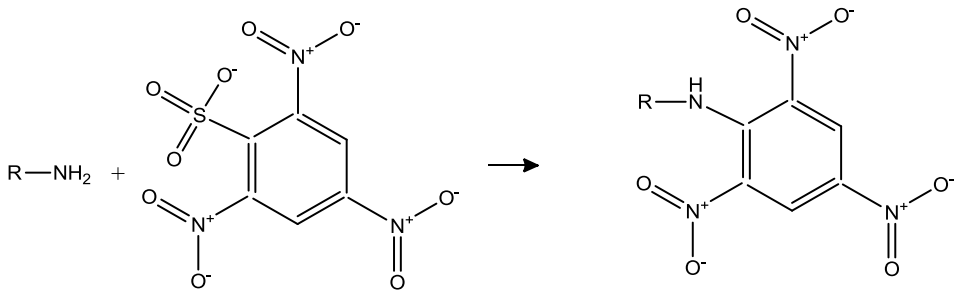

Figure 2.10. TNBS reaction with amine containing groups.(115)

Hydrazide containing groups are reacted with TNBS. However, method can be modified to determine aldehyde groups. Aldehyde groups react with hydrazide for the formation of hydrazone. In a similar manner, aldehyde groups interact with carbazates to constitute carbazones. Structure of tert-Butyl carbazate is as shown:

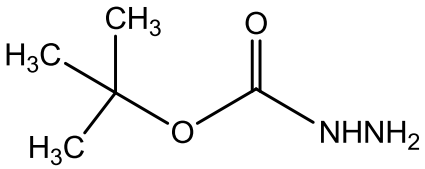

Figure 2.11. Structure of tert-Butyl carbazate (tBC).

The number of aldehyde groups in polymers can be determined via a modified TNBS Assay. Afterwards, unreacted carbazates are reacted with TNBS. Aldehyde amount is calculated via determination of remaining carbazate after carbazate reaction between aldehyde groups and tBC.

2.9.4.2 Bradford Assay for Protein Determination

Bradford assay is comparatively sensitive and easy method for the detection of proteins. It is stated that the method can be applied for the protein concentrations up to 2000 μg/ml. Since the assay is based on the Beer-Lambert Law, the standard calibration curve must be linear and the absorbance values should be lower than 1.5 value.(116) Thus, dilution is needed for decreasing the absorbance of the protein concentrations in the upper limit.

In the assay, Coomassie Blue G-250 is used as the reagent which has red-brown color in acidic buffers. When bradford reagent reacts with protein, blue color forms and the absorbance of the solution is measured at 595 nm.

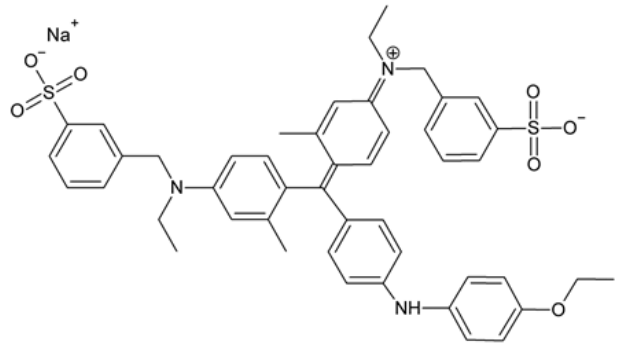

Figure 2.12. Structure of bradford reagent.

CHAPTER III

LITERATURE STUDIES

3.1. Polysaccharide Based Biodegradable Hydrogels

Polysaccharides are the most important biomolecules along with polynucleotides, proteins and lipids.(117) Many polysaccharides can be modified owing to the functional groups (-OH, -COOH, -NH_2) in their structure.(118) In addition, compositional similarities of carbohydrates with components of living tissues contribute to their biocompatibility.(91)

Carbohydrate based polymers are used for biomedical applications due to their enhanced biological properties. Dextran, chitosan, hyaluronic acid and alginate containing injectable hydrogels are used in a wide range of *in vivo* studies. Biodegradation products of these polymers are generally non-toxic and cleared from the body easily.

Dextran has attractive properties for injectable hydrogel production. Hydroxyl groups in the saccharide units provide oxidation sites to form aldehyde groups which enable diversity in cross linking techniques to form gels. Maia *et al.* produced injectable degradable hydrogel with hydrazone bond chemistry for potential drug delivery systems and tissue engineering applications.(119) Amphotericin B (AmB) was conjugated to cellulose and dextran based injectable hydrogels with hydrazone chemistry. Produced hydrogel was used as hydrophobic drug carrier for antifungal theraphy.(120) Injectable chitosan and dextran based hydrogels with imine bond formation were prepared for cell and protein delivery.(121) Chitosan and dextran

based hydrogels demonstrated nontoxic and biodegradable properties in *in vitro* cell culture studies.(122)

Hyaluronan and methyl cellulose based hydrogels were studied with a different view to obtain accelerated release of hydrophobic drug for spinal cord injury.(123) Hyaluronan based injectable hydrogels were also used for controlled protein delivery applications.(124) Schoichet et al. generated hyaluronan and methylcellulose (HAMC) containing injectable hydrogel system for localized sustained delivery of growth factors. Expanding the research to determine the small molecules delivery of neuroprotective agents, it was shown that hydrophobic agents can be released by tuning the properties of the injectable hydrogel network. HAMC polymer addition induced solubility of low soluble drugs and enabled adjusting the release profile. Carbohydrates were also used as protein carriers.(125) Chitosan is widely used for drug delivery applications.(29,121,126–128) Finally, there have been remarkable studies on polysaccharide based hydrogels which demonstrated biocompatibility with tissues and minimal cytotoxic effect.(129–131)

3.1.1 Alginate Based Hydrogels

Alginate is a linear hydrophilic polysaccharide derived from marine brown algae and consists of alternating α-L-guluronic and β-D-mannuronic acid blocks in the structure. Alginate polymer is shown in the Figure 3.1.

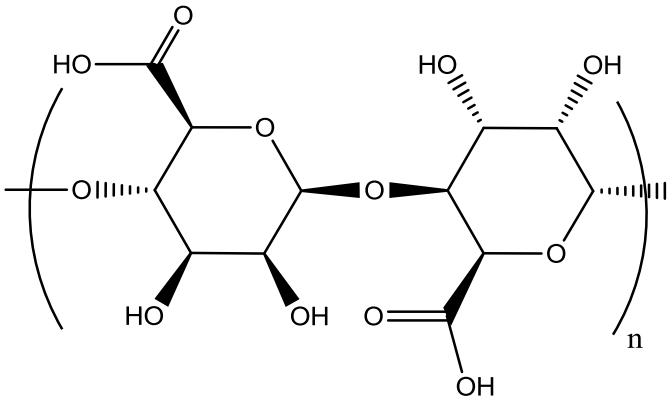

Figure 3.1 Structure of alginate.

The arrangement and composition of the repeating units in the alginate structure determine the physical properties of alginate. Due to the lack of degrading enzymes

in mammals, high molecular weight alginate degrades in body slowly.(47,132,133) The outstanding feature of the alginate is the gelation ability with divalent cations, mostly with calcium.(134) Guluronic acid block is responsible for "egg box" formation, which provides the usage for cell transplantation vehicles and wound dressing.(134) Yet, alginate hydrogels formed with divalent cations demonstrated uncontrollable degradation behaviour.(135)

There has not been a conclusive consideration about degradability of alginates *in vivo*. It is challenging to adjust degradation profiles of alginate based hydrogels due to the absence of degrading enzymes. Generally, it presents slow degradation.(136,137) In addition, high molecular weight alginic acid is non degradable.(138) However, alginates that have low molecular weight can be eliminated from the body.(139)

A few techniques were applied to increase the biodegradability of alginic acid via oxidation reaction. It was demonstrated that aldehyde addition into alginic acid resulted decrease in molecular weight and increase in biodegradability according to the work of Kristiansen and co-workers.(132)

Since the potential usage of polysaccharide is *in vivo*, bio responses gain importance. Thus, alginate materials that include low mannuronic acid components can be used in vivo applications to prevent inflammatory reactions. Moreover, it was reported that alginate implants have rich guluronic acid parts have relatively low immunological responses when implanted than polyvinyl alcohol and agarose containing gels.(140) Fibriotic reaction was observed in a few studies.(140–143) However, it was contended that chemical composition and mitogenic substances tends to immunogenic effects.

The structure of sodium alginate enables a few modification studies due to rich COO^- groups in the backbone. Oxidation or namely aldehyde modification is the most common. There has been a great deal of work related with oxidation of alginates with different substitution values.(118,144–146)

It was found that the degree of oxidation depends on sodium periodate concentration. Hydroxyl groups were oxidized with sodium periodate as a result of the breakage of carbon-carbon single bond. Finally, dialdehyde was formed in the monomers. Therefore, rotational flexibility was increased. It was also contend that molecular weight of polymer was decreased with an increase in substitution degree.(118) The oxidation yield was decreased at higher sodium periodate concentration, which caused by hemiacetal formation.

3.2 Hydrazone Bond Chemistry

Hydrazone bond can be defined as a type of Schiff base. However, the bond is more stable than a Schiff base formed by the reaction of an amine and an aldehyde. The aldehyde or ketone groups are reacted with materials containing hydrazide groups to form hydrazone bond as shown below:

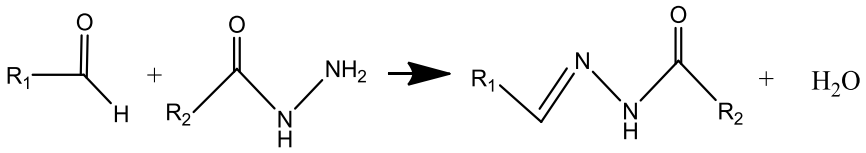

Figure 3.2. Formation of hydrazone bond.

Stability of the bond arises from the enhanced nucleophilicity of neighbour amines via alpha effect (92,147), blocking following reduction of the bond. The hydrazone bond formation between reactive species occurs spontaneously. High pH medium tends to increase the stability of the bond.(148) Hydrazone and oxime bonds possess greater hydrolytic stability than imine bond.(149)

3.2.1 Hydrazone Bond Formation

Since aldehyde and ketone groups ensure many modification and conjugation application, if the polymers do not contain such reactive groups to form hydrazone bonds, modifications can be performed to provide aldehyde or ketone groups in their

structures. It was observed that hydrazone bond created with ketone groups are more stable than with aldehyde groups.(93)

Homobifunctional hydrazide groups are reacted with aldehyde or ketone group containing polymers to form crosslinked structures. The most commonly used crosslinker molecule is named as adipic acid dihydrazide which is a water soluble homobifunctional hydrazide component. The molecule consists of 10 atom bridge, the backbone includes carbon atoms and the reactive sites ($CONHNH_2$) are found in the end as shown in the Figure 3.3.(12)

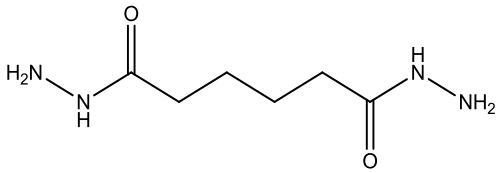

Figure 3.3. Structure of adipic acid dihydrazide (ADH).

1-ethyl-3-(3-dimethylaminopropyl) carbodiimide hydrochloride (EDC) is a homobifunctional cross linker used for conjugation to carboxyl groups. The structure of the material is given in the Figure 3.4.

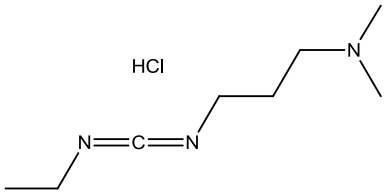

Figure 3.4. Structure of 1-ethyl-3-(3-dimethylaminopropyl) carbodiimide hydrochloride (EDC).

In such a reaction, the carboxyl group reacts with EDC and the intermediate product O-acylisourea is formed, then it reacts with an amine group for amide bond formation and isourea is formed as by the product. N-hydroxysuccinimide can be

used for stabilization O- acylisourea.(150) Hydrolysis of the intermediate product and reformation of the carboxyl and release of an N-substituted urea means the failure of the modification.(150) Krishna showed that hydrazide modification was realized for amine-PEG4-t-BOC with carbodiimide reaction. O-acylisourea intermediate was generated as a result of reaction with EDC and with the use of NHS a relatively more stable activated ester could be formed.(62)

3.2.2 Hydrazone Bond Chemistry *in Vivo* Applications

The linkages are biodegradable and hydrolytic in hydrazone bond. In addition, byproduct of the reaction, water, is safe. Hydrazone bond is relatively stable under physiological conditions whereas it hydrolyses relatively fast in media at acidic pH. Considering the acidic pH of the tumor tissues or endosomes, the chemistry is promising for *in vivo* targeted delivery applications.

The biocompatibility of the materials must be taken into account for successful tissue engineering practices. Elimination or minimization of host responses has vital importance for successful application. There are salient *in vivo* studies related with hydrazone network for biomedical applications.

Hydrazone bond is suitable for pH sensitive applications. The stability of HPMA copolymers were enhanced with hydrazone bond. Modified micelles were concentrated on tumors due to EPR effect and degraded due to acidic pH values.(151) In the same way, drug release occurred due to hydrolysis of hydrazone bond within hours at acidic pH mediums such as in endosomes or lysosomes of tumor cells.(151–153) pH sensivity provides targeted drug release for acidic environments. Therefore, toxic effects of drugs can be reduced.(154)

Another *in vivo* application showed that hydrazone hydrogels can be used for spinal fusion and initiated simultaneous angiogenesis.(155) In addition, the researchers demonstrated that hydrazone hydrogels creates insignificant host response in vocal fold tissue.(156)

A potential issue related with hydrogels is the reactivity of excess aldehyde groups, which is not participated hydrazone bond formation, can be reacted with amine

groups in tissues. Thus, a few design criteria should be considered when composing hydrogel to overcome this risk.(4) Addionally, it was reported that aldehyde groups were tended to interact with aminooxy groups to form oxime bond in the presence of amine and aminooxy groups rather than relatively unstable imine bond.(157) Yet, excess aldehyde groups can be used for specific purposes. For instance, hyaluronic acid base injectable hydrogels were produced with hydrazone bond. Excess aldehyde groups were reacted for obtaining tissue adhesive property.(155)

3.3 Hydrogels with Hydrazone Bonds

Hydrazone network ensures exceptional properties such as targeted delivery, pH sensitive application, stability of hydrogel in blood, controlled release, biodegradability and fast gelation. Fast gelation ranks in priority on injectable hydrogel formation. When aldehyde and hydrazide precursors encounter, the gelation occurs in a very short time. Therefore, this feature is conducive to *in situ* gelation. Polymers that have high substitution degree and concentration can form a gel prior to completion of mixing.(92) The study conducted by Hoare and Patenaude showed that hydrazone bond from synthetic based materials were formed within seconds which prevents diffusion of drugs out of target region.(31)

Patenaude *et al.* also demonstrated a tuning mechanism for gelation time with ketone and aldehyde counterparts.(93) Ketone groups are slower in terms of reactivity than aldehyde groups. Gelation time was adjusted between seconds to hours by adjusting the ratio of aldehyde and ketone groups in the poly (N-isopropylacrylamide) and carbohydrate containing hydrogels with hydrazone chemistry. Hydrazide groups were selected as 1.5 excess than aldehyde-ketone groups. It is apparent from Table 3.1. that gel formation time increases with increased ketone groups in the precursors. Functionalization degree was obtained as 0.42 for 100 Ket* whereas DS value of other ketone groups was defined as 0.12.

Table 3-1. Gelation time based on aldehyde and ketone groups in the hydrogel.(93)

Gel ID	Gel formation time (minutes)
100Ald/0Ket	0.09 ± 0.02
75Ald/25Ket	0.4 ± 0.1
50Ald/50Ket	24 ± 2
25Ald/75Ket	45 ± 6
0Ald/100Ket	65 ± 13
0Ald/100Ket*	2.0 ± 0.5

Ketone groups provide more gel formation time and enable well mixing of precursors. Yet, hydrogels with increased ketone groups demonstrated faster degradation as shown Figure 3.5. It was concluded that degradation rate can be adjusted with aldehyde and ketone ratio in the hydrogels.(93)

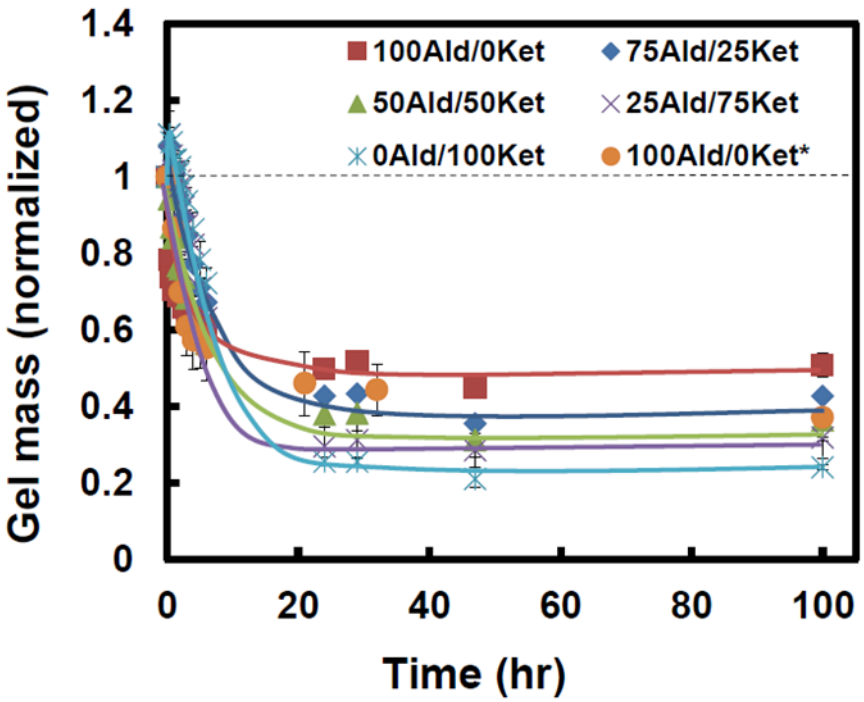

Figure 3.5. Mass loss versus time for hydrogel samples with different ratio of aldehyde to ketone. (93)

Krishna *et al.* also showed that gelation characteristics are related with mechanical properties. In the related study, high compressive modulus observed in gels with hydrazone bond chemistry and containing elastin like proteins which gelation occurs within seconds compared to other injectable hydrogels.(62)

Cranston and Hoare generated injectable nanocomposite hydrogel composed of polysaccharides - dextran and carboxymethyl cellulose (CMC) - and reinforced with cellulose nanocrystals (CNC) as a drug delivery agent.(158) The precursors were extruded and gel formation occurred within seconds. CNC was preferred due to its low toxic properties.(159,160) Concentration of CNC ranged between 0.05% and 1.0% in weight whereas 2% oxidized dextan and 2% in weight hydrazide modified carboxymethyl cellulose were present in final hydrogels. It was demonstrated that nanocomposite incorporation tends to lower swelling index due to possible reduced mobility of the chains and increased cross-link density. However, hydrogels had same swelling trend. Since swelling and degradation of hydrogels influence long term drug delivery, it was concluded that these hydrogels would be potential drug vehicles for long term therapies.(158)

Another work of Hoare and Mateen demonstrated that injectable degradable hydrogel formation for hydrophobic drug delivery from dextran and cyclodextrin.(161) Dexamethasone release was shown below:

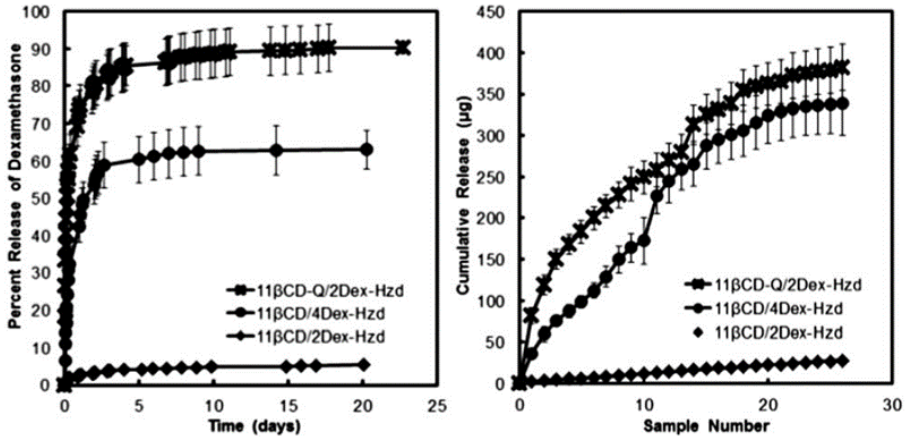

Figure 3.6. Dexamethasone release from hydrazone bonded hydrogels containing different hydrazide concentrations. (161)

Figure 3.6 reveals the effect of dextran hydrazide concentration on release profile. In comparison, while only 5.4% of the dexamethasone was released from hydrogel containing 2% wt. hydrazide modified dextran polymer, 65% of the drug was released from 4% wt. dextran hydrazide polymer at the end of 20 days. There was a significant change on burst release with small alterations on hydrazide amount on hydrogel.(161)

The group also generated injectable hydrogels composed of natural and synthetic polymers.(49) Carbohydrates–hyaluronic acid, carboxymethyl cellulose, dextran and methyl cellulose-were oxidized with sodium periodate. On the other hand, poly (N-isopropylacrylamide) was functionalized with hydrazide groups using adipic acid dihydrazide (ADH) in the presence of EDC. Swelling profile was adjusted with selection of oxidized carbohydrates. Dextran demonstrated the highest deswelling property.(49) A similar work of Hoare was related on elastic and degradable nanocomposite hydrogel production from carbohydrate and synthetic materials.(162) Composite materials were synthesized in the aldehyde ratio to hydrazide in the range between 0.85 and 4.26. Acceptable chronic inflammation was seen with no fibrous tissue formation.(162) Hydrazone bond chemistry was also used for small drug delivery from the combination microgel and hydrogel matrices.(94)

The reason of increased stability of hydrazone hydrogels is due to reduced electrophilicity of carbon atom connected with nitrogen which decreases reactivity of hydrazone bond.(92) The degradation rate can be adjusted by adjusting the cross linking degree and pH of the medium.(148,163)

3.3.1 Alginate Based Hydrazone Bonded Hydrogels

Dahlmann and his co-workers studied alginate and hyaluronic acid based hydrogels having hydrazone bond for myocardial tissue engineering applications. Aldehyde and hydrazide modification was done on each polymer to provide reactive sites for hydrazone bond formation. Oxidation functionality was confirmed with three independent techniques. C=O stretching was observed at 1726 cm^{-1}, which indicates aldehyde modification. In addition, the bond formation was verified via NMR

spectroscopy. The presence of hydrazide was tested with TNBS Assay. Swelling test was conducted for four different types of hydrogel (HyA-Ald/Alg-Hyd, HyA-Hyd/HyA-Alg, Alg-Ald/Alg-Hyd, Alg-Ald/Alg-Hyd) with 1:1 aldehyde/hydrazide ratio. HyA-Ald/Alg-Hyd had the lowest swelling index. It was thought that carbohydrate based hydrogels have enhanced properties for myocardial tissue engineering practices.(164)

Alginate based hydrogels were synthesized with gelatin and ethylenediamine in the presence of carbodiimide.(165,166) However, there have been limited study related with functionalization of sodium alginate with adipic acid dihydrazide (ADH) in the presence of EDC.

An important work demonstrated an insight about hydrazide modification of alginate.(167) In the study, sodium alginate was modified with ADH to form hydrazide groups and complexed with β-cyclodextrin. Hydrazide modification was done in the presence of EDC. Nucleophilic attack of primary amines upon o-acylisourea (intermediate form of activated carboxyl groups in the polymer) gives amide bond formation. Yet, a side reaction may be resulted with N-acylurea formation. In addition, side product formation was increased with EDC concentration. As a result, the degree of substitution was not adjusted eventually. The target of the hydrazide modification was to minimize N-acylurea. Sodium alginate was reacted with ADH in the presence of EDC at pH 4.75 and the pendant groups were modified with hydrazide. Low degree of modification provided similar gelation properties with unmodified alginate polymer. Moreover, it was observed that low modification degree contributed to prevention of physical aggregates. Relatively decreased ADH amount was used in modification studies due to high concentration of carboxylic acid groups in the structure of alginate.(167)

Another particular study was done about hydrazide modification of alginate by Tan *et al.*(168) A thermosensitive copolymer was produced with PNIPAAm-COOH and aminated alginate (AAlg). The structure of modified polymers was examined FTIR and ^{1}H NMR analysis for various grafting ratios. The potential aim of the work was the determination of control degradation by adjusting PNIPAAm modification.

Amidation procedure was applied with ADH via EDC-HOBt. HOBt was also used for stabilization of reaction product. The reaction was proceeding at pH 4.5 and 0.1 M HCl was added to set the pH value of the medium. Hydrazide group confirmation was done with ATR-FTIR analysis and TNBS Assay quantitatively. It was demonstrated that hydrogel degradation was adjusted with PNIPAAm modification degree according to in vitro experiments. In the study, alginate based biomaterial was obtained with hydrazide modification as seen from Figure 3.7.

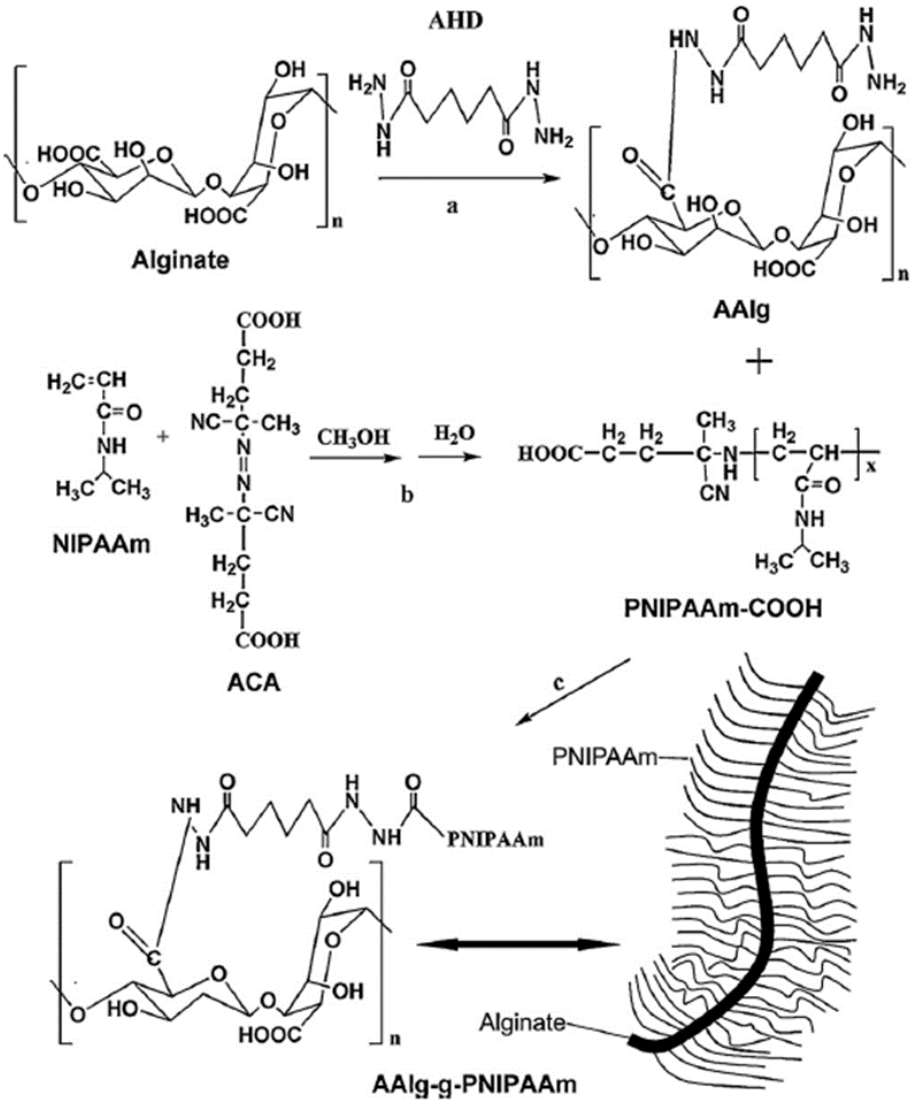

Figure 3.7. Synthesize route of comb-like AAlg-g-PNIPAAm polymer: A. Hydrazide modification of alginate, B.Synthesis of PNIPAAm , C. Comb-like structure formation.(168)

Wang *et al.* generated alginate and hyaluronic acid based scaffolds with hydrazone bond chemistry for spinal cord repair. Alginate and hyaluronic acid were crosslinked with ADH in the presence of EDC. It was noticed that higher concentration of EDC leads to more amide bonds. However, it was resulted with N-acylurea formation. Moreover, low pH values lead to crosslinked in a shorter period.(169) Finally, it was reported that amine groups in NH_2-Alginate can be detected with XPS analysis and photometric methods.(170)

3.4 Protein Delivery from Biodegradable Hydrogel Matrices

Hydrogels which are composed of biodegradable materials are used as drug delivery agents. Release of drugs can be achieved via adjusting degradation of polymers. There have been studies related to protein delivery and release from hydrogel matrices as summarized below.

Hiemstra *et al.* worked on protein delivery from injectable hydrogels composed of poly(ethylene glycol) and poly(lactide).(171) The study reveals that 90% of lysozyme was released in 10 days by depending on first order kinetics. On the other hand, 50 % of Immunoglobulin G was released in 16 days while 45% of therapeutic protein rhIL-2 was released in 7 days *in vitro* studies. Both proteins were released by following zero-order kinetics. Since protein release profiles had similarities for pH:5.0 and pH:7.0, it was concluded that release mechanism was dependent on diffusion.(171)

Dextran based hydrogels were studied for the release of three model proteins, namely immunoglobulin G, bovine serum albumin (BSA) and lysozyme for fibroblast growth factor. Hydrogels were formed with protein containing precursor solutions. 75% of the BSA was released in 16 days whereas 40% of lysozyme was released from hydrogel matrices in 14 days. The results revealed that injectable dextran hydrogels can be used for controlled release of proteins by adjusting DS and molecular weight of dextran.(172) BSA release was shown in Figure 3.8.

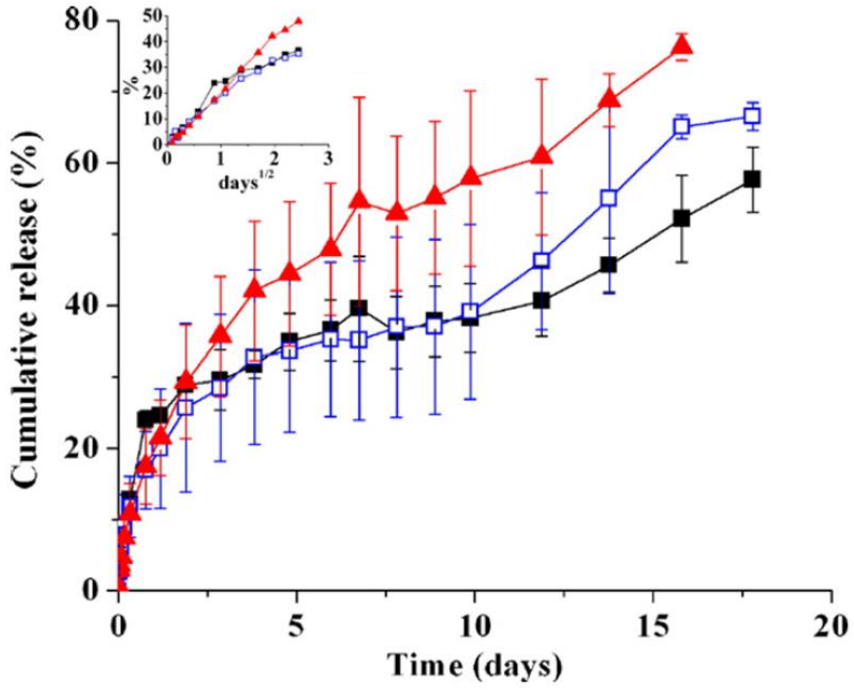

Figure 3.8 Cumulative BSA release from dextran based hydrogels.(64)

Tan studied thermosensitive alginate based injectable hydrogel for tissue engineering. Hydrazone bonded hydrogels were used as cell carrier by entrapping human bone mesenchymal stem cells (Hbm-SCS). Degradation was controlled by modification degree of PNIPAAm. (168)

Hydrazone hydrogels are promising materials for protein delivery. It was observed that low cellular toxicity was obtained for site specific protein delivery with carbohydrate based hydrazone hydrogels.(155) Spontaneous bond formation enables the conservation and stabilization of the three dimensional structure of proteins. In this manner, recombinant proteins are cross linked to form hydrazone bond in the conducted study. Recombinant elastins like polymers (ELP) based hydrogels are produced via the addition glutamic acid into ELP polymer backbone. Hydrazone chemistry provides enhanced mechanical properties to ELPs. Glutamic acid is modified to have aldehyde or hydrazide groups in the structure which provides the creation of hydrazone bond.(62)

3.5 Protein Clay Interaction

Proteins can interact with inorganic substances via mechanisms such as entrapment and adsorption. The key point is to preserve the native conformation of biomacromolecules after process.(173) A few studies were mentioned related with BSA adsorption onto clay.

The interaction between montmorillonite and BSA revealed higher adsorption values when reaching pI point. 2.4 mg BSA was adsorbed per mg montmorillonite for the weight ratio of BSA to montmorillonite equals to 4 at pH 4. Increased percentage adsorption was observed with increased protein to clay weight ratio. In addition, adsorbed protein amount was increased with increased weight ratio.(174)

Another study was related with adsorption of combination of BSA and Haemoglobin (Hb) proteins onto montmorillonite. As a result, adsorbed Hb amount was calculated as 0.08 mg for per mg montmorillonite whereas BSA was adsorbed in the range between 0.08 and 0.16 mg for per mg clay.(175)

BSA was interacted with various clays.(176) The adsorption profiles are given in Figure 3.9.

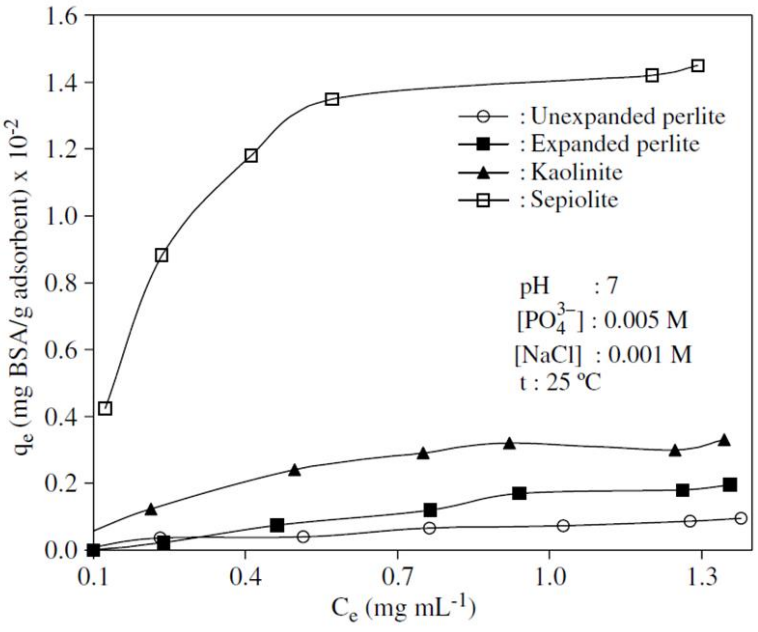

Figure 3.9 Adsorption capacity of BSA for various clays.(176)

The interaction between kaolinite and various proteins was examined by the work of Alkan.(176) It was found that kaolinite was a strong adsorbent with high retention capacity. Langmuir adsorption isotherm was observed. The adsorbed protein amounts was established as 0.131 mg α-lactalbumin , 0.018 mg β-lactoglobulin and 0.052 mg BSA for per mg kaolinite.(100)

3.6 Nanocomposite Hydrogels

Nanofillers are added into hydrogel matrices to enhance mechanical properties and to tune drug release profiles. In a study, halloysite nanotube (HNT, $Al_2Si_2O_5(OH)_4.nH2O$) was used as a nanofiller for nanocomposite hydrogel production to attain tunable mechanical properties and drug release behavior.(177) It is known by virtue of the previous literature studies that HNT is a promising agent for drug/protein delivery due to its tubular structure.(178) As the outputs of the work, BSA release was determined for hydrogels prepared with various polymers-TPT (oligo (trimethylene carbonate)-poly(ethylene glycol-oligo(trimethylene carbonate) diacrylate (TPT), AG (alginate sodium). According to the results of the study, sodium alginate had no significant impact on the drug release. However, the addition of HNT contributed to prolonged release of BSA from the hydrogels. The major effect of sodium alginate was on transport mechanism type. It is demonstrated that the transport mechanism can be set by adjusting the HNT and AG amount in the hydrogel. The AG containing hydrogels had Fickian diffusion and Case II transport with both diffusion and chain relaxation.

3.7 Laponite Containing Hydrogels

Laponite is a nanosilicate with formula $Na^{0.7+}[Mg_{5.5}Li_{0.3}\text{-}Si_8O_{20}(OH_4)]^{0.7}$ that forms disk shaped particles. This synthetic clay can be classified in 2:1 smectites class composed of two tetrahedral layer at the top and bottom and one octahedral layer

between the tetrahedral layers as shown in the Figure 3.10. It is also a kind of hectorite clay.

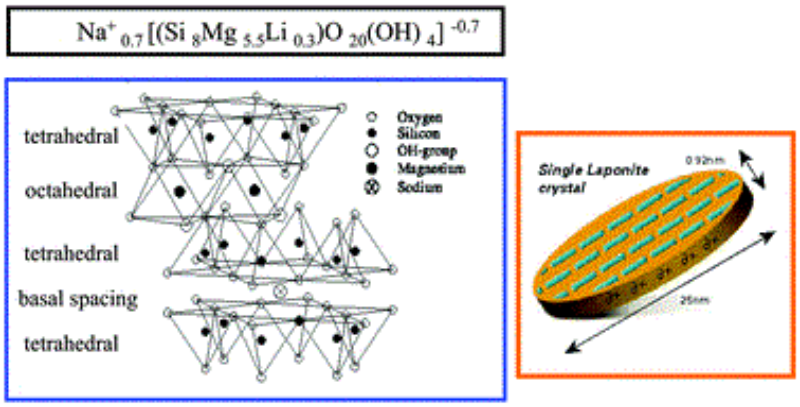

Figure 3.10 Molecular structure and dimensions of laponite.(179)

A novel study about use of Laponite in hydrogel formation was published in 2011. The anionic capability provides interaction with cationic molecules electrostatically. As a result, silicate nanodisks can form gel.(180)

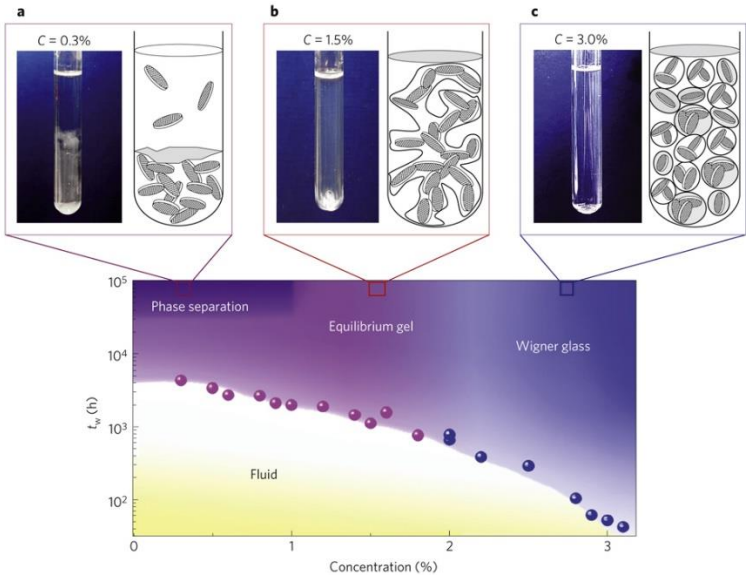

Figure 3.11 Gelation ability of laponite for 1.5% and 3.0% concentration.(180)

Laponite clay is used in biomedical applications with various aims as crosslinker or drug carrier. Figure 3.11 shows gel formation of laponite with 0.3%, 1.5% and 3.0% ratios.

Laponite reinforcement increases the mechanical abilities of the nanocomposite hydrogels. It was demonstrated that the Laponite addition into hydrogels provides enhanced toughness of the samples.(181–183) Yet, high amount of nanoparticle loading in weight between 5% and 10% was required for the remarkable material property change. However, the significant enhanced material properties can be provided for relatively low Laponite content in 1-3% (w/w) in a study.

It was reported that enhanced release of protein was provided with Laponite. Controlled cell adhesion and mineralization was targeted to achieve by using Laponite as crosslinker in the poly ethylene oxide base nanocomposite. The integration of PEO and Laponite provided controlled chemical and physical properties. Enhanced properties achieved due to the charged and degradable clay.(184)

Another work showed that laponite has the edge on montmorillonite due to its smaller particle size, dimensional uniformity in dispersion and higher stability.(185,186) There has been an interest on Laponite clay for the usage of drug carrier agents. In the work, tetracycline was used for the treatment of periodontal disease. The interaction mechanism between tetracycline and Laponite was obtained for different pH and concentration values. The release profile of the substrate was enhanced with clay addition. (185)

Laponite and dopamine methacrylamide (DMA) containing polyacrylamide (PAAm) hydrogels were synthesized. Increase laponite and DMA amount results in reduced water content and enhanced material properties as the outputs of the work. Additionally, it was sufficient that only laponite loading into gels toprovide moderate alterations in properties.(187)

Laponite was used for obtaining improved viscoelastic properties containing poly ethylene oxide (PEO) and chitosan.(48) In the study, Laponite were used as cross linker and providing the interaction between PEO and chitosan.

Nanocomposite hydrogel was produced with acrylamide, carrageenan and Laponite RD. Laponite RD was used as cross linker. There was not a significant change in

swelling with laponite addition between 2.7% and 12.5% wt. while laponite addition over 12% wt. leaded to decrease in swelling index due to limited macroradical movement.(188)

3.7.1 Toxicology and Degradation Properties of Laponite

Chemical composition and degradation products of Laponite are analogous with bioactive materials. It is demonstrated that the degradation products are Na^+, $Si(OH)_4$, Mg^{2+}, Li^+ which are nontoxic.(189) Cancer treatment was done with cytotoxic chemotherapy agents via intravenous route. Performance of the therapy was determined according to secondary toxicity and drug loading capacity.(190) Thus, nanoparticle containing injectable materials are used to reduce systematic toxicity.

Laponite was used as nanocarrier mainly due to the interlayer spacing of clay, which ensures high retention capacity with active substances.(25,191) Another reason point is that for choice of Laponite for studies was that Laponite can be degraded into nontoxic products *in vivo*.(5)

Doxorubicin interacted with Laponite for cancer treatment in a salient work.(192) The previous study of the group showed that Laponite did not possess in vitro cytotoxicity.(192) Laponite-doxorubicin complexes were examined in terms of antitumor efficacy and toxicology. (193) Magnesium ions and doxorubicin were analysed in different organs with blood and histology examinations as shown in Figure 3.12.

It is apparent from the information supplied that Laponite-doxorubicin complexes had lower systematic toxicity than doxorubicin. Magnesium amount was obtained for certain organs after treatment in selected time intervals, which are given in the Figure 3.13. Bio distribution results revealed that the level of magnesium was relatively low after 45 days. Additionally, there did not observe significant organ damage or abnormalities in mice.

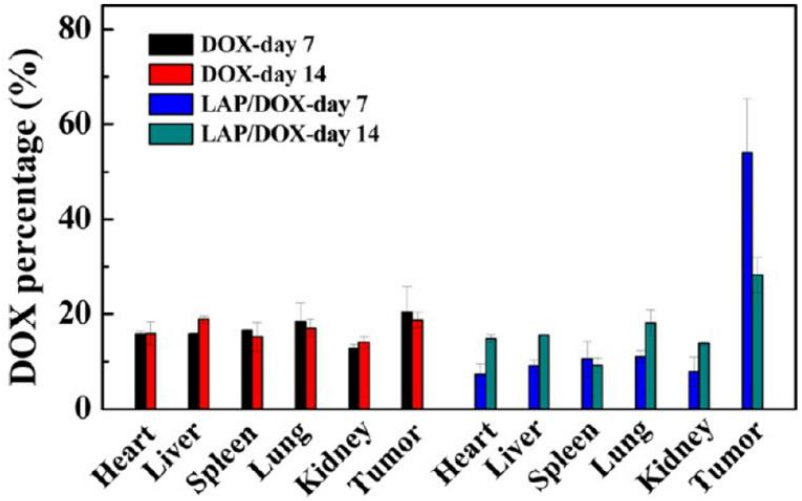

Figure 3.12 Bio distribution of doxorubicin and Laponite-doxorubicin complexes in certain organs after 7 days and 14 days. (193)

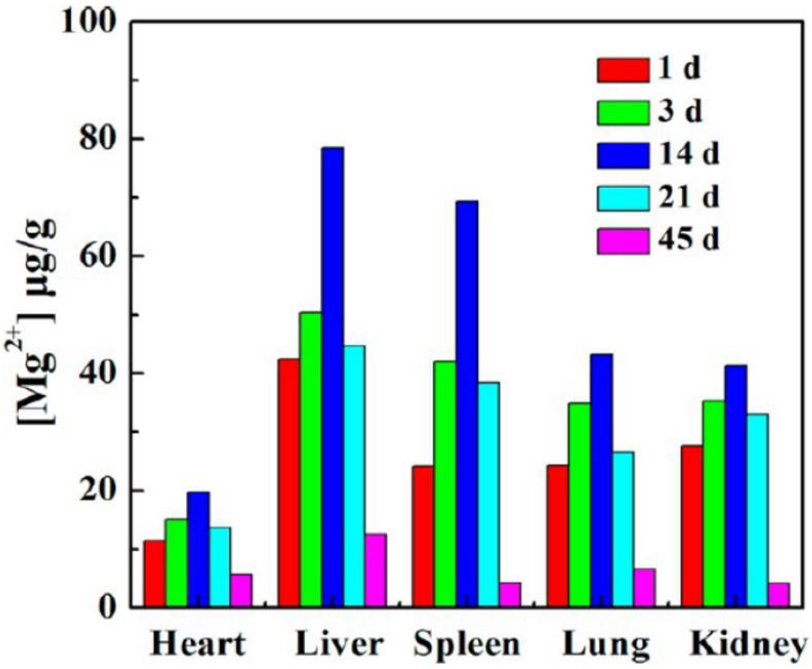

Figure 3.13 Bio distribution of magnesium ions in certain organs at selected time. (193)

Li *et al.* concluded that Laponite-doxorubicin provided reduced tumor volume, increased drug loading and increased animal survival.(193) It was indicated that negatively charge surfaces would initiates blood clot formation. Therefore, Laponite

content was kept below 2% wt. for laponite containing nanocomposite hydrogel production.(194)

Laponite-doxorubicin alginate was generated as nanocarrier.(195) The nanohybrid demonstrated that high doxorubicin loading capacity with pH sensitive sustained release of drug. It was conducted that laponite is cytocompatible according to cell culture tests.(195) Lastly, Chang *et. al.* studied on enhanced mechanical properties with Laponite addition along with cell culture studies. It was demonstrated that Laponite did not show harmful effects on cells.(182)

3.8 Motivation of the Work

A successful drug development involves accurate substance selection, transmittance of therapeutic agents into target without decomposing and releasing the substances at a desired rate. All steps must be handled appropriately to obtain a comprehensive therapy. It is required that after delivery of protein into tissues effectively, bio macromolecules are released in a controlled way. The objective is that design the drug delivery system to deliver biomacromolecules into target tissue successfully and manipulate the release profile of the protein by preventing uncontrolled high or low release rates.

The literature was examined for the evaluation of the current applications of protein delivery techniques. Since considerable effort is required for the delivery to proteins into target tissue by oral administration, intravenous route is more convenient for delivering these agents. Hydrogels are by far the most used materials in biomedical industry due to biocompatibility with tissues.

Equally importantly, though, the reliability and biocompatibility of the developed formula should be considered. It should not lead to host immune responses and toxic effects. Thus, there is a tendency to use the natural polymers as matrix components. Yet, it is more challenging to govern the degradation behaviour and release mechanism.

Another issue is the weak interaction between polymer and protein which is confronted in release systems. Nanotechnology can be applied in the development of drug carrier clays, which are used to protect drugs. There have been studies about adsorption of proteins onto inorganic particles to enhance stabilization or interaction.

This work consists of the combination of two separate subjects with the aim of maintaining controlled release of proteins. There are systems related with nanocomposite hydrogels to improve hydrogel characteristics. However, there is a gap related with generation of nanocomposite injectable hydrogel model which assures an adsorption mechanism between protein and clay to enhance release profiles in hydrogels. The aim of the study is to generate a system which supplies patient compliance, bio reliability along with performance. The prominent point of the work is about the way of incorporation of protein into biodegradable injectable hydrogel matrix. It was thought that the adsorption process contributes to release of protein in a controlled manner. In addition to this, protein loading capacity can be increased into hydrogel. Burst release resulted from weak interaction between protein and polymer can be reduced.

In this study, model protein BSA was adsorbed into Laponite XLG under various conditions. Alginate based injectable hydrogels were prepared with hydrazone chemistry. These hydrogels were prepared to contain polymer precursors with BSA, Laponite XLG, or BSA-Laponite XLG. The literature studies section highlights the recent works about injectable biodegradable nanocomposite hydrogels for biomedical applications along with adsorption studies. There were no studies in literature on BSA-Laponite XLG interaction. In addition, alginate based hydrogels with hydrazone chemistry that are composed of oxidized alginate and alginate hydrazide are not reported. In conclusion, a synergetic work which containing both studies was done to enhance drug release profile.

CHAPTER IV

EXPERIMENTAL

4.1 Materials

Protein-Clay Interaction Experiments

The materials used in protein-clay interaction experiments are as follows:

- *Laponite XLG* was kindly supplied by BYK Additives & Instruments, Germany.
- *Bovine serum albumin* (BSA) was used as a model protein and purchased from Biowest.
- *Phosphate buffer* (PB) was prepared from *potassium dihydrogen phosphate* (KH_2PO_4) and *dipotassium hydrogen phosphate* (K_2HPO_4), which were obtained from Merck Millipore.
- *Hydrochloric acid* (HCl) and *sodium hydroxide* (NaOH) respectively from Sigma-Aldrich and Merck Millipore were used to prepare solutions for adjusting the pH value of PB.
- *Sodium azide* was purchased from TCI and used for preventing bacterial growth in PB.
- Ultrapure water was used in all experimental stages.

Hydrogel Formation Experiments

Below are the materials used for the hydrogel formation:

- *Sodium alginate* from Aldrich in the molecular weight range between 120 000 g/mol and 190 000 g/mol, was used in the gel formation experiments.
- *Adipic acid dihydrazide* (ADH), *1-ethyl-3-3-dimethylaminopropyl carbodiimide hydrochloride* (EDC), and *N-hydroxysuccinimide* (NHS) were purchased from TCI and Sigma Aldrich and used in the hydrazide modification of sodium alginate.
- *Sodium periodate* ($NaIO_4$) and *Ethylene glycol* were supplied from Sigma Aldrich for aldehyde modification studies.
- *tert-Butyl carbazate* (tBC) and *2,4,6-trinitrobenzenesulfonic acid* (TNBS) from Sigma Aldrich were used in determination of modification degree in the carbazate assay.
- *Bradford reagent* was supplied from Sigma Aldrich for protein concentration determination assays.
- *Acetate buffer* was prepared using *acetic acid* and *sodium acetate* while *borate buffer* was made from *boric acid* and *sodium tetraborate*.

4.2 Protein Clay Interaction

4.2.1 Protein Clay Interaction Assay Parameters

BSA was used as a model protein for studying protein clay interaction. Laponite XLG was used as a clay mineral. The interaction medium was chosen as phosphate buffer at selected molarity (0.01 M and 0.05 M) with different pH values as 5.5 and 7.4. Since the most effective parameter on adsorption is known as the protein to clay ratio, the weight ratio was chosen between 0.33 and 10 protein: clay. Minimum 5 samples were prepared with the same conditions for each test set for reliability. Finally, interaction time was chosen as 18 hours.

4.2.2 Protein-Clay Adsorption Experiments

BSA was interacted with Laponite XLG for various conditions such as pH, weight ratio and molarity. The main steps were described in Figure 4.1. To summarize, after dissolving solutions, BSA solution was added into Laponite XLG solution drop by

drop. It was waited about 18 hours to complete interaction. Then, interacted sample was centrifuged to separate solid complexes and noninteracted solution. Solid samples were dried for structural analysis while supernatant solution was tested for the determination of protein amount.

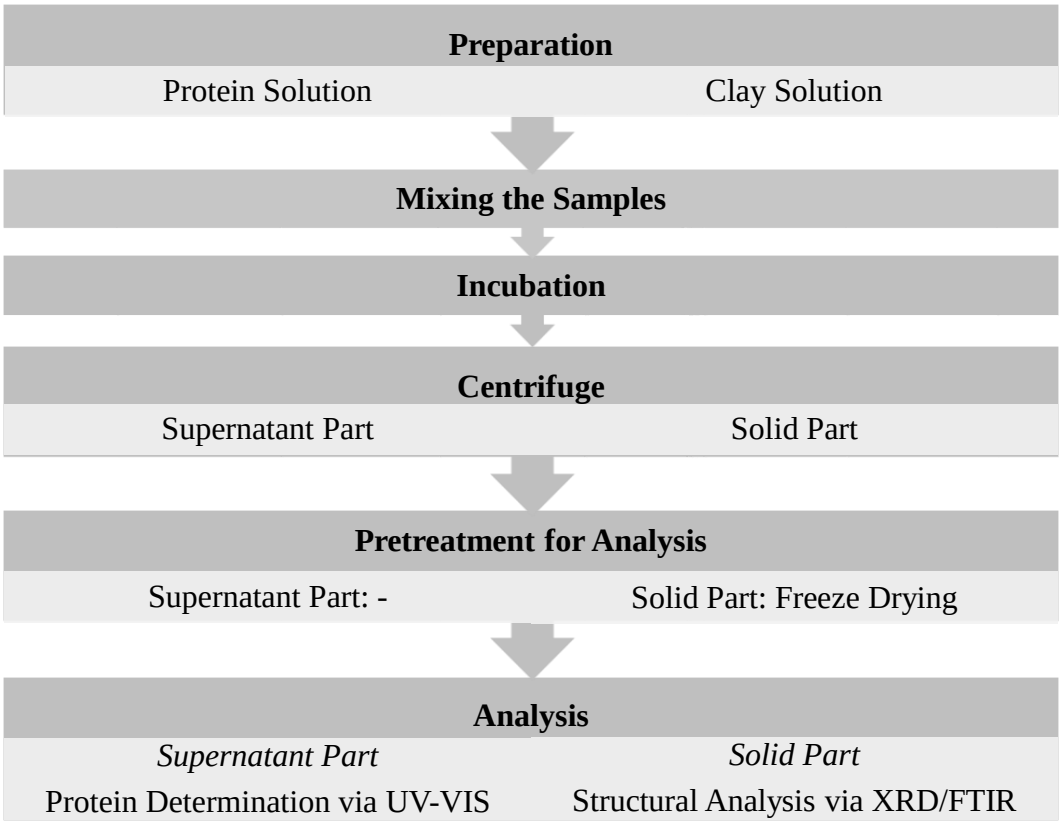

Figure 4.1 Summary of BSA-Laponite XLG experimental procedure.

BSA solution was prepared in phosphate buffer (PB) with desired pH (5.5 or 7.4) and then incubated about 1.5 hours at 4 ^{o}C to provide easy dissolution. Laponite XLG was added to distilled water and mixed about 1.5 hour by using magnetic stirrer at room temperature. Afterwards, Laponite XLG solution was added to the 0.05 M PB solution or kept in distilled water. Protein solution was then added drop by drop into clay solution with desired ratio. The final molarity was set equal for each samples within a set. The complex was then placed into a refrigerator kept at 4 ^{o}C at least for 18 hours. At the end of the interaction time, each solution was

centrifuged at 8 000 rpm for 20 minutes. After the completion of the centrifuge step, the supernatant part and solid part were separated.

The adsorbed BSA percentage, adsorbed BSA amount for per Laponite XLG was determined by measuring the absorbance of supernatant part with a UV-VIS spectrophotometer. The solid part was freeze-dried for XRD and FTIR analysis.

Preparation of Calibration Curve Samples

In order to calculate the adsorbed protein amount with UV analysis, the calibration curve was prepared for quantification of non-modified/supernatant part in the complex. BSA samples were prepared between 0.2 and 1.5 mg/ml to constitute a calibration graph. For each concentration minimum 4 samples were prepared. The prepared samples were kept at 4 ^{o}C for 18 hours in the refrigerator and then centrifuged at 8000 rpm for 20 minutes to maintain same experimental conditions. After completion of the previous steps, the absorbance of the samples was measured by UV spectrophotometer at 280 nm and a calibration curve graph was attained.

The XRD and FTIR analysis of the produced complexes were given in the characterization section.

4.3 Hydrogel Production

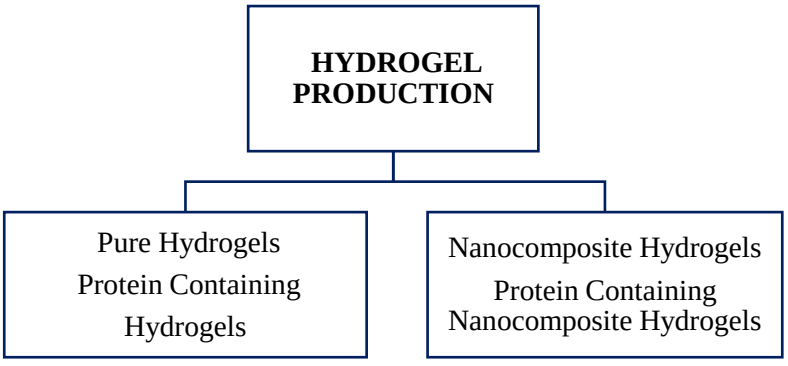

Figure 4.2 Classification of hydrogel production with pure, nanocomposite, protein containing and protein containing nanocomposite.

Hydrogel production can be classified in two parts. Pure hydrogels and protein containing hydrogels were primarily prepared with biodegradable polysaccharides. Nanocomposite and protein adsorbed nanocomposite containing hydrogels were generated as a final step.

Given are figures concerning production techniques of alginate based hydrogels. Alginate was shown as A symbol, alginate aldehyde with A-A while A-H implied alginate hydrazide.

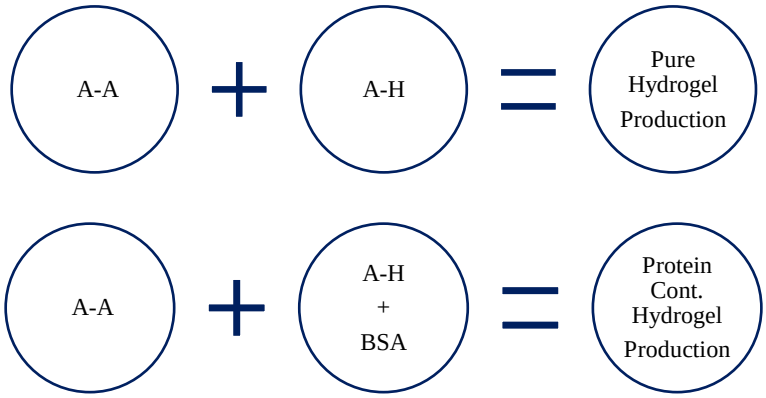

Figure 4.3 Alginate based hydrogel production schematic for pure and protein containing types.

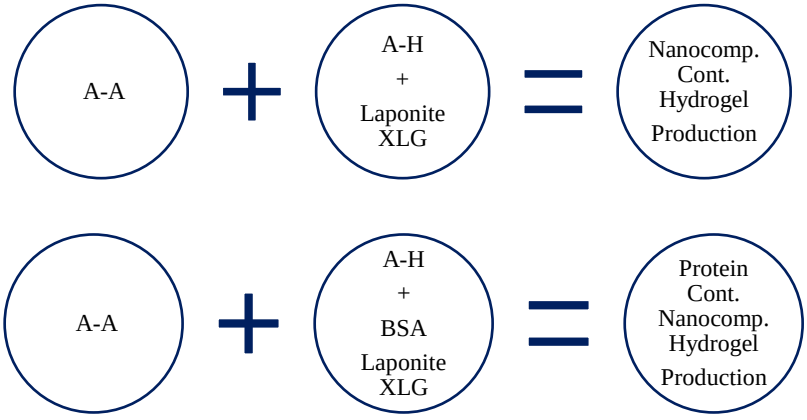

Figure 4.4 Alginate based hydrogel production schematic for nanocomposite and protein containing nanocomposite types.

Figure 4.3 and Figure 4.4 provide basic schematic of alginate based hydrogels with addition of protein, clay and protein-clay complexes.

4.4 Production of Alginate Based Hydrogels (Hydrazone 01)

Hydrazone bonded hydrogels were formed via the reaction between Alginate aldehyde (A-A) and alginate hydrazide (A-H). The formation procedure consists of 5 main steps as follows:

- Oxidation of alginate
- Hydrazide modification of alginate
- Preparation of pure and protein containing precursors
- Preparation of nanocomposite and protein adsorbed nanocomposite precursors
- Hydrogel formation

4.4.1 Oxidation of Alginate

The oxidation procedure of alginate includes reaction, purification and drying processes. There have been two techniques for the aldehyde group addition into sodium alginate. Although both methods have the same reaction application, the purification steps are different from each other. Technique 1 was used in most of the modification studies. The summary of the oxidation procedure is below:

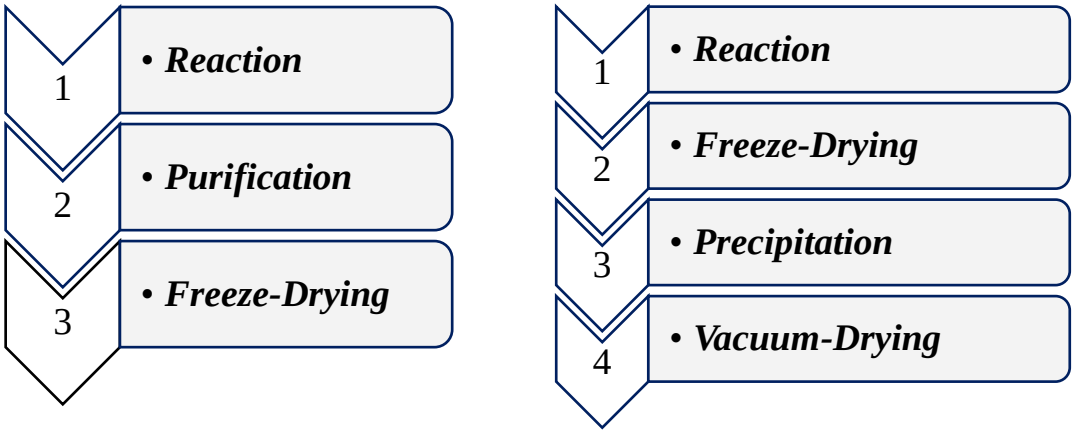

Figure 4.5 Oxidation of alginate – Technique 1 (left side) and Technique 2 (right side).

4.4.1.1 Oxidation of Alginate (Technique 1)

The oxidation study done by Mooney was used for the oxidation of sodium alginate with different degree of substitution values.(146) The procedure was described for 50% theoretical degree of substitution as followed:

1500 mg alginate was added slowly to distilled water to give 10 mg/ml concentration. The mixture was then mixed with a magnetic stirrer. Meanwhile, 809 mg sodium periodate was also dissolved in 30 ml distilled water and wrapped with aluminium foil due to the light sensivity of sodium periodate ($NaIO_4$). The mixture was stirred using a magnetic stirrer. After it was waited for an hour for dissolution of both materials, sodium periodate solution was added dropwise to the erlenmeyer flask containing sodium alginate solution, which was also wrapped with aluminum foil. The solutions were mixed for 24 hours in the dark. Ethylene glycol was added to inactivate unreacted $NaIO_4$, which presented in the reaction mixture at the end of the reaction duration. The solutions were allowed to stir for another an hour. The reaction was completed at the end of the duration. Afterwards, reaction product was purified.

A dialysis tubing with 3.5 kDa M_WCO was used for purification of the reaction product. Firstly, the membrane tubing was immersed in distilled water to wet about 30 minutes. Afterwards, the reaction product was poured into tubing and both ends were clipped. The membrane tubing was placed into a beaker having 2 liters of water. The water was exchanged at least 3 times in a day in the beaker. The purification application proceeded for 3 days.

After the completion of the dialysis, the purified materials were transferred to the vortex tubes or borosilicate glass for drying. Samples were frozen by using dry ice or liquid nitrogen to place in freeze dryer. The specimens were dried using a freeze dryer for 3 days. The dried samples were stored at -20 ^oC for further applications and tests.

4.4.1.2 Oxidation of Alginate (Technique 2)

Since the reaction step of oxidation process is common for both techniques, reaction procedure is also valid for Technique 2 given in the "Oxidation of alginate (Technique 1)" part.

The reaction product was transferred to the vortex tubes or borosilicate glass for the drying application. Samples were freeze-dried for 3 days.

The dried materials were then dissolved in distilled water. Then, approximately 2 ml alginate aldehyde solution was added into 20 ml ethanol drop by drop. The solution was centrifuged at 8000 rpm for 20 minutes. The centrifuge application was repeated at least 3 times. The supernatant part was pulled and solid part was taken.

After supernatant part was separated, solid part was dried at vacuum oven. The final dried product was stored at -20 ^{o}C for further applications.

4.4.2 Hydrazide Modification of Alginate

The hydrazide modification was carried out following the procedures in the literature conducted by Tan *et al*. and Gomez *et al*. (167,168)

The hydrazide modification of alginate, also includes reaction, purification and drying steps as in aldehyde group modification. Since methodology of Technique 1 was used most of the modification studies, the procedure of hydrazide modification study was described in accordance with Technique 1. However, Technique 2 can also be applied. The hydrazide modification procedure is given below:

Hydrazide group addition into alginate was achieved by reacting the polysaccharide with ADH and EDC with various substitution degrees. Firstly, 50 mg alginate was dissolved in distilled water whereas 1000 mg ADH were added into distilled water slowly. Then, both solutions were stirred using a magnetic stirrer to increase the dissolution rate. After providing homogeneous form of both solutions, ADH solution was added into alginate solution and it was waited to reach a homogeneous appearance by mixing at 400 rpm using a magnetic stirrer. Then, pH of the solution was adjusted between 4.9 and 5.2 by adding 0.1 M HCl.

80 mg EDC and 70 mg NHS were dissolved in water and then added to polymer solution slowly. After mixing rate of the magnetic stirrer was increased, 0.1 M HCl solution was added to the mixture for adjusting pH value to 4.7. pH value of the solution was checked in every 15 minutes for the first 4 hours. The pH of solution was set between 4.7 and 5.0 during 24 hours. At the end of the duration, pH adjustment was not done and the reaction product was prepared for purification step. The same purification and drying procedure was used described in "Oxidation of alginate (Technique 1)".

4.4.3 Preparation of Hydrogel Precursors

Pure hydrogel samples contain only polymer precursors–alginate aldehyde and alginate hydrazide to form hydrogels via hydrazone bond formation.

Precursors were dissolved in PB (0.05 M and pH 7.4). Alginate aldehyde was dissolved in PB for 2 hours to obtain homogeneous fluid. On the other hand, alginate hydrazide was dissolved in PB with same properties overnight for pure hydrogel samples.

Protein containing specimens were prepared with polymer precursors along with BSA solution. BSA was dissolved in buffer and then added to the hydrazide solution, which was waited overnight, for the preparation of protein containing samples. The amount of the alginate hydrazide was the same for pure and protein containing hydrogel samples. In addition, volume of the alginate hydrazide solution was kept equal in preparation of pure hydrogels and protein containing hydrogels.

4.4.4 Preparation of Precursors for Nanocomposite Hydrogels

Alginate aldehyde was dissolved in PB (0.05 M and pH 7.4) for 2 hours to obtain a homogeneous solution. On the other hand, alginate hydrazide was dissolved in PB buffer overnight. Laponite XLG was dissolved in distilled water for the preparation of nanocomposite containing samples. A predetermined amount was taken and added into alginate hydrazide solution-waited overnight. The solution was mixed for another an hour for complete dissolution. The final molarity and pH value was set as 0.05 M and pH 7.4 for alginate hydrazide and Laponite XLG mixture.

In a similar manner, BSA adsorbed Laponite XLG was taken from the sample after 18 hours duration and then added slowly into alginate hydrazide solution, which was waited overnight. One more hour was waited for obtaining homogeneous solution of alginate hydrazide and BSA-Laponite XLG complex.

4.4.5 Hydrogel Formation

Hydrogels were synthesized by mixing precursors with selected polymer concentration and volume, nanocomposite weight ratio and protein weight ratio in precursors with different DS values. Gel formation was done at room temperature.

Pure hydrogels were synthesized by mixing of alginate aldehyde and alginate hydrazide solutions. Protein containing hydrogels were prepared via mixing of alginate aldehyde and alginate hydrazide-BSA precursors. Alginate based nanocomposite hydrogels were generated from alginate aldehyde and alginate hydrazide-Laponite XLG. Lastly, the mixture of alginate aldehyde and alginate hydrazide-BSA-Laponite XLG complex were formed protein containing nanocomposite hydrogels.

AA code were used to identify pure hydrogels and AAP was defined as protein containing hydrogel samples. AAN code was used to refer to nanocomposite containing hydrogels with AANP code, which was defined as protein containing nanocomposite hydrogel samples.

4.5 Characterization

4.5.1 UV-VIS Spectrophotometer

UV-VIS spectrophotometer was used for the determination of the adsorbed BSA amount. Measuring of supernatant concentration was presented the non-interacted BSA amount in the BSA-Laponite XLG complexes. The protein determination analysis was conducted using a Shimadzu 2550 double monochromator UV-VIS spectrophotometer. Measurements were taken at 280 nm. Each measurement was done for 4 times and each sample set had minimum 5 samples.

In addition, the protein release tests were done via Bradford Assay at 595 nm. Each measurement was done for 3 times and each sample set had minimum 5 samples.

4.5.2 Carbazate and TNBS Assay

Aldehyde groups react with hydrazide and form a hydrazone bond. In a similar manner, aldehyde groups react with carbazates to constitute carbazones. The degree of substitution values of aldehyde and hydrazide modified polymers were determined with the carbazate-TNBS Assay by means of this phenomena.

The number of aldehyde groups in polymers were determined via a modified TNBS Assay. The method was modified from the procedure taken by Sivakumaran and Hoare for obtaining aldehyde group modification for alginate.(94) Alginate aldehyde was dissolved in sodium acetate buffer. After complete dissolution, tBC was added into aldehyde solution and then waited for 24 hours. At the end of time, a little amount was pulled for adding borate buffer. TNBS solution was then added into borate buffer and reacted more 2 hours. Final solution was diluted with HCl solution with 1:1 ratio. Finally a minimal amount was added into HCl solution. DS values of alginate aldehyde (A-A) components were detected by measuring of the composed complex absorbance at 334 nm by UV-VIS spectrophotometer.

The TNBS Assay for aldehyde determination described above was valid without carbazate addition for the hydrazide group detection. Modified polymer was reacted without tert-Butyl carbazate and hydrazide modification percentage was lastly obtained with this technique.

The detailed procedure for carbazate-TNBS Assay procedures are found in the Appendix B.

4.5.3 Bradford Assay

Bradford Assay was used for the determination of released BSA from the hydrogel matrix. Detection method is based on measuring of the composed complex absorbance at the selected wavelength by using UV-VIS spectrophotometer. The micro assay technique was used for the determination of protein in the range between 1 µg and 10 µg. Bradford Assay procedure is given in Appendix C in detail.

4.5.4 Swelling Tests

The initial hydrogel weight was determined and recorded as W_o at time zero. Afterwards, the hydrogels were immersed in PB (0.05 M and pH: 7.4) at 37 ^{o}C. The medium was refreshed for obtaining hydrogel weight in chosen time intervals and weight of hydrogel at selected time W_t value was recorded. The medium was refreshed at each measurement point.

Degree of swelling was determined using the following formula:

$$\text{Swelling Index} = \frac{W_t}{W_o} \quad (2)$$

in which:

W_t: Hydrogel weight at selected time, mg

W_o: Hydrogel weight at formation, mg

4.5.5 Fourier Transformed Infrared Spectroscopy (FTIR-ATR)

FTIR analysis was mainly used for obtaining the alterations in the structures after modification studies. FTIR analysis was done to determine the structure of alginate (A) and modified alginate materials, which are alginate aldehyde (A-A) and alginate hydrazide (A-H), with different modification degrees. Additionally, FTIR spectroscopy was used to specify the adsorption between BSA and Laponite XLG clay with produced different corresponding weight ratios.

Perkin Elmer Spectrum Two model FTIR spectroscopy with ATR was used in analysis. The composition of polymers and hydrogels were confirmed in the range between 500 cm^{-1} and 4000 cm^{-1} accumulated of 256 scans with 4 cm^{-1} resolution while the protein-clay samples were detected in the same range accumulated of 64 scans with 4 cm^{-1} resolution.

4.5.6 XRD Analysis

XRD analysis was done for the determination of structure of protein clay complexes. The analysis was conducted at METU Central Laboratory from 2^o to 70^o with 1^o/min for clay samples and complexes. In addition, the complexes were detected from 2^o to 15^o with 0.1^o/min scan rate.

CHAPTER V

RESULTS AND DISCUSSION

The results of the studies are comprised of four main section, which are interaction of BSA and Laponite XLG, preliminary studies about hydrogel formation with imine and hydrazone chemistry, generation of alginate based hydrogels with hydrazone chemistry and production of protein containing alginate based nanocomposite hydrogels.

5.1 Interaction of BSA and Laponite XLG

An adsorption study was conducted between BSA and Laponite XLG to enhance the drug loading capacity of protein. It was also presumed that a better release mechanism from hydrogel matrices is provided due to increased interaction of BSA-Laponite XLG complexes. Interaction between BSA and Laponite XLG was investigated for various conditions. Main parameters that influence the adsorption of protein onto the clay were selected as pH, weight ratio of BSA to Laponite XLG (BSA/Laponite XLG) and molarity of the medium.

Since the produced complexes are planned to be used in biomedical applications, the interaction studies were done for pH values of 5.5 and 7.4, which are correspond to the pH of skin and blood respectively. In addition, the pI point of BSA is known as approximately 4.7.(196) The influence of proximity to the pI point on adsorption was also investigated. The weight ratio of BSA to Laponite XLG was chosen between 0.33 and 10 to detect optimal conditions in terms of adsorption percentage

and adsorption capacity. Since produced complexes were to be used in the formation of protein containing nanocomposite hydrogels, adsorption profiles were generated based on weight ratio to obtain suitable point selection for the production of complexes with desired BSA to Laponite XLG ratio. Adsorption process is dependent on incubation time. Moreover, the time which requires complete adsorption of BSA is influenced on clay type. For instance, adsorption of BSA was nearly complete after 10 hours on sepiolite surfaces and 8 hours on kaolinite clay minerals whereas only 3 hours were sufficient for the complete adsorption of BSA on perlite.(176) A few studies were conducted to obtain the incubation time, in which adsorption was finalized for BSA-Laponite XLG mixtures. It was not seen any difference in adsorption data when experimented the incubation time as 18 hours and 24 hours for BSA-Laponite XLG complexes. Therefore, Interaction time was selected as 18 hours to reach saturation for each test set.

5.2 Adsorption of BSA onto Laponite XLG under Different Conditions

After BSA-Laponite XLG mixture was waited for 18 hours at 4 ^{o}C, solution was centrifuged. The interacted solid part and non-interacted supernatant part was separated. Adsorbed BSA amount was calculated by determining the protein concentration in the supernatant via UV-VIS spectroscopy performed at 280 nm, which is based on the detection of tyrosine and transient receptor potential (TRP) with relatively low content of phenylalanine and disulphide bonds.(197)

Performance of adsorption was evaluated with adsorption percentage expression, which is defined as the percentage ratio of adsorbed protein amount in clay surface to initial protein amount in interaction medium while adsorption capacity was expressed as adsorbed protein amount for per clay amount. It was investigated the effects of weight ratio, pH and molarity on adsorption in regard to adsorption percentage and adsorption capacity.

Impact of weight ratio on adsorption was examined for the samples prepared using 0.05 M phosphate buffer at pH 7.4. In a set of experiments (Set A), the concentration of Laponite XLG and BSA was varied whereas, in another set (Set B) clay

concentration was kept constant with *variable BSA concentration*. The properties of the sample sets are in the Table 5.1.

Table 5-1 Concentration of BSA, Laponite XLG and weight ratio in interaction medium of the samples in the Set A and Set B.

Sample Code	Laponite XLG Concentration (mg/ml)	BSA Concentration (mg/ml)	Weight Ratio (mg BSA/mg Laponite XLG)
A	6.25	4.17	0.67
	5.77	5.77	1.00
	5.36	7.14	1.33
	4.69	9.38	2.00
	3.75	12.50	3.33
	3.00	15.00	5.00
B	1.00	0.33	0.33
	1.00	0.50	0.50
	1.00	0.67	0.67
	1.00	1.00	1.00
	1.00	1.67	1.67
	1.00	2.50	2.50
	1.00	6.67	6.67
	1.00	10.00	10.00

Effect of variable Laponite XLG concentration on adsorption was investigated by comparison of A and B sample sets in terms of percentage adsorption and adsorption capacity. From the calculated adsorption percentage values in the Table 5.2, it is evident that adsorption percentage decreased with increasing ratio for both test sets. Almost all BSA macromolecules were adsorbed at Laponite XLG surface for 0.33 weight ratio. Adsorption capacity increased up to 2.5 weight ratio, then decreased to 0.57 mg/mg adsorption capacity for 6.67 weight ratio. Adsorption capacity was evaluated with literature works. BSA adsorbed on various clay mineral with 0.22 for sepiolite and for 0.029 kaolinite in terms of adsorption capacity (mg adsorbed BSA/mg clay minerals).(176)

Table 5-2 Calculated adsorption percentage and adsorption capacity values based on weight ratio of samples in the Set A and Set B.

Sample Code	Weight Ratio (mg BSA/mg Laponite XLG)	Adsorption Percentage (%)	Adsorption Capacity (mg BSA/mg Laponite XLG)
A	0.67	79.0±0.07	0.53±0.01
	1.00	58.7±0.25	0.59±0.01
	1.33	47.3±0.17	0.63±0.01
	2.00	35.6±0.65	0.71±0.01
	3.33	23.0±0.97	0.77±0.03
	5.00	17.7±0.57	0.88±0.03
B	0.33	98.4±3.11	0.33±0.01
	0.50	82.7±1.62	0.41±0.01
	0.67	73.7±0.93	0.49±0.01
	1.00	61.3±1.02	0.61±0.01
	1.67	41.9±1.30	0.70±0.02
	2.50	29.6±1.03	0.74±0.03
	6.67	8.56±4.20	0.57±0.28
	10.00	7.08±1.40	0.71±0.14

When percentage adsorption values were plotted to weight ratio, logarithmic relation was obtained between percentage adsorption and weight ratio. An equation was fitted as $y=-29.76\ln(x)+60.366$ and $r^2=0.96$ for Set A. $y=-27.65\ln(x)+62.257$ logarithmic equation was attained with $r^2=0.98$ for Set B. x and y axis showed respectively weight ratio and adsorption percentage.

Additionally, Figure 5.1 shows the similarity between the adsorption percentage curves of A and B. The data were fitted with logarithmic equations. Both lines were coherent with each other. However, there were deviations at higher weight ratios from the fitted equation, which can be resulted from reduced sensitivity in UV measurement at higher weight ratios.

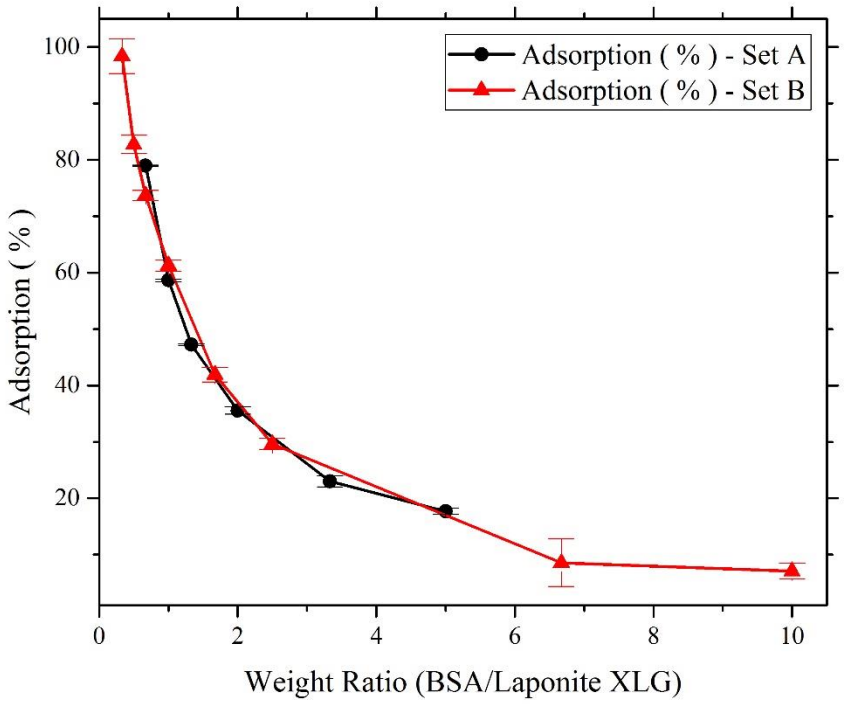

Figure 5.1 Adsorption percentage profiles based on weight ratio for samples in the Set A and Set B, which interacted in 0.05 M PB at pH 7.4.

Relatively high standard deviation was also observed for the samples with high BSA to Laponite XLG ratio, which was the probable reason of the alteration from fitted line for higher corresponding ratios. When weight ratio value was lower than 2, attained adsorption percentage profiles were nearly the same for both sample sets. Thus, it was concluded that weight ratio has significant effect on adsorption. Concentrations of BSA and Laponite XLG, which are presented in the interaction medium, had minor influence on adsorption process.

Adsorption capacity was expressed as mg adsorbed BSA amount for per mg Laponite XLG. Logarithmic increase was provided up to 2.5 weight ratio for B samples and 3.33 weight ratio for A samples as shown in the Figure 5.2.

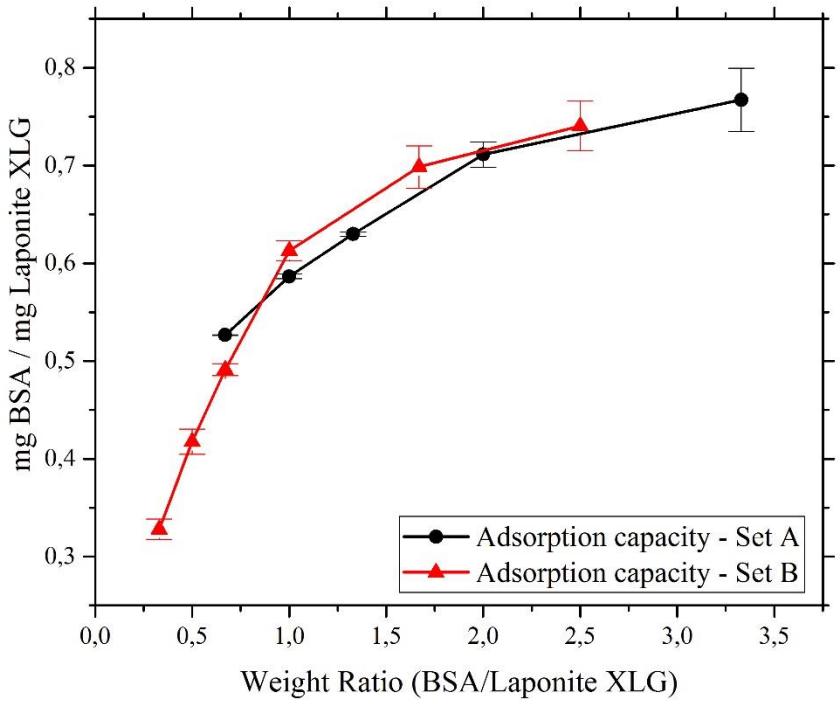

Figure 5.2 Adsorption capacity profiles based on weight ratio for samples in the Set A and Set B, which interacted in 0.05 M PB at pH 7.4.

Protein charge varies with pH, which manipulates adsorption. Influence of pH on adsorption was tested with pH values of 5.5 and 7.4 for samples in set B. It is known that BSA is negatively charged for both pH values.

Adsorption percentage and adsorption capacity values were given in Table 5.3 with respect to pH. Among these pH values, adsorption percentage was higher for each data point at pH 5.5. Similarly, higher adsorption capacity was acquired for all samples prepared at pH 5.5 due to the closeness to the pI point of BSA. The highest difference in adsorption values was seen at 0.67 weight ratio among samples had same weight ratio while minimum difference between adsorption values were seen at 0.33 weight ratio.

Table 5-3 Influence of pH on adsorption percentage and adsorption capacity based on weight ratio.

Weight Ratio (mg BSA/mg Laponite XLG)	Adsorption Percentage (%)		Adsorption Capacity (mg BSA/mg Laponite XLG)	
	pH: 5.5	**pH:7.4**	**pH: 5.5**	**pH:7.4**
0.33	98.1±1.85	98.4±3.11	0.33±0.01	0.33±0.01
0.50	99.2±0.57	82.7±1.62	0.50±0.01	0.41±0.01
0.67	95.5±0.31	73.7±0.93	0.64±0.01	0.49±0.01
1.00	79.1±0.25	61.3±1.02	0.79±0.01	0.61±0.01
1.67	51.8±0.14	41.9±1.30	0.86±0.01	0.70±0.02
2.50	35.0±0.11	29.6±1.03	0.87±0.01	0.74±0.03
6.67	15.3±0.46	8.56±4.20	1.02±0.03	0.57±0.28
10.00	11.1±0.12	7.08±1.40	1.11±0.01	0.71±0.14

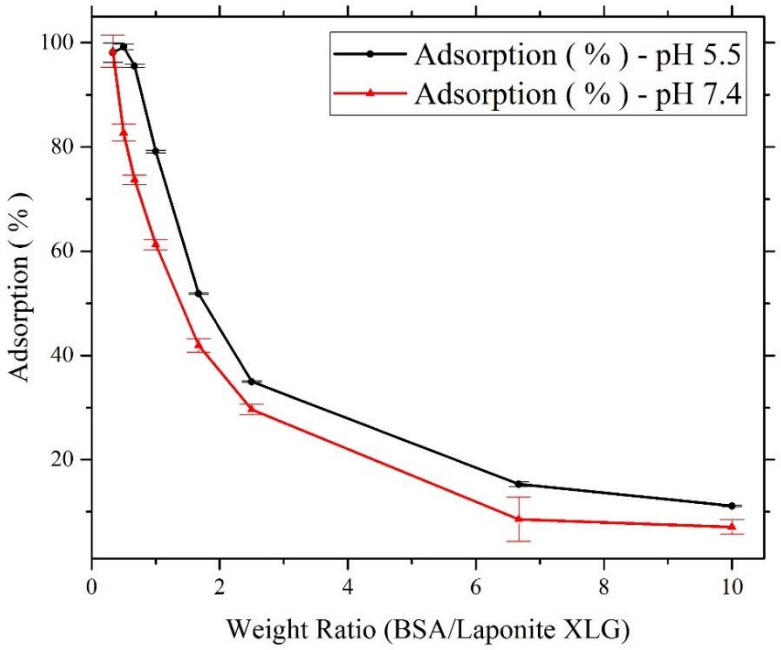

Figure 5.3 Effect of pH on adsorption percentage of BSA onto Laponite XLG

Effect of pH on percentage adsorption was more clearly seen from the Figure 5.4. The exponential increment was observed up to 2.5 weight ratio.

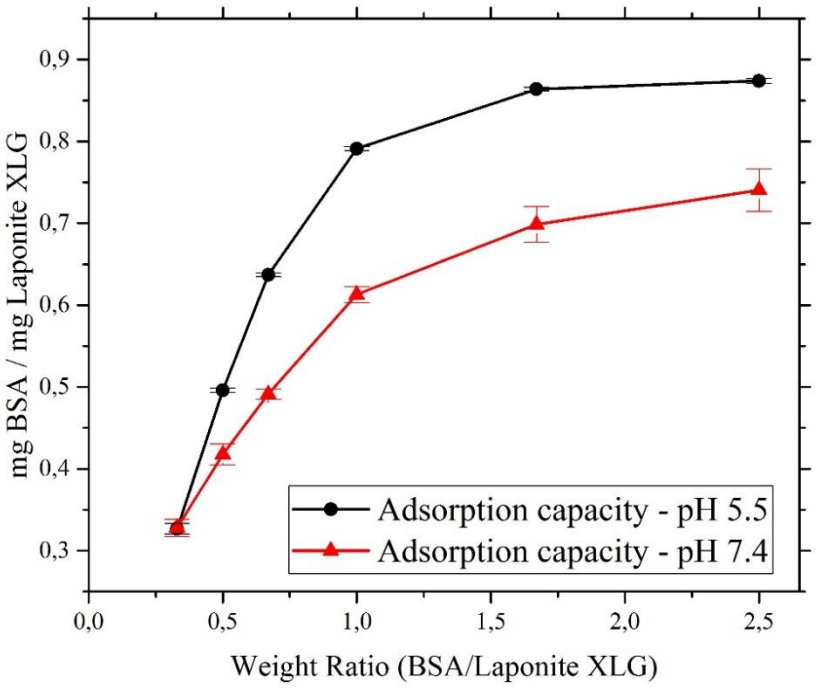

Figure 5.4 Effect of pH on adsorption capacity.

Influence of molarity on adsorption was determined based on weight ratio as given Table 5.4. Molarity of the medium was adjusted to 0.01 M or 0.05 M. Experiment was conducted at pH: 7.4 for sample Set A.

Table 5-4 Influence of molarity on adsorption percentage and adsorption capacity based on weight ratio.

Weight Ratio (mg BSA/mg Laponite XLG)	**Adsorption Percentage (%)**		**Adsorption Capacity (mg BSA/mg Laponite XLG)**	
	0.01 M	**0.05 M**	**0.01 M**	**0.05 M**
0.67	70.1±0.07	79.0±0.07	0.47±0.01	0.53±0.01
1.00	55.6±0.76	58.7±0.25	0.56±0.01	0.59±0.01
1.33	43.0±0.34	47.3±0.17	0.57±0.01	0.63±0.01
2.00	28.0±0.56	35.6±0.65	0.56±0.01	0.71±0.01
3.33	14.0±0.69	23.0±0.97	0.47±0.02	0.77±0.03

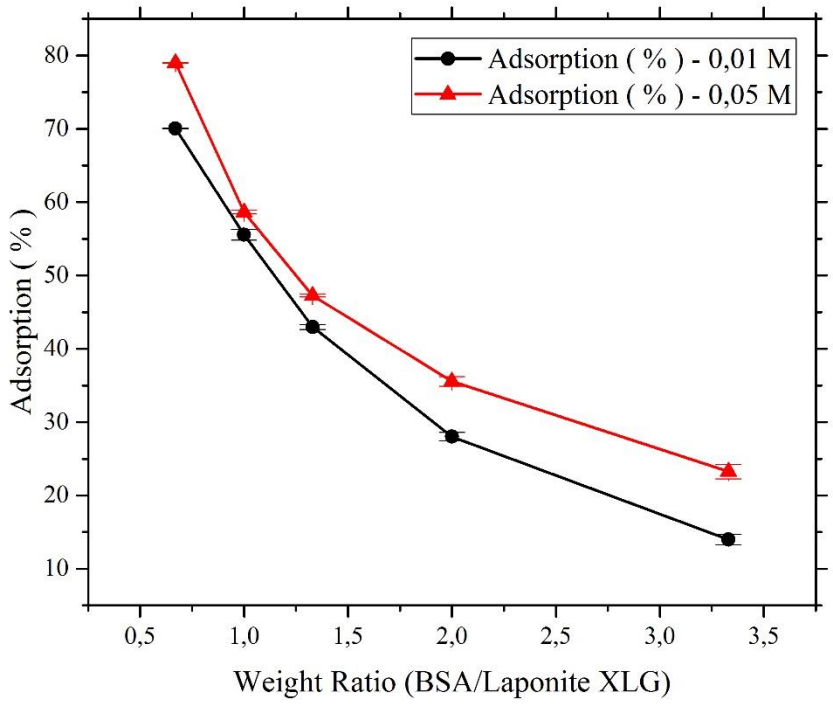

Figure 5.5 Effect of molarity on adsorption percentage.

Adsorbed BSA amount in per Laponite XLG increased from 0.47 for 0.67 weight ratio to 0.57 for 1.33 weight ratio, adsorbed BSA amount then decreased to 0.47 for 3.33 weight ratio for samples which were prepared at 0.01 M. The samples prepared in 0.05 M buffer, however, demonstrated a consistent exponential rise in adsorbed BSA amount. The most noticeable change was in the influence of molarity on adsorption capacity; however, it is clear that the difference was relatively decreased for lower weight ratios.

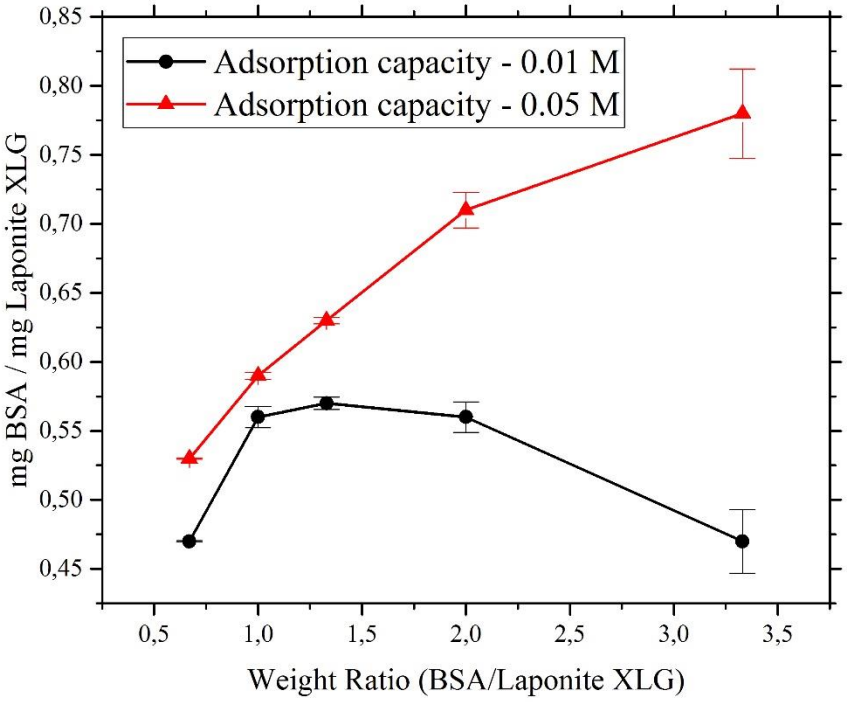

Figure 5.6 Molarity effect on percentage adsorption.

A turbid appearance was observed after interaction for the samples prepared at 0.05 M. It is required to inhibit the repulsive interaction energy between protein and clay particles for binding of BSA protein to negatively charged Laponite XLG. It was set forth that turbidity was a result of repulsive forces based on similar type of protein clay interaction.(198) Furthermore, when molarity of the medium was adjusted to 0.01 M, there was not observed any flocculation or two phases system which is consistent with the information provided that laponite suspensions form flocculate at ionic strength over than 0.01 M .(199)

5.2.1 Structural Analysis of BSA-Laponite XLG Complexes

The produced complexes were characterized with Fourier Transform Infrared Spectroscopy (FTIR), X-Ray Diffraction (XRD) to obtain the structure along with alterations in the morphology of Laponite XLG and BSA complexes.

Empirical formula of Laponite XLG is known as $Na_{0.7}^{+}[(Si_8Mg_{5.5}Li_{0.3})O_{20}(OH)_4]^{-0.7}$. The structure of Laponite XLG was detected via FTIR to obtain the corresponding peaks.

It has been stated that the broad band between 3400 cm^{-1} and 3700 cm^{-1} is due to the stretching and bending of surface hydroxyl groups and absorbed water.(200) Thus, the broad peak observed at 3408 cm^{-1} could be due to hydroxyl groups in the structure or absorbed water present in the sample. The peak observed at 963 cm^{-1} corresponds to Si-O bond whereas Mg_3OH bending was seen at 648 cm^{-1}. Si-O stretching vibration was seen at 1633 cm^{-1}. The obtained spectrum for Laponite XLG is in agreement with the literature.(201–203)

FTIR spectrum shows the characteristic peaks of BSA which are identified as amide I band, amide II band and amide III band. Amide I band was determined at 1651 cm^{-1}. Moreover, the peaks observed at 1532 cm^{-1} were interpreted to be due to amide II band with N-H bending vibration and C-N stretching vibration. The peak observed at 1241 cm^{-1} was assigned to amide III band. N-H bending vibration was detected at 3290 cm^{-1}. Peak belonging to symmetric stretch of COO^{-} at 1391 cm^{-1} is due to the side chains of BSA. The peak was observed at 3063 cm^{-1} due to the C=O stretching vibration of amide I band.

FTIR Spectrum of BSA was compared with the spectra given in the literature and it was seen that the obtained spectrum matched well with those given in the literature.(204–206) Laponite XLG and BSA complexes were analyzed for samples with various adsorption capacity. The legends are specified the adsorption capacity values which was calculated with protein determination technique via UV-VIS spectrophotometer in the Figure 5.7 and 5.8.

A glance at the FTIR spectra given in Figure 5.7 reveals that the complexes have the characteristic peaks of both BSA and Laponite XLG. Intensity of the peak at 646 cm^{-1} was decreased for all samples and there were minor position changes.

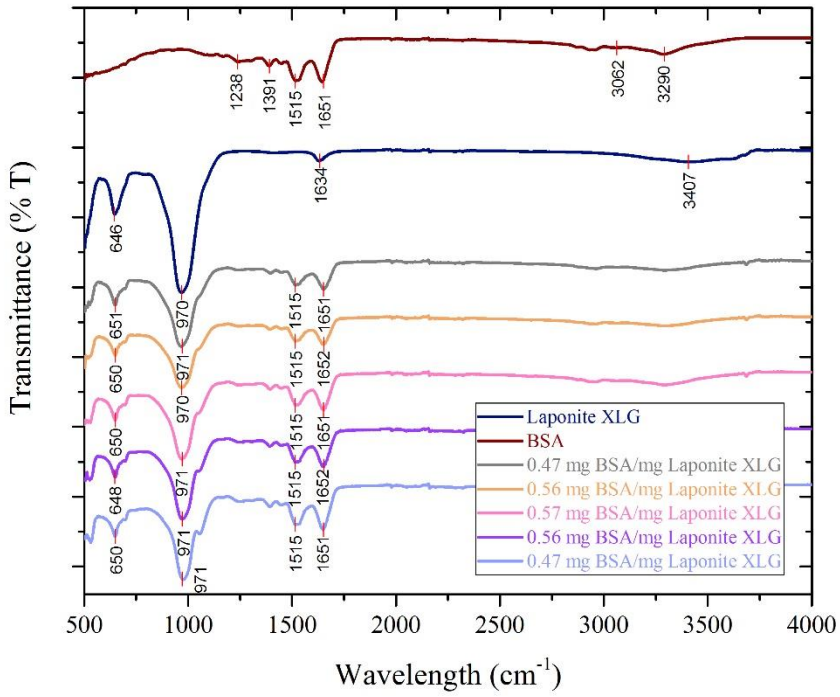

Figure 5.7 FTIR Spectrum of BSA-Laponite XLG complexes prepared in 0.01 M PB at pH 7.4.

Amide I band, consists of C=O stretching and C-N stretching, was investigated to whether obtaining the conservation of secondary structure of protein. The distinctive point is that the components should not contain water due to strong absorbance bands of water. Water demonstrates absorption bands at 1640 cm^{-1}, 2125 cm^{-1} and 3400 cm^{-1} while amide I band also shows absorption between 1600 cm^{-1} and 1700 cm^{-1}. Thus, it was challenging that the determination of corresponding bands in the presence of water. It is evident that there was no sharp alteration on the peak positioned at 1651 cm^{-1} for samples which were prepared using 0.01 M PB. Hence, the peak analysis suggested that the secondary structure of BSA was conserved in the BSA-Laponite XLG complexes. Specimens which were prepared using 0.05 M buffer were also tested. Similarly, there was not seen a shift at the amide I band position, which changes in a very narrow band between 1651 cm^{-1} and 1652 cm^{-1}

for BSA samples. Only sample with 0.63 adsorption capacity demonstrated the amide I peak at 1648 cm^{-1}.

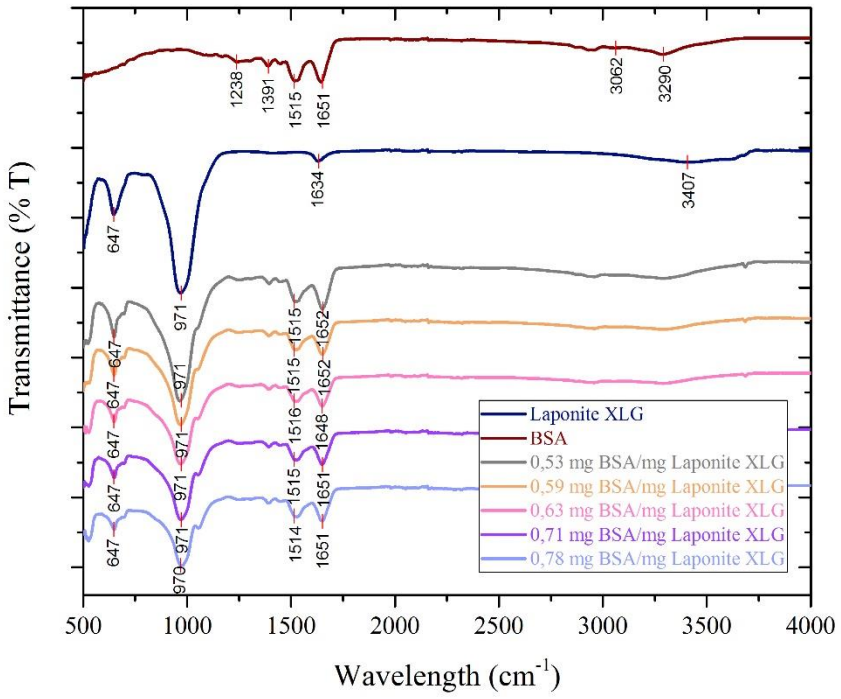

Figure 5.8 FTIR Spectrum of BSA-Laponite XLG complexes prepared in 0.05 M.

The alteration can be interpretated as random coil formation(204), which indicates as an increase in disordered structure. It was observed for new peak positioned at 1063 cm^{-1} for both samples prepared at 0.01 M and 0.05 M which was due to interaction between BSA and Laponite XLG. FTIR analysis is commonly used for obtaining protein conformation and changes in the structure resulted from lyophilization.(15) It was not seen a significant alterations in secondary structure of the BSA in the complexes. However, an additional technique is required for confirmation such as circular dichroism spectroscopy.

The interaction type between BSA and Laponite XLG was evaluated with X-Ray Diffraction (XRD) technique. Amorphous materials such as BSA do not show sharp peaks in XRD analysis. However, crystalline materials can be characterized by

XRD. XRD analysis was done for the Laponite XLG. There are characteristic peaks in the spectra due to crystalline structure of the clay.

Figure 5.9 presents the XRD spectra of the Laponite XLG and BSA-Laponite XLG complexes. Laponite XLG demonstrated broad basal reflections which were detected at 5.95º, which is close to the value reported by Zhang.(207) There were also peaks detected at 19.67º, 27.7º, 34.65º, 53.52º and 60.62º positions. The interaction type between Laponite XLG and BSA was examined. The tested sample had 0.59 mg BSA/mg Laponite XLG adsorption capacity.

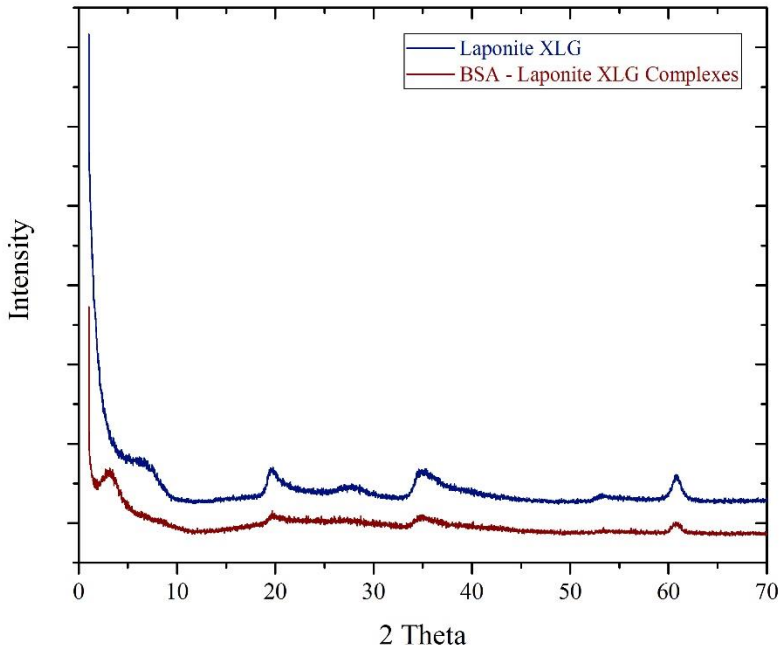

Figure 5.9 XRD Spectrum of Laponite XLG and Laponite XLG-BSA complex.

It is apparent from XRD Spectra that there was a peak at 3.08° with 28.66 A. Characteristic peak of Laponite at 5.95° was not observed in the complex. Moreover, intensities of the remaining peaks were decreased.

Composed peaks and their basal spacing values prove the intercalated formation. Moreover, alterations in positions and their intensities showed interaction between protein and clay. Figure 5.10 reveals formed peaks at complex explicitly below.

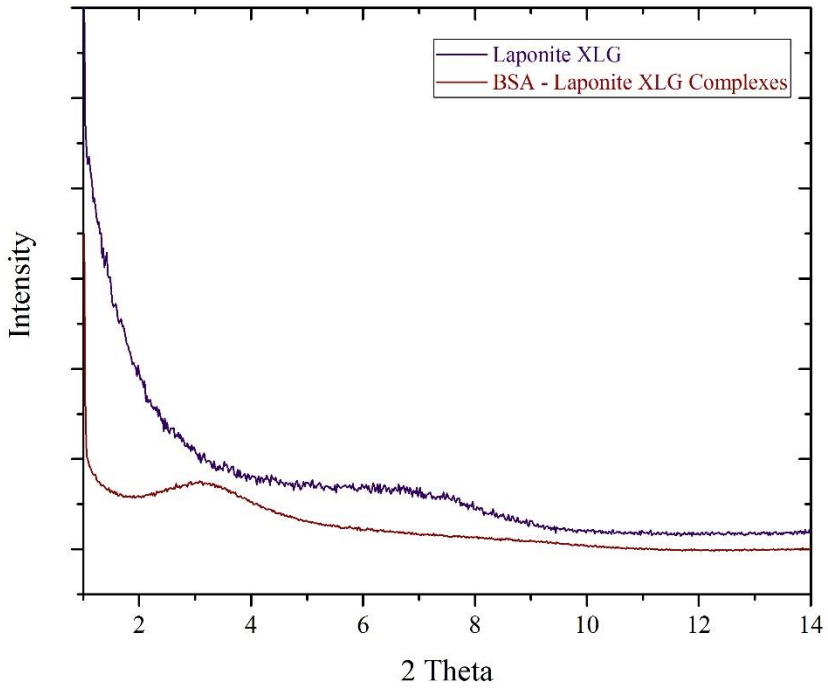

Figure 5.10 XRD Spectrum of Laponite XLG and Laponite XLG-BSA Complex scanned at slow rate.

5.3 Preliminary Hydrogel Formation Studies

HEMA (2-Hydroxylethyl methacrylate) based hydrogels were produced as pure, laponite containing and enzyme containing at first. The procedure of the studies is given in the Appendix H.

Preliminary studies were performed to verify polysaccharide based hydrogel formation with imine and hydrazone chemistry. Stability of hydrazone bond is greater than imine bond. The influence of this condition on protein release mechanism from hydrogel matrices was investigated. Therefore, chitosan and dextran aldehyde polymers were used to form hydrogels via imine bond formation as a result of the reaction between the aldehyde group on dextran and amine groups on chitosan, which is in Appendix E. Dextran was oxidized to create reactive sites

for imine cross linking.The oxidation of dextran is found from the Appendix D. The carbonyl group formation of dextran and imine bond formation were confirmed with FTIR. Since gel formation time is another important criteria on performance of injectable hydrogels, gelation time was obtained for various polymer concentrations. It was observed that gel formation can be ensured by increasing pH value for low polymer concentrations. Protein containing imine bond hydrogels were generated to investigate the release mechanism. It was determined that release of protein was realized in a couple of hours. Produced hydrogels is given in the Table 5.5 with reactive parts for gel formation.

Table 5-5. Produced hydrogels with imine and hydrazone bond chemistry.

Hydrogel Code	Aldehyde Component	Hydrazide/Amine Component
Imine01	Dextran Aldehyde	Chitosan
Hydrazone 01	Alginate Aldehyde	Alginate Hydrazide
Hydrazone 02	Dextran Aldehyde	Alginate Hydrazide
Hydrazone 03	Dextran Aldehyde	Adipic Acid Dihydrazide
Hydrazone 04	Alginate Aldehyde	Adipic Acid Dihydrazide

Hydrazone 03 coded hydrogels were generated with oxidized dextran and adipic acid dihydrazide to obtain minimum polymer concentration required to form a gel. The relation between aldehyde and hydrazide counterparts on gel formation time was studied. It was found that with increasing aldehyde amount that gel formation could be realized in a shorter time as given in Appendix G.

Hydrazone 02 coded hydrogels were synthesized with several polymer concentrations with 5% and 60% substitution degrees of hydrazide. The procedure and related parts is in Appendix F. Swelling test demonstrated that hydrogels had low swelling index. Thus, it was concluded that Hydazone 02 hydrogels could be useful for (bio-) applications which require low swelling.

Conducted modification studies to form hydrogels with imine bond and hydrazone bond is seen from Table 5.6.

Table 5-6 Conducted modification studies to functionalize polysaccharides for hydrazone bond formation.

Polymer	Modification	Modified Polymer
Dextran	Aldehyde group modification	Dextran Aldehyde
Alginate	Aldehyde group modification	Alginate Aldehyde
Alginate	Hydrazide group functionalization	Alginate Hydrazide

The outputs of the works provided an insight for the potential hydrogel model for protein release studies in terms of degree of substitution, polymer concentration, moles of aldehyde and hydrazide counterparts in the polymers, release and swelling characteristics. As a result, Hydrazone 01 hydrogels composed of alginate was chosen for the protein delivery applications.

5.4 Alginate Based Hydrogels with Hydrazone Chemistry

Alginate term implies alginic acid together with salts of alginic acid such as sodium alginate in the context. The prominent feature of sodium alginate is high solubility in water on the contrary to other forms.

Hydrazone bond chemistry can be formed via reaction between aldehyde or ketone groups and hydrazide groups. Hydrazone bond chemistry was selected for protein release study due to fast gelation property which prevents diffusion of therapeutic agents out of matrix in a short period of time. Hydrolytic degradation of chains can be adjusted with alteration of polymer concentration and degree of substitution of alginate components. Alginate contains hydroxyl groups which make modification studies convenient. Alginate (A) was modified to form alginate aldehyde (A-A) and alginate hydrazide (A-H) with different degree of substitution values to form hydrogels with hydrazone chemistry.

5.4.1 Functionalization of Alginate with Aldehyde Groups

Alginate does not contain aldehyde group in the structure to form hydrazone chemistry. Hence, carbohydrate was reacted with sodium periodate to transform hydroxyl groups to carbonyl groups. There have been many studies about oxidation of alginate. (47,134,146,164) Modification provided both creation of reactive sites on the polymer and enhanced biocompatibility.(163)

The procedure used was developed by Mooney *et al.*(146) Due to light sensivity of sodium periodate, oxidation process was conducted in the dark. Theoretical degree of modification is defined as the molar ratio of sodium periodate to molar ratio of repeating unit of alginate. In the work, theoretical modification degrees were selected as 10%, % 25% and 50%. It was reported that higher oxidation degrees cause deterioration in polysaccharide nature.(208) Therefore, degree of substitution was limited to 50%. The prominent point was that average molecular weight of a repeating unit was not changed greatly after modification. However, it was assumed that increased degree of substitution tended to decreased molecular weight of alginate according to the study of Mooney *et al.*.(146) It is known that molecular weight of the polymer precursors highly influence on gel formation. Figure 5.11 shows the oxidation reaction of alginate:

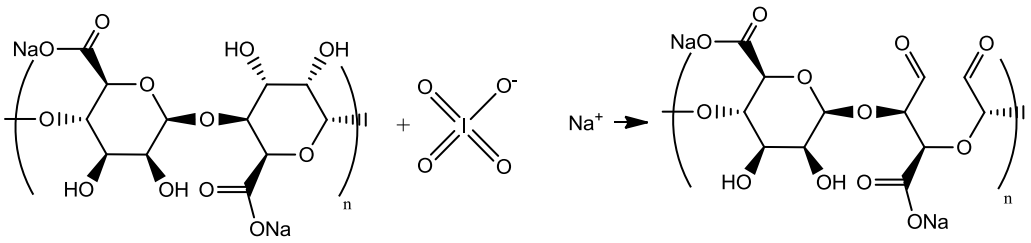

Figure 5.11 Oxidation reaction of alginate with sodium periodate.

Table 5.7 and 5.8 give the materials and its amounts for oxidation of alginate with respected modification degrees. Two types of method was used based on constant final volume and variable final volume of the reaction mixture.

Table 5-7 Amounts of alginate and sodium periodate were used in the oxidation study with various degree of substitution values. (Constant Final Volume)

Alginate (mg)	Alginate (mg/ml)	Sodium Periodate (mg)	Final Volume (ml)	Alginate (mmol)	Sodium Periodate (mmol)	Theoretical DS (%)
1500	10	809	180	7.56	3.78	50
1500	10	406	180	7.56	1.90	25
1500	10	162	180	7.56	0.759	10

Since reaction yield was not changed greatly for % 50 theoretical degree of substitution in both techniques, oxidation of alginate was done based on constant final volume.

Table 5-8 Amounts of alginate and sodium periodate were used in the oxidation study with various degree of substitution values. (Variable Final Volume)

Alginate (mg)	Alginate (mg/ml)	Sodium Periodate (mg)	Final Volume (ml)	Alginate (mmol)	Sodium Periodate (mmol)	Theoretical DS
1500	10	809	165	7.56	3.78	50
1500	10	406	157.6	7.56	1.90	25
1500	10	162	153	7.56	0.759	10

The structure of the native and modified alginate were analyzed with Fourier Transform Infrared Spectroscopy (FTIR) to evaluate the alteration in the carbohydrate structure as a result of the modification. FTIR spectrum of alginate is given in Figure 5.12.

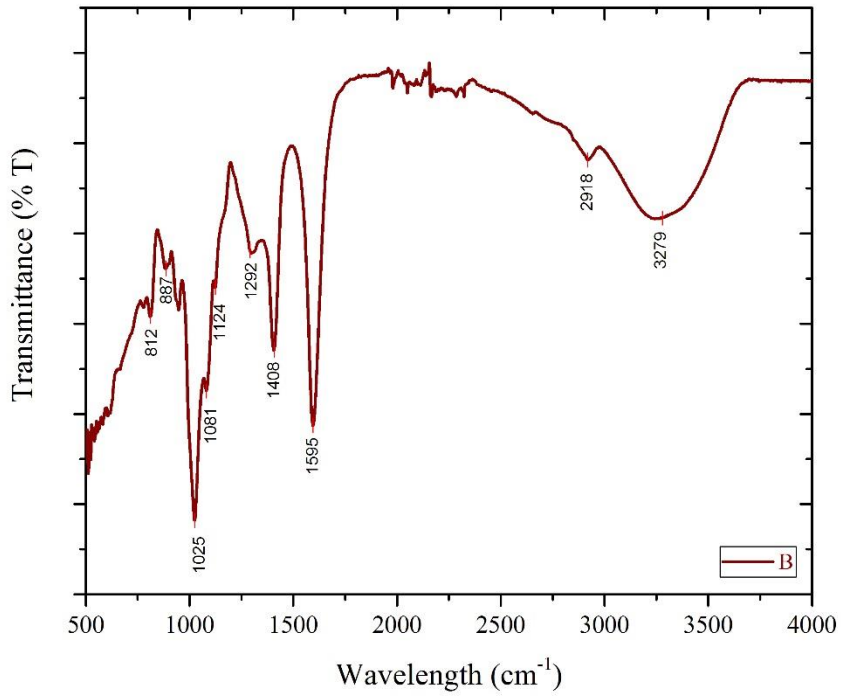

Figure 5.12 FTIR Spectrum of alginate.

The band detected at approximately 1025 cm^{-1} was due to C-O-C stretching. Asymmetric and symmetric stretching were observed at 1595 cm^{-1} and 1408 cm^{-1} resulting from carboxylate salt groups. The OH bond was seen from the peak observed around 3279 cm^{-1} in the sodium alginate structure. It was stated that C-O-C antisymmetric stretching is seen with the peaks between 1024 cm^{-1} and 1081 cm^{-1} whereas the peaks related to carboxyl and carboxylate molecules can be seen from the peaks from 1000 cm^{-1} to 1400 cm^{-1}.(209) In addition, peak observed at 1292 cm^{-1} were assigned to C-C-H and O-C-H stretching. The results are coherent with literature works.(127,210)

It was seen from the Figure 5.13 that the polysaccharide structure was partly conserved despite the oxidation reaction. Native alginate peaks could be observed in the spectrum of modified alginate spectra too. However, there were changes in intensities of the peaks belonging to alginate structure. Carbonyl peak formation around 1730 cm^{-1} indicated that the materials were oxidized.(119,146,211) New

peak formation was observed at 1731 cm^{-1} for the samples theoretically modified with 25% and 50%. The C=O bond, stretching of carbonyl groups, indicates aldehyde group formation.

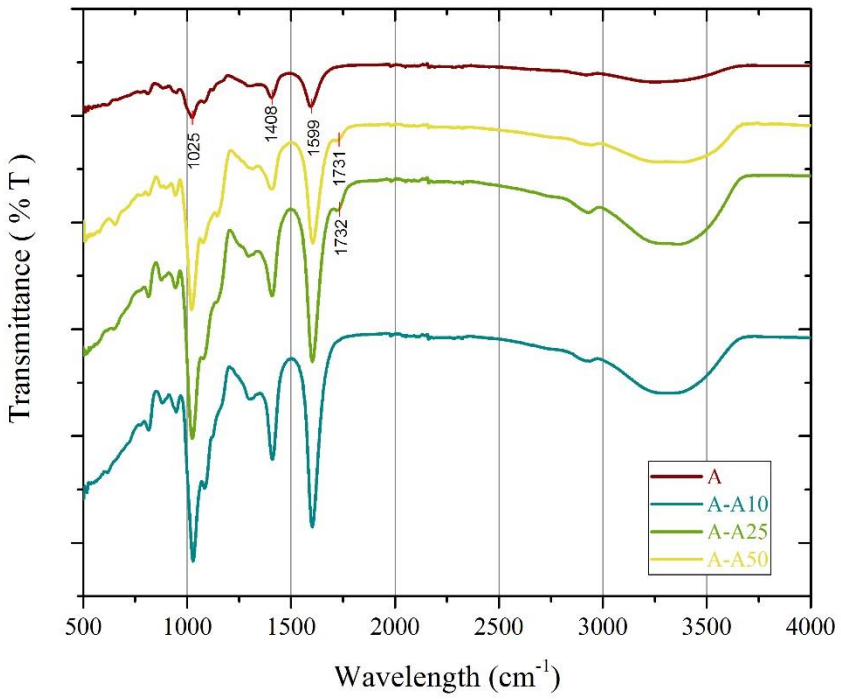

Figure 5.13 FTIR Spectrum of alginate aldehyde samples.

Samples, which had 10% theoretical modification degree, did not demonstrate the C=O stretching. This could be due to low modification degree or hemi-acetal formation. A similar result was reported by Gil *et al.* that materials which had low degree of substitution did not show carbonyl peak.(119) Moreover, many oxidized materials showed no peak around 1730 cm^{-1} in the FTIR analysis even the modification was proved with other techniques.(119,121)

Oxidation degree was determined with carbazate assay. Aldehyde groups in the modified polymers were reacted with tert-butyl carbazate in excess amount to form carbazones. Unreacted tert-butyl carbazate then reacted with TNBS at alkaline

medium and formed a colored derivative based on concentration as shown in the Figure 5.14:

Figure 5.14 tBC - TNBS complexes with various concentration.

Solution was diluted with HCl to measure absorbance of the colored derivative was measured at 334 nm as shown Figure 5.15. Unreacted tBC amount was calculated by using calibration curve. Based on the carbazate assay, the degree of substitution was measured as 45±3% for 50% theoretical degree of substitution. Similarly, for theoretical degree of substitution of 25% and 10%, measured degree of substitution values were 23±2% and 9±2%, respectively. It is evident that modification yield decreased with increased theoretical substitution value.

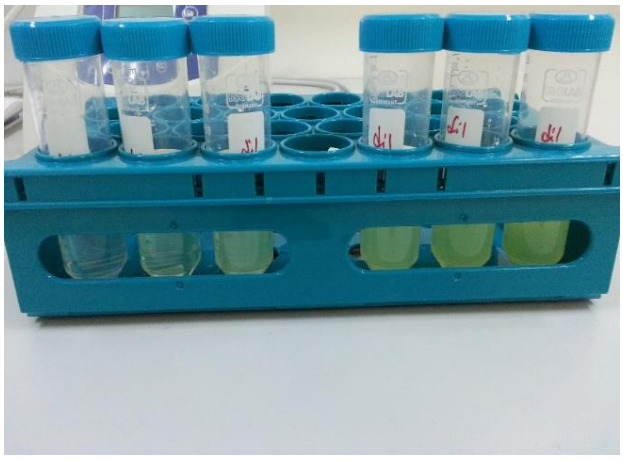

Figure 5.15 Samples diluted with HCl solution for UV-VIS measurement.

5.4.2 Functionalization of Alginate with Hydrazide Groups

Hydrazide modification was done through the reaction of alginate with ADH in the presence of EDC and NHS at room conditions for 24 hours. Functionalization of alginate was conducted to create reactive sites for hydrogel production with hydrazone chemistry.

Required amounts of reactants were investigated to occur hydrazide modification with desired degree of substitution-which is given in Table 5.9.

Table 5-9 Alginate, ADH and EDC amounts were used for functionalization of alginate with hydrazide.

Synthesis No.	Alginate (A) (mmol)	ADH (mmol)	EDC (mmol)
1	0.117	4.388	2.925
2	0.117	1.117	0.585
3	0.117	0.117	0.117
4	0.932	0.932	0.05592
5	0.233	5.35	0.417

Functionalization of alginate with hydrazide groups was difficult due to pre-gel formation during reaction due to high reactivity of alginate. Reaction was carried out under acidic conditions with pH values between 4.5 and 5.0. Reaction yield was greatly reduced when pH value of the reaction mixture exceeded over pH 5.5. Secondly, it was not suggested pH adjustment with HCl directly in ADH modification which applied for hyaluronic acid and other polysaccharides.(169) When HCl solutions were in between 0.5 M and 1 M HCl, high acidic zones became and gel formation occurred prior to modification study. The pH of the solution, therefore, was set at approximately 4.7 by adding 0.1 M HCl at certain intervals. It was reported that when pH value of the solution becomes lower than 3.5, precipitation could be occurred based on molecular weight of alginate.(169,212)

EDC, is highly humid sensitive, must be stored at suitable conditions preferably at -20 ^{o}C to prevent loss of activity. EDC was dissolved in distilled water, then added

into reaction mixture as immediate as possible. NHS solution was also added to increase stability of the complex together with EDC solution.

The reaction was firstly done for higher mol ratio of adipic acid dihydrazide (ADH) to alginate (A) with relatively high mole ratio of EDC to A for modification practices, which were numbered 1 and 2. Hydrazide modification was unsuccessful due to high reactivity of alginate for synthesis number 1 and 2. Addition of EDC into reaction mixture tended to flocculation in a shorter time.

Afterwards, synthesis no. 3 was applied with the given ratios in the Table 5.10. When the reaction was completed, no aggregate formation was observed and then purification and drying steps were completed. However, purified alginate hydrazide was dissolved in PB and formed gel.

Table 5-10 Corresponding ratios of ADH and EDC to alginate were used for functionalization of alginate with hydrazide.

Synthesis No.	ADH/A (mol/mol)	EDC/A (mol/mol)	ADH/EDC (mol/mol)
1	37.5	25	1.5
2	10	5	2
3	1	1	1
4	1	1	16.65
5	22.96	1.79	12.83

Synthesis number 4 was applied based on the work of Gomez *et al.* with low modification degree to prevention of physical aggregates. The prominent part was comparatively high ratio between ADH and EDC.(167) The modification study was completed successfully. Hydrazide modification was tested with FTIR analysis and quantitatively TNBS Assay. In spite of the reaction can be occurred in both guluronate and mannuronate blocks(169), only one block of alginate was shown in the Figure 5.16.

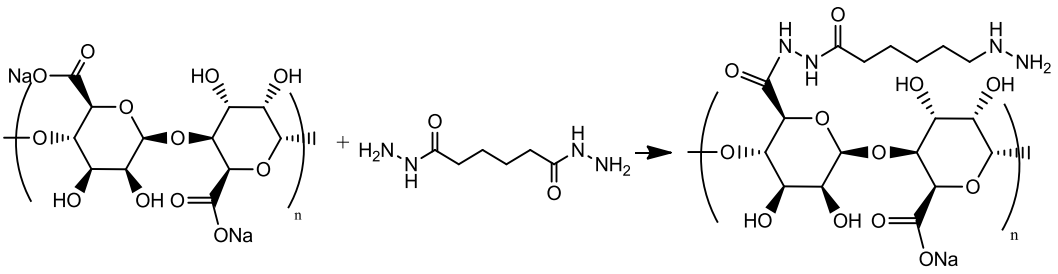

Figure 5.16 Hydrazide modification of alginate in the presence of EDC and NHS.

Low degree of hydrazide modification was attained with this technique, which was inefficient for hydrazone bond formation. The work of Tan *et al.* (168) was conducted for higher degree of substitution, which was coded as synthesis number 5. The remarkable point was that high ratio of ADH to EDC provided successful hydrazide modification for synthesis number 4 and 5 with low ratio of EDC to alginate.

Hydrazide group formation was detected with FTIR analysis and TNBS Assay. The alterations in polysaccharide nature was detected with FTIR for alginate hydrazide samples.

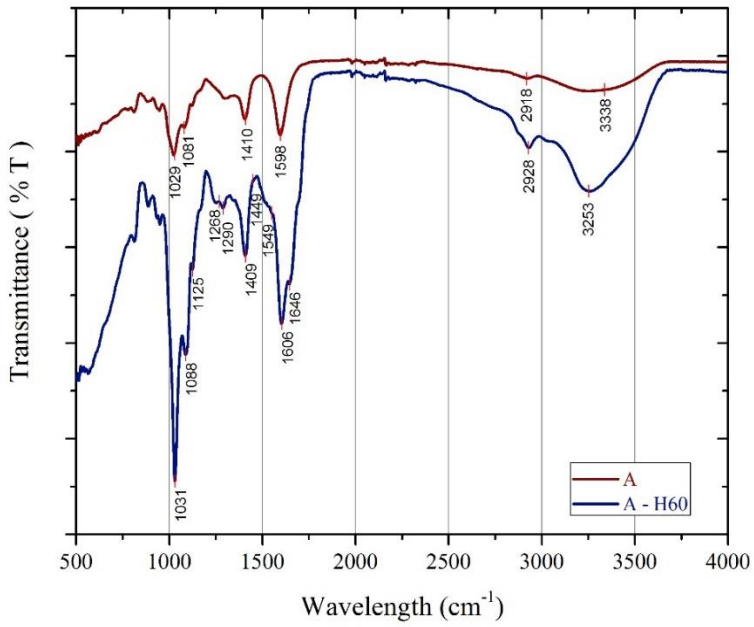

Figure 5.17 FTIR Spectrum of native alginate and alginate hydrazide.

The examination of the peak positions reveals the similarities between alginate and alginate hydrazide in the Figure 5.17. The new peaks observed for alginate hydrazide lined with navy color were examined. The peak observed at 1268 cm^{-1} could be belonging to C-N- stretch and 2928 cm^{-1} was due to C=O and H-C=O stretch, The peak observed at 3253 cm^{-1} became much intense due to addition of N-H stretch.

Characteristic peaks were observed at 1646 cm^{-1} due to C=O stretching of secondary amine and 1549 cm^{-1} due to N-H bending for amide bonds. The peak at 1606 cm^{-1}, demonstrated the presence of carbonyl groups. The peak indicates that uncompleted transformation of carbonyl groups into amide bond.(169)

The degree of hydrazide modification was assessed via TNBS assay, which was modified from Hoare *et al.* for aldehyde group determination.(94) Hydrazide groups in the modified polymers were directly reacted with TNBS at alkaline medium and formed a colored derivative. The solution was diluted with HCl. Afterwards, the absorbance of the colored derivative was measured at 334 nm. Reacted hydrazide amount was calculated by using a calibration curve-composed from adipic acid dihydrazide samples. The degree of substitution was calculated as 55±5%.

5.4.3 Alginate Based Hydrogels with Hydrazone Chemistry

Alginate based hydrogels were produced with hydrazone chemistry. Alginate was oxidized with sodium periodate in various substitution degrees. On the other hand, alginate was also modified with adipic acid dihydrazide at high substitution degree. Biodegradable linkages of hydrazone bond can be adjusted via polymer concentration and crosslinking density. Fast gelation was provided with hydrazone chemistry, which prevents diffusion of drugs at an instant. However, this condition raises issues related with homogeneous mixing of precursors.

Hydrogels were prepared in polydimethylsiloxane (PDMS) cast which has 250 µl volume of a segment with cylindrical shape. Hydrazide precursor was firstly added with desired volume following aldehyde solution addition. The mixture was pulled and pushed via a micropipettor a couple of times to ensure homogeneity. Precursors, which form gel within seconds, hinder providing a homogeneous mixture

throughout hydrogel. PDMS cast was putted in a closed vessel containing humid air for the completion of gel formation.

Four types of hydrogels were studied, which are alginate based, protein containing alginate based, alginate based nanocomposite and protein containing nanocomposite hydrogel. Model protein was used as BSA whereas Laponite XLG was used as clay and nano drug carrier.

Alginate based hydrogels were prepared simply via mixing of alginate aldehyde and alginate hydrazide. Protein containing alginate based hydrogels were prepared via addition of BSA solution into hydrazide solution before mixing of aldehyde precursor.

Laponite XLG was dissolved in distilled water, then added into alginate hydrazide sample. Afterwards, alginate aldehyde was mixed with hydrazide solution to form alginate based nanocomposite hydrogels. Laponite XLG was kept in lower concentrations than 1% (w/v) both in water and in hydrazide solution. Lastly, BSA-Laponite complexes, which were interacted about 18 hours, were added into hydrazide solution, then mixed with alginate aldehyde precursor to form protein containing nanocomposite hydrogel.

When the hydrogel is injected into the target tissue, the excess aldehyde groups present in the hydrogel may interact with the tissues and it constitutes a potential risk.(4) The total number of hydrazide groups; therefore, should be equal to or higher than the total number of aldehyde groups in the hydrogel for the optimal conditions. The total number of hydrazide groups was selected equal or higher than the total number of aldehyde groups in the hydrogel as a design parameter for further protein containing hydrogel production works so that all aldehyde groups would react with hydrazide groups by forming hydrazone bonds.

It was also reported that aldehyde groups tended to interact with aminooxy groups to form oxime bond in the presence of amine and aminooxy groups rather than relatively unstable imine bond.(157) This point can also be evaluated valid for hydrazone bond chemistry due to higher stability than imine bond. In other words,

it was presumed that protein do not react with aldehyde precursor in hydrazide solution due to low stability of imine bond.

Average molecular weight of repeating units was calculated to determine total number of aldehyde and hydrazide groups in the polymers.

Average molecular weight of polymers can be calculated as follows:

$$\boldsymbol{Mw_{average}} = \frac{\left(\boldsymbol{DS} * \boldsymbol{Mw_{modified}}\right) + \left((\mathbf{1} - \boldsymbol{DS}) * \boldsymbol{Mw_{unmodified}}\right)}{\mathbf{100}} \qquad (\mathbf{3})$$

In here:

$M_{waverage}$: Average molecular weight of a repeating unit in g/mol

$M_{wmodified}$: Molecular weight of a repeating unit in modified polymer in g/mol

$M_{wunmodified}$: Molecular weight of a repeating unit in umodified polymer in g/mol

DS: Degree of substitution value in percentage

The total number of reactive groups are obtained as given below:

Total moles of aldehyde groups in the polymer

$$\frac{\boldsymbol{m_A}}{\boldsymbol{M_A}}(\boldsymbol{DS_A}) \qquad (\mathbf{4})$$

In the formula:

m_A: Mass of modified polymer in g

M_A: Molecular weight of a repeating unit in modified polymer have aldehyde group in g/mol

D_{SA}: Degree of substitution of modified polymer have aldehyde group in percentage

It is seen from the information in Table 5.11 that there was insignificant change in average molecular weight of a repeating unit of alginate aldehyde polymers after oxidation.

Table 5-11 Average molecular weight of repeating units in alginate aldehyde with different degree of substitution values.

DS	$Mw_{modified}$ (g/repeating unit mole)	$Mw_{unmodified}$ (g/repeating unit mole)	$Mw_{average}$ (g/repeating unit mole)
10	196	198	197.8
25	196	198	197.5
50	196	198	197

Total moles of hydrazide groups in the polymer

$$\frac{m_H}{M_H}(DS_H) \quad (5)$$

m_H: mass of modified polymer in g

M_H: Molecular weight of a repeating unit in modified polymer have hydrazide group in g/mol

D_{SH}: Degree of substitution of modified polymer have hydrazide group in percentage

Table 5-12 Average molecular weight of repeating units in alginate hydrazide with different degree of substitution values.

DS	$Mw_{modified}$ *(g/repeating unit mole)*	$Mw_{unmodified}$ *(g/repeating unit mole)*	$Mw_{average}$ *(g/repeating unit mole)*
60	354	198	291.6

There was great change in average molecular weight after functionalization of hydrazide due to intense pendant group addition and high substitution degree. Degree of substitution was selected as high due to the necessity of greater hydrazide amount in the hydrogel.

Total moles of hydrazide number was selected as greater than total moles of aldehyde number in the polymer due to eliminate potential interactions.

$$\frac{m_H}{M_H}(DS_H) \geq \frac{m_A}{M_A}(DS_A) \quad \textbf{(6)}$$

Apart from the ratio of hydrazide to aldehyde, gel formation was investigated under different conditions such as degree of substitution values, polymer concentration, Laponite XLG and BSA amounts. The hydrogels were produced in the Table 5.13. Each sample was produced with only alginate based hydrogel, protein containing alginate based hydrogel, alginate based nanocomposite hydrogel and protein containing alginate based nanocomposite hydrogel.

BSA addition was done in 0.2% (w/v) of alginate polymer in hydrogel. Laponite XLG addition was done between 0.1% and 0.5% (w/v) of polymer. Degree of substitution values were ranged from 10% to 50% for alginate aldehyde by theoretically whereas hydrazide modification degree was set at 60%.

Maximum individual alginate aldehyde concentration was selected as 10% (w/v) whereas alginate hydrazide concentration was set as 1.5% (w/v) due to high viscosity when preparation of hydrogels.

Minimum polymer concentration was obtained for hydrogel samples with various modification degrees. Gelation time was observed for various polymer concentrations.

Table 5-13 Alginate based hydrogel production.

Hydrogel Code	Degree of Substitution	Individual Aldehyde Concentration (w/v)	Individual Hydrazide Concentration (w/v)	Total Polymer Concentration (w/v)	Hydrazide/ Aldehyde (mole/mole)
AA50-3.2	Aldehyde	10	1.5	3.2	1.06
AA50-2.2	DS: % 50 Hydrazide	5	1.5	2.2	2.12
AA50-1.7	DS: % 60	2.5	1.5	1.7	4.24
AA50(2)-4.05	Aldehyde	10	1.5	4.05	0.62
AA50(2)-2.55	DS: % 50	5	1.5	2.55	1.24
AA50(2)-1.8	Hydrazide DS: % 60	2.5	1.5	1.8	2.47
AA25-5.75	Aldehyde DS: % 50	10	1.5	5.75	0.53
AA25-3.25	Hydrazide DS: % 60	5	1.5	3.25	1.06
AA25-2		2.5	1.5	2	2.12
AA10-5.75	Aldehyde	10	1.5	5.75	1.33
AA10-3.25	DS: % 10	5	1.5	3.25	2.65
AA10-2	Hydrazide DS: % 60	2.5	1.5	2	5.30

Based on the preliminary experiments, it was concluded that polymer concentration was the main parameter which reduces gelation time. Hydrogels that had higher polymer concentration were formed in a shorter time for each hydrogel type. The fastest gel formation was observed for hydrogel coded as AA10-5.75 within seconds. It is interesting to note that gelation time of AA10-5.75 was lower than AA25-5.75 even for the same polymer concentration. However, the gelation occurred less in a minute for hydrogel AA25-5.75.

At this point, it can be presumed that higher hydrazide/ aldehyde ratio tended to faster gel formation. It was also concluded that gel formation was observed even at very low polymer concentrations within 10 minutes for theoretical aldehyde substitution of 10%, 25% and 50%.

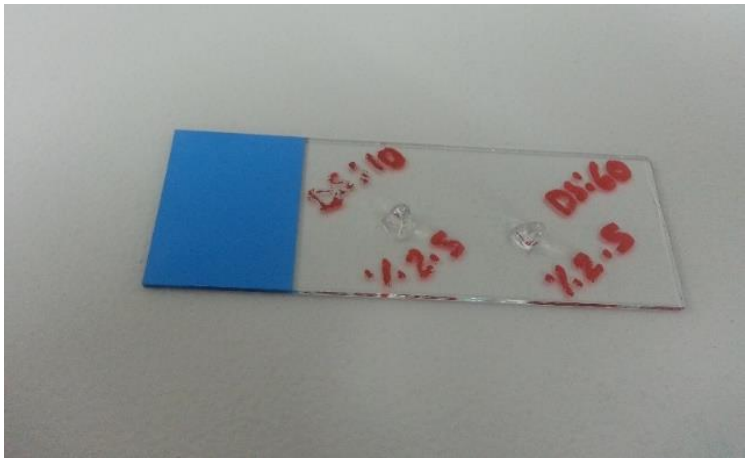

Figure 5.18 Alginate based hydrogels with number AA10-2 and AA50-1.8.

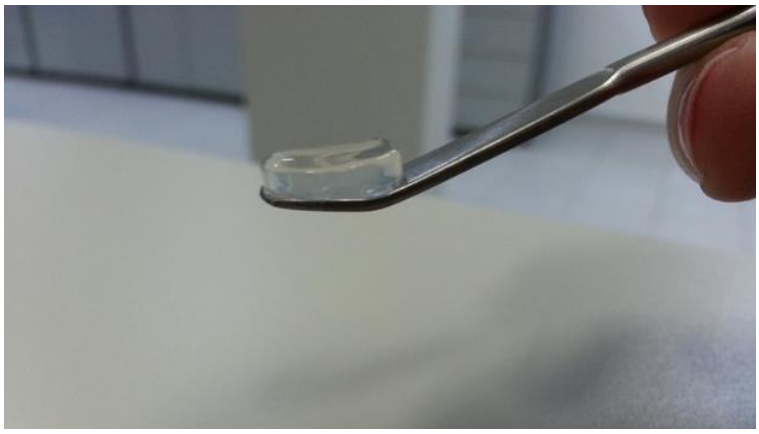

Figure 5.19 Alginate based hydrogel with number AA50-2.2.

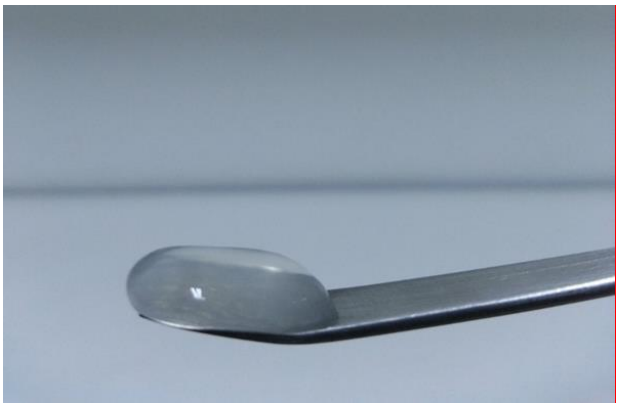

Figure 5.20 Alginate based hydrogel with number AA50-1.7.

Since mole ratio of aldehyde to hydrazide was kept lower than 1.0 to eliminate toxic effects *in vivo* due to potential reactivity of free aldehyde groups with amine groups in tissues, gels with higher relative aldehyde numbers were not prepared for protein containing hydrogel studies. Protein containing hydrogels were produced with AAP50(2)-2.55, AAP25-3.25 and AAP10-5.75. Laponite XLG containing hydrogels were also produced between 0.1% and 0.5% (w/v) in concentration.

5.4.4 Influence of Clay Addition on Swelling Behavior of Hydrogels

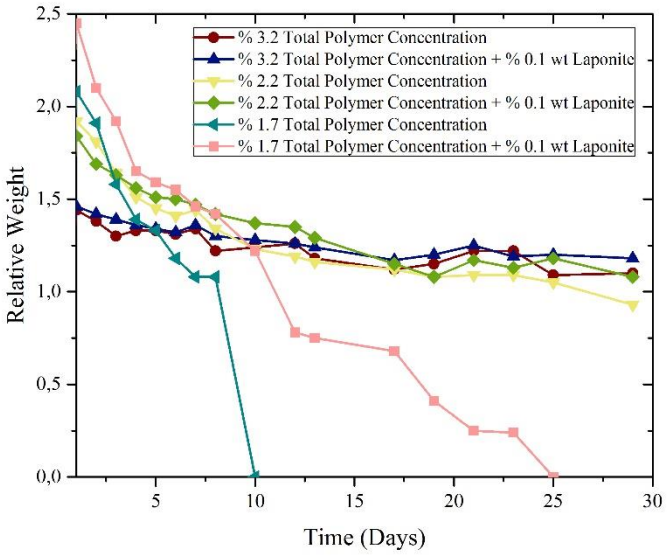

Figure 5.21 Relative weight ratio (w/w) change for alginate based hydrogels with number AA50-3.2, AA50-2.2 and AA50-1.7 and alginate based nanocomposite hydrogels for AAN50-3.2-0.1, AAN50-2.2-0.1 and AAN50-1.7-0.1 based on time.

Swelling has influence on degradation behavior of hydrogels. In addition, release mechanism is also affected by swelling characteristics. Thus, the influence of Laponite XLG addition on swelling was investigated for hydrogels with different total polymer concentrations.

Theoretical degree of substitution values of components were selected as 50% for aldehyde component and 60% for hydrazide components. Volumetric ratio of aldehyde to hydrazide parts were equal to 0.25 when hydrogel preparation. The moles of hydrazide groups were higher than aldehyde groups for all polymer concentration tested. It was seen that AA50-1.7 hydrogels with 1.7% (w/v) total polymer concentration degraded much faster compared to the other hydrogel samples. However, it is clear that incorporation of Laponite XLG delayed degradation time by approximately 15 days. Swelling profile became more stable with Laponite XLG addition for hydrogels number AAN50-3.2-0.1 and AAN50-2.2-0.1. Yet, it did not affect their degradation time significantly.

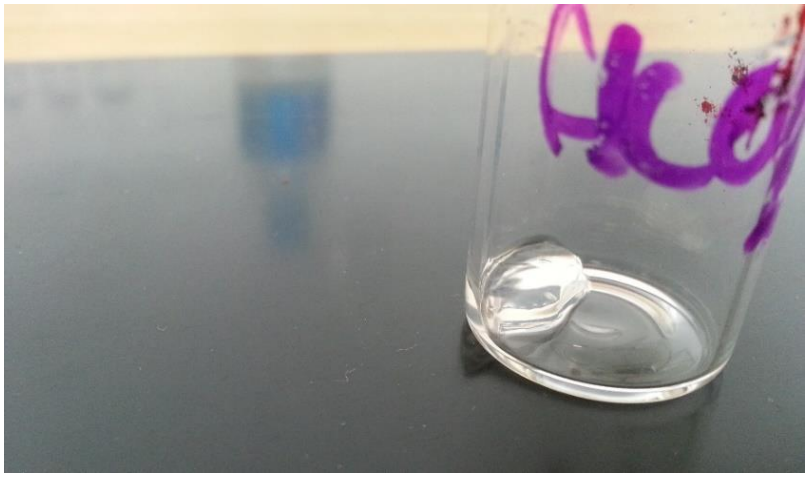

Figure 5.22 AAN50-3.2-0.1 numbered nanocomposite hydrogel with 3.2% polymer concentration and 0.1% Laponite XLG addition after 30 days.

Hydrogels with 3.2% total polymer concentration conserved their shape after 30 days as seen from Figure 5.22. After 5 months period, hydrogels with 3.2% polymer concentration completely degraded.

Secondly, Laponite XLG was added in the range between 0.1% and 0.5% (w/v) to AA50(2)-2.55 coded hydrogel with 1.24 hydrazide to aldehyde ratio. Pure hydrogels were degraded much faster. Incorporation of Laponite XLG was increased degradation time for all addition degrees. Produced hydrogels became rigid and fragile with 0.5% (w/v) Laponite XLG addition. Thus, it was contended that Laponite XLG addition must be kept lower than % 0.5 (w/v). Laponite XLG addition was selected between % 0.1 and % 0.3 for further hydrogel formation works. Swelling test are in the Appendix G.

5.4.5 Protein Release from Hydrogel Matrices

Protein was loaded into hydrogel with 0.2% (w/v) BSA addition. Protein was dissolved in buffer at the desired pH and molarity. Afterwards, protein solution was added into the hydrazide precursor. Protein was not loaded into aldehyde precursor due to possible reaction between aldehyde groups and amine groups. As discussed, it was presumed that protein do not react with aldehyde precursor in hydrazide solution due to low stability of imine bond. (157)

Release of BSA from hydrogel matrices was measured via Bradford Assay. Protein amount was measured in the medium to obtain released protein amount from hydrogel. Protein was loaded into hydrogels with % 0.2 (w/v) to AAP50(2)-2.55, AAP25-3.25 and AAP10-5.75. It was obtained for AAP50(2)-2.55 hydrogels that BSA was entrapped in the hydrogel after 3 days. Thus, release of protein was nearly completed.

Secondly, BSA-Laponite XLG complexes, which was interacted for 18 hours, were added into hydrazide precursor. Then it was mixed with aldehyde precursor. As a result, % 0.2 (w/v) BSA with % 0.2 (w/v) Laponite XLG addition was done to hydrogel coded AANP50(2)-2.55.

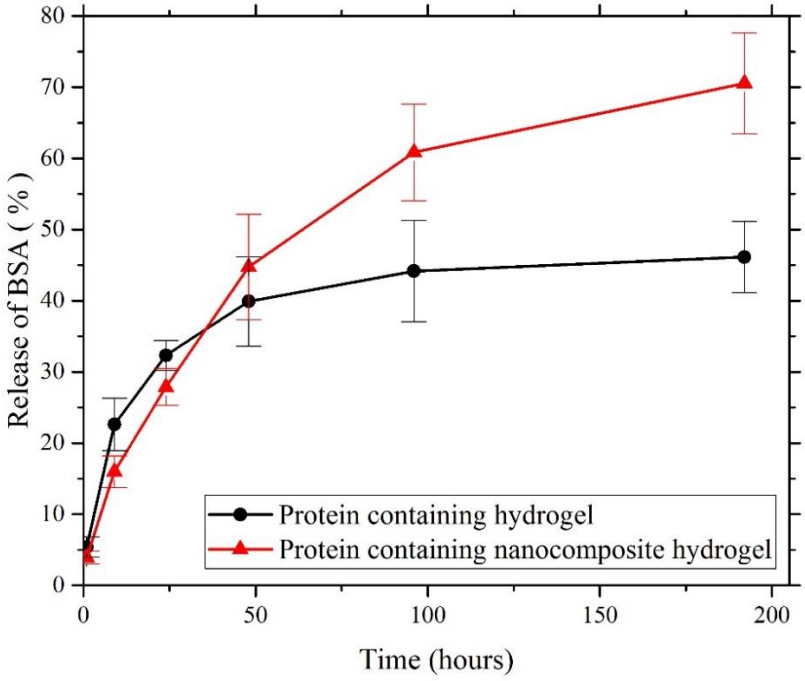

Figure 5.23 Comparison of release profiles of BSA and BSA-Laponite containing hydrogels.

Figure 5.23 showed that Laponite XLG addition has positive impact on burst release due to enhanced interaction between BSA and Laponite XLG. However, BSA release was comparably higher but more stable in the protein containing nanocomposite hydrogels.

CHAPTER VI

CONCLUSION

In this study, the outputs of the two research, the determination of interaction between BSA and Laponite XLG and hydrogel formation with hydrazone chemistry, were aimed to serve for controlled release of proteins. It was presumed that due to the incorporation of clay minerals, these hydrogels have higher drug loading capacity and provide a better control of protein release due to enhanced interaction. Drug loading capability was evaluated with adsorption capacity for different experimental conditions. It was found that increased weight ratio (BSA/Laponite XLG) led to an increase in adsorption capacity. In a same manner, higher adsorption capacity was attained for the samples prepared at pH 5.5 due to the closeness of the pI point of BSA. Effect of molarity was examined on adsorption for the samples prepared in 0.01 M and 0.05 M medium. Higher adsorption capacity data was found for the samples interacted in higher molarity. The outputs of the interaction study reveal that secondary protein structure was conserved for many interaction conditions, weight ratio, pH and molarity, according to FTIR analysis. Intercalated formation was analyzed with XRD for BSA-Laponite XLG complexes.

Secondly, hydrazone bond formation with biodegradable polymers namely alginate polysaccharide was designed. Hydrazone bond formation occurs within a short period, which prevents the diffusion of protein out of the matrix in an instant. The chemistry was comprised of biodegradable nature with linkages and components.

Injectable nanocomposite hydrogel formation was mainly aimed with various polymer concentration and degree of substitution values. Due to absence of reactive sites in alginate for hydrazone bond formation, aldehyde and hydrazide modification of alginate were conducted. Oxidation was done through the reaction between sodium periodate and alginate with % 10, % 25 and % 50 theoretical substitution degree. Secondly, alginate was reacted with adipic acid dihydrazide in the presence of 1-ethyl-3-(3-dimethylaminopropyl) carbodiimide/N-hydroxysuccinimide to obtain hydrazide modification. Modification was tested via FTIR, TNBS and carbazate assays.

After modification, alginate based injectable hydrogels were formed with various concentration of aldehyde and hydrazide components ranging from 1.7% to 5.75% (w/v). Fast gelation provides release of proteins in a controlled manner. It was obtained that polymer concentration had a great influence on decreasing gelation time. Gel formation was occured within seconds for AA50-5.75 coded hydrogels and within minutes for AA25-5.75 numbered hydrogels. Swelling test was conducted for pure hydrogels and Laponite XLG containing nanocomposite hydrogels with several polymer concentration to determine degradation behaviour. Laponite XLG addition increased degradation time approximately 15 days and swelling profile became more stable for hydrogels with 1.7% (w/v) polymer concentration.

Lastly, protein containing nanocomposite hydrogels were generated. The prominent part is that protein administered via BSA-Laponite XLG complexes, which were produced with an adsorption mechanism, into injectable hydrogel. Release of BSA was measured via Bradford Assay for hydrogels coded with AAP50(2)-2.55 and AANP50(2)-2.55. The model release study showed that BSA, which was adsorbed onto Laponite XLG, was released from hydrogel matrix in a more controlled manner. Thus, the generated hydrogel chemistry along with adsorption mechanism is a promising alternative for protein delivery and release applications.

CHAPTER VII

RECOMMENDATIONS

Alginate based hydrogel with hydrazone chemistry is promising due to fast gelation property and high stability for drug release applications. Bond chemistry is stable under neutral pH values while degrades in acidic pH values. This feature gains advantage for pH sensitive drug applications and cancer therapies. According to degradation studies, hydrogel samples conserve their shape after a long period. Degradation was relatively slow under pH 7.4 for hydrogels with hydrazone chemistry. The stability of the bond and degradation kinetic should be investigated under acidic pH values for the potential pH sensitive release applications.

Produced alginate based hydrogels can be utilized also for tissue engineering applications due to biodegradable features. For instance, most of the cartilage tissue engineering studies were done with biodegradable polymers and polysaccharides. Alginate based hydrogels can be used for cartilage tissue engineering studies instead of hyaluronic acid based injectable hydrogels. Another point is about the lack of degrading enzymes of alginate in mammals, which provide a better control of degradation and hydrogel properties *in vivo* than dextran based materials.

The hydrazide modification study of alginate was challenging due to high reactivity of alginate and increased pH value during reaction. pH adjustment via HCl solution may be tricky due to composed high acidic zones. Moreover, a significant molecular weight rise was occurred due to addition of dense pendant groups.

Thus, alginate hydrazide samples have high viscosity, which make inconvenience for gel formation. Hence, it is offered to use relatively low molecular weight alginate for hydrazide modification studies.

There is a gap in the literature about interaction of BSA and Laponite XLG. The outputs of the work can be adapted to stabilization of protein studies and nanocomposite hydrogel production with several chemistries.

Finally, protein release test was done with Bradford Assay. The assay is reliable and fast for protein determination. However, the interference could be occurred due to alginate based materials and Laponite XLG. Thus, the results of the protein release should be supported an additional test technique. HPLC detection for protein determination would enable a more sensitive measurement.

REFERENCES

1. Vermonden T, Censi R, Hennink WE. Hydrogels for Protein Delivery. Chem Rev. 2012;112:2853−288.
2. Manning MC, Chou DK, Murphy BM, Payne RW, Katayama DS. Expert Review Stability of Protein Pharmaceuticals : An Update. Pharm Res. 2010;27(4):544–75.
3. Harris JM, Chess RB. Effect of pegylation on pharmaceuticals. Nat Rev Drug Discov. 2003;2(3):214–21.
4. Patenaude MJ. Designing Injectable Hydrogel Biomaterials with Highly-Tunable Properties. 2014.
5. Li Y, Maciel D, Tomás H, Rodrigues J, Ma H, Shi X. pH sensitive Laponite/alginate hybrid hydrogels: swelling behaviour and release mechanism. Soft Matter. 2011;7(13):6231.
6. Huang X, Brazel CS. On the importance and mechanisms of burst release in matrix-controlled drug delivery systems. J Control Release. 2001;73:121–36.
7. Paul DR, Robeson LM. Polymer nanotechnology : Nanocomposites. Polymer (Guildf). 2008;49(15):3187–204.
8. Kiliaris P, Papaspyrides CD. Progress in Polymer Science Polymer / layered silicate (clay) nanocomposites : An overview of flame retardancy. Prog Polym Sci. 2010;35(7):902–58.
9. Dawson JI, Oreffo ROC. Clay : New Opportunities for Tissue Regeneration and Biomaterial Design. Adv Mater. 2013;4069–86.
10. Carretero MI. Clay minerals and their beneficial effects upon human health . A review. Appl Clay Sci. 2002;21:155–63.
11. Calamai L, Lozzi I, Stotzky G, Fusi P, Ristori GG. Interaction of catalase with montmorillonite homoionic to cations with different hydrophobicity: effect on enzymatic activity and microbial utilization. Soil Biol Biochem. 2000;32:815–23.
12. Hermanson GT. Bioconjugate Techniques. 3rd ed. Academic Press; 2013.
13. Vugmeyster Y. Pharmacokinetics and toxicology of therapeutic proteins: Advances and challenges. World J Biol Chem. 2012;3(4):73.
14. Walsh G. Pharmaceutical biotechnology products approved within the European Union. European Journal of Pharmaceutics and Biopharmaceutics.

2003. p. 3–10.

15. Banga AK. Therapeutic Peptides and Proteins: Formulation, Processing, and Delivery Systems. 2nd ed. Boca Raton, FL: CRC Press; 2006.

16. Small and large molecules [Internet]. [cited 2016 Aug 27]. Available from: http://pharma.bayer.com/en/innovation-partnering/technologies-and-trends/small-and-large-molecules/

17. Mahato RI. Biomaterials for Delivery and Targeting of Proteins and Nucleic Acids. New York. CRC Press; 2005.

18. Tessmar JK, Göpferich AM. Matrices and scaffolds for protein delivery in tissue engineering. Advanced Drug Delivery Reviews. 2007. p. 274–91.

19. Uchegbu, Ijeoma, Schatzlein A. Polymers in drug delivery. Boca Raton, FL: CRC Press; 2006.

20. Brange J, Andersen L, Laursen ED, Meyn G, Rasmussen E. Toward understanding insulin fibrillation. J Pharm Sci. 1997;86(5):517–25.

21. Kanematsu A, Marui A, Yamamoto S, Ozeki M, Hirano Y, Yamamoto M, et al. Type I collagen can function as a reservoir of basic fibroblast growth factor. J Control Release. 2004;99(2):281–92.

22. Schönherr E, Hausser HJ. Extracellular matrix and cytokines: a functional unit. Dev Immunol. 2000;7(2–4):89–101.

23. Mahato, Ram, Narang A. Pharmaceutical dosage forms and drug delivery. 2nd ed. CRC Press; 2011.

24. Uchegbu, Ijeoma, Schatzlein A. Polymers in drug delivery. Boca Raton, FL: CRC Press;

25. Viseras C, Cerezo P, Sanchez R, Salcedo I, Aguzzi C. Current challenges in clay minerals for drug delivery. Applied Clay Science. 2010. p. 291–5.

26. Controlled Release Delivery System [Internet]. [cited 2016 Sep 1]. Available from: https://www.maynepharma.com/our-capabilities/specialty-technologies/controlled-release-delivery-system/

27. Jensen KJ. Peptide and Protein Design for Biopharmaceutical Applications. Peptide and Protein Design for Biopharmaceutical Applications. 2009. 1-294 p.

28. Accurate Detection of API Release from Sustained-Release Tablets Using Near-Infrared Spectroscopy [Internet]. [cited 2016 Aug 29]. Available from: http://www.news-medical.net/whitepaper/20151208/Accurate-Detection-of-API-Release-from-Sustained-Release-Tablets-Using-Near-Infrared-Spectroscopy.aspx

29. Bhattarai N, Gunn J, Zhang M. Chitosan-based hydrogels for controlled, localized drug delivery. Advanced Drug Delivery Reviews. 2010. p. 83–99.

30. Lin CC, Metters AT. Hydrogels in controlled release formulations: Network design and mathematical modeling. Adv Drug Deliv Rev. 2006;58(12–13):1379–408.

31. Patenaude M, Hoare T. Injectable, Degradable Thermoresponsive Poly(N -isopropylacrylamide) Hydrogels. ACS Macro Lett. 2012;1(3):409–13.

32. Deng KL, Zhong HB, Tian T, Gou YB, Li Q, Dong LR. Drug release behavior of a pH/temperature sensitive calcium alginate/poly(N-acryloylglycine) bead with core-shelled structure. Express Polym Lett. 2010;4(12):773–80.

33. Peppas NA, Khare AR. Preparation, structure and diffusional behavior of hydrogels in controlled release. Adv Drug Deliv Rev. 1993;11(1–2):1–35.

34. Peppas NA, Bures P, Leobandung W, Ichikawa H. Hydrogels in pharmaceutical formulations. Eur J Pharm Biopharm. 2000;50(1):27–46.

35. Wichterle O, Lím D. Hydrophilic Gels for Biological Use. Nature. 1960;185(4706):117–8.

36. Bat E, Lin EW, Saxer S, Maynard HD. Morphing hydrogel patterns by thermo-reversible fluorescence switching. Macromol Rapid Commun. 2014;35(14):1260–5.

37. Boehnke N, Cam C, Bat E, Segura T, Maynard HD. Imine Hydrogels with Tunable Degradability for Tissue Engineering. Biomacromolecules. 2015;16(7):2101–8.

38. Qiu Y, Park K. Environment-sensitive hydrogels for drug delivery. Advanced Drug Delivery Reviews. 2012. p. 49–60.

39. Peppas NA, Hilt JZ, Khademhosseini A, Langer R. Hydrogels in biology and medicine: From molecular principles to bionanotechnology. Advanced Materials. 2006. p. 1345–60.

40. Jeong B, Bae YH, Lee DS, Kim SW. Biodegradable block copolymers as injectable drug-delivery systems. Nature. 1997;388(6645):860–2.

41. Holtz JH, Asher SA. Polymerized colloidal crystal hydrogel films as intelligent chemical sensing materials. Nature. 1997;389:829–32.

42. Beebe DJ, Moore JS, Bauer JM, Yu Q, Liu RH, Devadoss C, et al. Functional hydrogel structures for autonomous flow control inside microfluidic channels : Abstract : Nature. Nature. 2000;404(6778):588–90.

43. Rowley JA, Madlambayan G, Mooney DJ. Alginate hydrogels as synthetic extracellular matrix materials. Biomaterials. 1999;20(1):45–53.

44. Flory PJ, Rehner J. Statistical Mechanics of Cross-Linked Polymer Networks II. Swelling. J Chem Phys. 1943;11(11):521.

45. Flory PJ. Statistical Mechanics of Swelling of Network Structures. J Chem Phys. 1950;18(1950):108–11.

46. Bae KH, Wang L-S, Kurisawa M. Injectable biodegradable hydrogels: Progress and challenges. J Mater Chem B. 2013;1(40):5371–88.

47. Yan S, Wang T, Feng L, Zhu J, Zhang K, Chen X, et al. Injectable in situ self-cross-linking hydrogels based on poly(l -glutamic acid) and alginate for cartilage tissue engineering. Biomacromolecules. 2014;15(12):4495–508.

48. Jin Q, Schexnailder P, Gaharwar AK, Schmidt G. Silicate cross-linked bio-nanocomposite hydrogels from PEO and chitosan. Macromol Biosci. 2009;9(10):1028–38.

49. Patenaude M, Hoare T. Injectable, mixed natural-synthetic polymer hydrogels with modular properties. Biomacromolecules. 2012;13(2):369–78.

50. Jukes JM, van der Aa LJ, Hiemstra C, van Veen T, Dijkstra PJ, Zhong Z, et al. A newly developed chemically crosslinked dextran-poly(ethylene glycol) hydrogel for cartilage tissue engineering. Tissue Eng Part A. 2010;16(2):565–73.

51. Gaharwar AK, Peppas NA, Khademhosseini A. Nanocomposite hydrogels for biomedical applications. Biotechnol Bioeng. 2014;111(3):441–53.

52. Park H, Park K. Biocompatibility issues of implantable drug delivery systems. Pharmaceutical Research. 1996. p. 1770–6.

53. Fang J. Injectable Implant: goes in as a liquid, light locks it in place. [Internet]. [cited 2016 Aug]. Available from: http://www.zdnet.com/article/sap-allots-2-billion-for-iot-investments-buys-software-firm-plat-one/

54. Guan J, Hong Y, Ma Z, Wagner WR. Protein-reactive, thermoresponsive copolymers with high flexibility and biodegradability. Biomacromolecules. 2008;9(4):1283–92.

55. Moreira Teixeira LS, Leijten JCH, Wennink JWH, Chatterjea AG, Feijen J, van Blitterswijk CA, et al. The effect of platelet lysate supplementation of a dextran-based hydrogel on cartilage formation. Biomaterials. 2012;33(14):3651–61.

56. Hoemann CD, Sun J, Légaré A, McKee MD, Buschmann MD. Tissue engineering of cartilage using an injectable and adhesive chitosan-based cell-delivery vehicle. Osteoarthr Cartil. 2005;13(4):318–29.

57. Park H, Choi B, Hu J, Lee M. Injectable chitosan hyaluronic acid hydrogels for cartilage tissue engineering. Acta Biomater. 2013;9(1):4779–86.

58. Suh JK, Matthew HW. Application of chitosan-based polysaccharide biomaterials in cartilage tissue engineering: a review. Biomaterials. 2000;21(24):2589–98.

59. A different way to treat osteoarthritis knee pain [Internet]. [cited 2016 Aug 29]. Available from: http://www.synviscone.com/what-is-synvisc-one.aspx

60. Jin R, Teixeira LSM, Krouwels A, Dijkstra PJ, Van Blitterswijk CA, Karperien M, et al. Synthesis and characterization of hyaluronic acid-poly(ethylene glycol) hydrogels via Michael addition: An injectable biomaterial for cartilage repair. Acta Biomater. 2010;6(6):1968–77.

61. Choh S-Y, Cross D, Wang C. Facile synthesis and characterization of disulfide-cross-linked hyaluronic acid hydrogels for protein delivery and cell encapsulation. Biomacromolecules. 2011;12(4):1126–36.

62. Krishna UM, Martinez AW, Caves JM, Chaikof EL. Hydrazone self-crosslinking of multiphase elastin-like block copolymer networks. Acta Biomater. Acta Materialia Inc.; 2012;8(3):988–97.

63. Hardy JG, Lin P, Schmidt CE. Biodegradable hydrogels composed of oxime crosslinked poly(ethylene glycol), hyaluronic acid and collagen: a tunable platform for soft tissue engineering. J Biomater Sci Polym Ed. 2015;26(3):143–61.

64. Hiemstra C. In situ forming biodegradable hydrogels and their application for protein delivery. PhD [dissertion] University of Twente, 2007.

65. Ko DY, Shinde UP, Yeon B, Jeong B. Recent progress of in situ formed gels for biomedical applications. Prog Polym Sci. 2013;38(3–4):672–701.

66. Gaharwar AK, Dammu SA, Canter JM, Wu CJ, Schmidt G. Highly extensible, tough, and elastomeric nanocomposite hydrogels from poly(ethylene glycol) and hydroxyapatite nanoparticles. Biomacromolecules. 2011;12(5):1641–50.

67. Schexnailder P, Schmidt G. Nanocomposite polymer hydrogels. Colloid Polym Sci. 2009;287(1):1–11.

68. Wu CJ, Gaharwar AK, Schexnailder PJ, Schmidt G. Development of biomedical polymer-silicate nanocomposites: A materials science perspective. Materials (Basel). 2010;3(5):2986–3005.

69. Cypes SH, Saltzman WM, Giannelis EP. Organosilicate-polymer drug delivery systems: controlled release and enhanced mechanical properties. J Control Release. 2003;90(2):163–9.

70. Wu CJ, Schmidt G. Thermosensitive and dissolution properties in nanocomposite polymer hydrogels. Macromol Rapid Commun. 2009;30(17):1492–7.

71. Schoener CA, Peppas NA. pH-responsive hydrogels containing PMMA nanoparticles: an analysis of controlled release of a chemotherapeutic conjugate and transport properties. J Biomater Sci Polym Ed. 2013;24(9):1027–40.

72. Kamath KR, Park K. Biodegradable hydrogels in drug delivery. Adv Drug Deliv Rev. 1993;11(1–2):59–84.

73. Li Y, Tang Y, Narain R, Lewis AL, Armes SP. Biomimetic stimulus-responsive star diblock gelators. Langmuir. 2005;21(22):9946–54.

74. Hu Z, Xia X, Marquez M, Weng H, Tang L. Controlled release from and tissue response to physically bonded hydrogel nanoparticle assembly. In: Macromolecular Symposia. 2005. p. 275–84.

75. Bezemer JM, Radersma R, Grijpma DW, Dijkstra PJ, Feijen J, Van Blitterswijk CA. Zero-order release of lysozyme from poly(ethylene glycol)/poly(butylene terephthalate) matrices. J Control Release. 2000;64(1–3):179–92.

76. Larsson A, Ekblad T, Andersson O, Liedberg B. Photografted poly(ethylene glycol) matrix for affinity interaction studies. Biomacromolecules. 2007;8(1):287–95.

77. Werner C, Maitz MF, Sperling C. Current strategies towards hemocompatible coatings. J Mater Chem. 2007;17(32):3376.

78. Thienen TG Van, Thienen TG Van, Raemdonck K, Raemdonck K, Demeester J, Demeester J, et al. Protein Release form Biodegradable Dextran Nanogels. Langmuir. 2007;23(19):9794–801.

79. Censi R, Di Martino P, Vermonden T, Hennink WE. Hydrogels for protein delivery in tissue engineering. J Control Release. 2012;161(2):680–92.

80. Sinha VR, Trehan A. Biodegradable microspheres for protein delivery. J Control Release. 2003;90(3):261–80.

81. Caldorera-Moore M, Peppas NA. Micro- and nanotechnologies for intelligent and responsive biomaterial-based medical systems. Adv Drug Deliv Rev. 2009;61(15):1391–401.

82. He C, Kim SW, Lee DS. In situ gelling stimuli-sensitive block copolymer hydrogels for drug delivery. J Control Release. 2008;127(3):189–207.

83. Schweizer D, Serno T, Goepferich A. Controlled release of therapeutic antibody formats. Eur J Pharm Biopharm. 2014;88(2):291–309.

84. Pal B, Morris J. Perceived risks of joint infection following intra-articular corticosteroid injections: A survey of rheumatologists. Clin Rheumatol. 1999;18(3):264–5.

85. Cleland JL. Immunogenicity and injection site consideration. Protein Deliv: Phys Syst. 1997;30–4.

86. Rungseevijitprapa W, Bodmeier R. Injectability of biodegradable in situ forming microparticle systems (ISM). Eur J Pharm Sci. 2009;36(4–5):524–31.

87. Saluja A, Kalonia DS. Nature and consequences of protein-protein interactions in high protein concentration solutions. International Journal of

Pharmaceutics. 2008. p. 1–15.

88. Schweizer D, Schönhammer K, Jahn M, Göpferich A. Protein-polyanion interactions for the controlled release of monoclonal antibodies. Biomacromolecules. 2013;14(1):75–83.

89. Zhang Y, Chan HF, Leong KW. Advanced materials and processing for drug delivery: the past and the future. Adv Drug Deliv Rev. 2013;65(1):104–20.

90. Kretlow JD, Klouda L, Mikos AG. Injectable matrices and scaffolds for drug delivery in tissue engineering. Adv Drug Deliv Rev. 2007;59(4–5):263–73.

91. Hoare TR, Kohane DS. Hydrogels in drug delivery: Progress and challenges. Polymer (Guildf). Elsevier Ltd; 2008;49(8):1993–2007.

92. Patenaude M, Smeets NMB, Hoare T. Designing injectable, covalently cross-linked hydrogels for biomedical applications. Macromol Rapid Commun. 2014;35(6):598–617.

93. Patenaude MJ. Designing Injectable Hydrogel Biomaterials with Highly-Tuneable Properties. PhD [dissertion]. McMaster University, 2014.

94. Sivakumaran D, Maitland D, Hoare T. Injectable microgel-hydrogel composites for prolonged small-molecule drug delivery. Biomacromolecules. 2011;12(11):4112–20.

95. MIXPAC™ L-System [Internet]. [cited 2016 Aug 29]. Available from: https://www.sulzer.com/da/Products-and-Services/Mixpac-Cartridges-Applications-Static-Mixers/Healthcare-Mixing-Systems/Dental/MIXPAC-L-System

96. C.A. H, Norde W. Globular proteins at solid/liquid interfaces. Colloids Surfaces B Biointerfaces. 1994;2:517–66.

97. Ding X, Henrichs SM. Adsorption and desorption of proteins and polyamino acids by clay minerals and marine sediments. Mar Chem. 2002;77(4):225–37.

98. Yu WH, Li N, Tong DS, Zhou CH, Lin CX, Xu CY. Adsorption of proteins and nucleic acids on clay minerals and their interactions: A review. Applied Clay Science. 2013. p. 443–52.

99. Aguzzi C, Cerezo P, Viseras C, Caramella C. Use of clays as drug delivery systems: Possibilities and limitations. Appl Clay Sci. 2007;36(1–3):22–36.

100. Barral S, Villa-García MA, Rendueles M, Díaz M. Interactions between whey proteins and kaolinite surfaces. Acta Mater. 2008;56(12):2784–90.

101. Fejer I, Kata M, Eross I, Dekany I. Interaction of monovalent cationic drugs with montmorillonite. Colloid Polym Sci. 2002;280(4):372–9.

102. Chen GJ, Yen MC, Wang JM, Lin JJ, Chiu HC. Layered inorganic/enzyme nanohybrids with selectivity and structural stability upon interacting with

biomolecules. Bioconjug Chem. 2008;19(1):138–44.

103. Castela-Papin N, Cai S, Vatier J, Keller F, Souleau CH, Farinotti R. Drug interactions with diosmectite: A study using the artificial stomach-duodenum model. Int J Pharm. 1999;182(1):111–9.

104. Johnston CT, Premachandra GS, Szabo T, Lok J, Schoonheydt RA. Interaction of biological molecules with clay minerals: A combined spectroscopic and sorption study of lysozyme on saponite. Langmuir. 2012;28(1):611–9.

105. Rodrigues LA de S, Figueiras A, Veiga F, de Freitas RM, Nunes LCC, da Silva Filho EC, et al. The systems containing clays and clay minerals from modified drug release: A review. Colloids Surfaces B Biointerfaces. 2013;103:642–51.

106. Perkins WD. Fourier transform-infrared spectroscopy: Part l. Instrumentation. J Chem Educ. 1986;63(1):A5.

107. Berthomieu C, Hienerwadel R. Fourier transform infrared (FTIR) spectroscopy. Photosynth Res. 2009;101(2–3):157–70.

108. Barth A. Infrared spectroscopy of proteins. Biochimica et Biophysica Acta - Bioenergetics. 2007. p. 1073–101.

109. Perkins WD. Fourier transform infrared spectroscopy. Part III. Applications. J Chem Educ. 1987;64(12):A296–305.

110. Thermal Gravimetric Analysis [Internet]. [cited 2016 Sep 1]. Available from: https://www.uab.edu/engineering/home/images/downloads/TGA_UAB_TA_MAy_absolute_final_2014.pdf

111. Agilent Te. UV-visible spectroscopy. Royal Society of Chemistry. 2000. p. 22.

112. Habeeb AFSA. Determination of free amino groups in protein by trinitrobenzene sulfonic acid. Anal Biochem 14, 328. 1966;14:328.

113. TNBS [Internet]. [cited 2016 Aug 29]. Available from: http://www.gbiosciences.com/pdf/protocol/tnbs.pdf

114. Otles, S. Methods of Analysis of Food Components and Additives, 2nd ed. CRC Press; 2011.

115. Taratula O. Nanotechnology in Developing Multifunctional Non-viral Gene Delivery Systems. 2008.

116. Bradford protein assay [Internet]. Available from: https://en.wikipedia.org/wiki/Bradford_protein_assay

117. Liu J, Willför S, Xu C. A review of bioactive plant polysaccharides: Biological activities, functionalization, and biomedical applications. Bioact Carbohydrates Diet Fibre. 2015;5(1):31–61.

118. Gomez CG, Rinaudo M, Villar MA. Oxidation of sodium alginate and characterization of the oxidized derivatives. Carbohydr Polym. 2007;67(3):296–304.

119. Maia J, Ferreira L, Carvalho R, Ramos MA, Gil MH. Synthesis and characterization of new injectable and degradable dextran-based hydrogels. Polymer (Guildf). 2005;46(23):9604–14.

120. Hudson SP, Langer R, Fink GR, Kohane DS. Injectable in situ cross-linking hydrogels for local antifungal therapy. Biomaterials. 2010;31(6):1444–52.

121. Cheng Y, Nada AA, Valmikinathan CM, Lee P, Liang D, Yu X, et al. In situ gelling polysaccharide-based hydrogel for cell and drug delivery in tissue engineering. J Appl Polym Sci. 2014;131(4):1–11.

122. Weng L, Romanov A, Rooney J, Chen W. Non-cytotoxic, in situ gelable hydrogels composed of N-carboxyethyl chitosan and oxidized dextran. Biomaterials. 2008;29(29):3905–13.

123. Wang Y, Lapitsky Y, Kang CE, Shoichet MS. Accelerated release of a sparingly soluble drug from an injectable hyaluronan-methylcellulose hydrogel. J Control Release. 2009;140(3):218–23.

124. Baumann MD, Kang CE, Stanwick JC, Wang Y, Kim H, Lapitsky Y, et al. An injectable drug delivery platform for sustained combination therapy. J Control Release. 2009;138(3):205–13.

125. Hirakura T, Yasugi K, Nemoto T, Sato M, Shimoboji T, Aso Y, et al. Hybrid hyaluronan hydrogel encapsulating nanogel as a protein nanocarrier: New system for sustained delivery of protein with a chaperone-like function. J Control Release. 2010;142(3):483–9.

126. Ishihara M, Obara K, Nakamura S, Fujita M, Masuoka K, Kanatani Y, et al. Chitosan hydrogel as a drug delivery carrier to control angiogenesis. J Artif Organs. 2006;9(1):8–16.

127. Malesu kumar, Vijay SD. Chitosan–sodium alginate nanocomposites blended with Cloisite 30B as a novel drug delivery system for anticancer drug curcumin. Int J Appl Biol Pharm Technol. 2011;2(3):402–11.

128. Li X, Weng Y, Kong X, Zhang B, Li M, Diao K, et al. A covalently crosslinked polysaccharide hydrogel for potential applications in drug delivery and tissue engineering. J Mater Sci Mater Med. 2012;23(12):2857–65.

129. Lee KY, Alsberg E, Mooney DJ. Degradable and injectable poly(aldehyde guluronate) hydrogels for bone tissue engineering. J Biomed Mater Res. 2001;56(2):228–33.

130. Bhatia SK, Arthur SD, Chenault HK, Kodokian GK. Interactions of polysaccharide-based tissue adhesives with clinically relevant fibroblast and

macrophage cell lines. Biotechnol Lett. 2007;29(11):1645–9.

131. Jia X, Colombo G, Padera R, Langer R, Kohane DS. Prolongation of sciatic nerve blockade by in situ cross-linked hyaluronic acid. Biomaterials. 2004;25(19):4797–804.

132. Kristiansen KA, Tomren HB, Christensen BE. Periodate oxidized alginates: Depolymerization kinetics. Carbohydr Polym. 2011;86(4):1595–601.

133. Song Z, Yin J, Luo K, Zheng Y, Yang Y, Li Q, et al. Layer-by-Layer buildup of Poly(L-glutamic acid)/Chitosan film for biologically active coating. Macromol Biosci. 2009;9(3):268–78.

134. Balakrishnan B, Jayakrishnan A. Self-cross-linking biopolymers as injectable in situ forming biodegradable scaffolds. Biomaterials. 2005;26(18):3941–51.

135. Shoichet MS, Li RH, White ML, Winn SR. Stability of hydrogels used in cell encapsulation: An in vitro comparison of alginate and agarose. Biotechnol Bioeng. 1996;50(4):374–81.

136. Boontheekul T, Kong HJ, Mooney DJ. Controlling alginate gel degradation utilizing partial oxidation and bimodal molecular weight distribution. Biomaterials. 2005;26(15):2455–65.

137. Tan R, Feng Q, She Z, Wang M, Jin H, Li J, et al. In vitro and in vivo degradation of an injectable bone repair composite. Polym Degrad Stab. 2010;95(9):1736–42.

138. Bouhadir KH, Lee KY, Alsberg E, Damm KL, Anderson KW, Mooney DJ. Degradation of partially oxidized alginate and its potential application for tissue engineering. Biotechnol Prog. 2001;17(5):945–50.

139. Al-Shamkhani A, Duncan R. Synthesis, controlled release properties and antitumour activity of alginate-cis-aconityl-daunomycin conjugates. Int J Pharm. 1995;122(1–2):107–19.

140. Spargo BJ, Rudolph AS, Rollwagen FM. Recruitment of tissue resident cells to hydrogel composites: in vivo response to implant materials. Biomaterials. 1994;15(10):853–8.

141. Otterlei M, Ostgaard K, Skjåk-Braek G, Smidsrød O, Soon-Shiong P, Espevik T. Induction of cytokine production from human monocytes stimulated with alginate. J Immunother (1991). 1991;10(4):286–91.

142. Cappai A, Petruzzo P, Ruiu G, Congiu T, Dessy E, De Seta W, et al. Evaluation of new small barium alginate microcapsules. Int J Artif Organs. 1995;18(2):96–102.

143. Gombotz WR, Wee S. Protein release from alginate matrixes. Adv Drug Deliv Rev. 1998;31(3):267–85.

144. Balakrishnan B, Lesieur S, Labarre D, Jayakrishnan A. Periodate oxidation

of sodium alginate in water and in ethanol-water mixture: A comparative study. Carbohydr Res. 2005;340(7):1425–9.

145. Jeon O, Alt DS, Ahmed SM, Alsberg E. The effect of oxidation on the degradation of photocrosslinkable alginate hydrogels. Biomaterials. 2012;33(13):3503–14.

146. Bouhadir KH, Alsberg E, Mooney DJ. Hydrogels for combination delivery of antineoplastic agents. Biomaterials. 2001;22(19):2625–33.

147. Garver JM, Gronert S, Bierbaum VM. Experimental Validation of the α-Effect in the Gas Phase. J Am Chem Soc. 2011;133(35):13894–7.

148. Vetrik M, Pradny M, Hruby M, Michalek J. Hydrazone-based hydrogel hydrolytically degradable in acidic environment. Polym Degrad Stab. 2011;96(5):756–9.

149. Kalia J, Raines RT. Hydrolytic stability of hydrazones and oximes. Angew Chemie - Int Ed. 2008;47(39):7523–6.

150. Carbodiimide Crosslinker Chemistry [Internet]. Thermo Fischer. [cited 2016 Sep 1]. Available from: https://www.thermofisher.com/tr/en/home/life-science/protein-biology/protein-biology-learning-center/protein-biology-resource-library/pierce-protein-methods/carbodiimide-crosslinker-chemistry.html

151. Etrych T, Kovar L, Strohalm J, Chytil P, Rihova B, Ulbrich K. Biodegradable star HPMA polymer-drug conjugates: Biodegradability, distribution and anti-tumor efficacy. J Control Release. 2011;154(3):241–8.

152. Zhou Z, Li L, Yang Y, Xu X, Huang Y. Tumor targeting by pH-sensitive, biodegradable, cross-linked N-(2-hydroxypropyl) methacrylamide copolymer micelles. Biomaterials. 2014;35(24):6622–35.

153. Xu Z, Liu S, Kang Y, Wang M. Glutathione- and pH-responsive nonporous silica prodrug nanoparticles for controlled release and cancer therapy. Nanoscale. 2015;7(13):5859–68.

154. Ulbrich K, Etrych T, Chytil P, Pechar M, Jelinkova M, Rihova B. Polymeric anticancer drugs with pH-controlled activation. In: International Journal of Pharmaceutics. 2004. p. 63–72.

155. Martínez-Sanz E, Ossipov DA, Hilborn J, Larsson S, Jonsson KB, Varghese OP. Bone reservoir: Injectable hyaluronic acid hydrogel for minimal invasive bone augmentation. J Control Release. 2011;152(2):232–40.

156. Luo Y, Kobler JB, Heaton JT, Jia X, Zeitels SM, Langer R. Injectable hyaluronic acid-dextran hydrogels and effects of implantation in ferret vocal fold. J Biomed Mater Res - Part B Appl Biomater. 2010;93(2):386–93.

157. Maynard HD, Broyer RM KC. In: Click Chemistry for Biotechnology and Materials Science. In: J L, editor. In: Click Chemistry for Biotechnology and

Materials Science. West Sussex, UK: Wiley, Inc.; 2009. p. 53–68.

158. Yang X, Bakaic E, Hoare T, Cranston ED. Injectable polysaccharide hydrogels reinforced with cellulose nanocrystals: Morphology, rheology, degradation, and cytotoxicity. Biomacromolecules. 2013;14(12):4447–55.

159. De Figueirêdo MCB, De Freitas Rosa M, Lie Ugaya CM, De Souza Filho MDSM, Da Silva Braid ACC, De Melo LFL. Life cycle assessment of cellulose nanowhiskers. J Clean Prod. 2012;35:130–9.

160. Jackson JK, Letchford K, Wasserman BZ, Ye L, Hamad WY, Burt HM. The use of nanocrystalline cellulose for the binding and controlled release of drugs. Int J Nanomedicine. 2011;6:321–30.

161. Mateen R, Hoare T. Injectable, in situ gelling, cyclodextrin–dextran hydrogels for the partitioning-driven release of hydrophobic drugs. J Mater Chem B. Royal Society of Chemistry; 2014;2(32):5157.

162. Campbell SB, Patenaude M, Hoare T. Injectable superparamagnets: Highly elastic and degradable poly(N-isopropylacrylamide)-superparamagnetic iron oxide nanoparticle (SPION) composite hydrogels. Biomacromolecules. 2013;14(3):644–53.

163. Lee KY, Bouhadir KH, Mooney DJ. Degradation behavior of covalently cross-linked poly(aldehyde guluronate) hydrogels. Macromolecules. 2000;33(1):97–101.

164. Dahlmann J, Krause A, Moller L, Kensah G, Mowes M, Diekmann A, et al. Fully defined in situ cross-linkable alginate and hyaluronic acid hydrogels for myocardial tissue engineering. Biomaterials. Elsevier Ltd; 2013;34(4):940–51.

165. Choi YS, Hong SR, Lee YM, Song KW, Park MH, Nam YS. Study on gelatin-containing artificial skin: I. Preparation and characteristics of novel gelatin-alginate sponge. Biomaterials. 1999;20(5):409–17.

166. Suzuki Y, Nishimura Y, Tanihara M, Suzuki K, Nakamura T, Shimizu Y, et al. Evaluation of a novel alginate gel dressing: Cytotoxicity to fibroblasts in vitro and foreign-body reaction in pig skin in vivo. J Biomed Mater Res. 1998;39(2):317–22.

167. Gomez CG, Chambat G, Heyraud A, Villar M, Auzely-Velty R. Synthesis and characterization of a b-CD-alginate conjugate. Polymer (Guildf). 2006;47(26):8509–16.

168. Tan R, She Z, Wang M, Fang Z, Liu Y, Feng Q. Thermo-sensitive alginate-based injectable hydrogel for tissue engineering. Carbohydr Polym. 2012;87(2):1515–21.

169. Wang M. Preliminary study on the fabrication of Alginate/Hyaluronic Acid scaffolds for spinal cord injury repair. Ms. [Thesis], University of

Saskatchewan, 2012.

170. Li J, Ma J, Jiang T, Wang Y, Wen X, Li G. Constructing Biopolymer-Inorganic Nanocomposite through a Biomimetic Mineralization Process for Enzyme Immobilization. Materials (Basel). 2015;8(9):6004–17.

171. Hiemstra C, Zhong Z, Van Tomme SR, van Steenbergen MJ, Jacobs JJL, Otter W Den, et al. In vitro and in vivo protein delivery from in situ forming poly(ethylene glycol)-poly(lactide) hydrogels. J Control Release. 2007;119(3):320–7.

172. Hiemstra C, Zhong Z, van Steenbergen MJ, Hennink WE, Feijen J. Release of model proteins and basic fibroblast growth factor from in situ forming degradable dextran hydrogels. J Control Release. 2007;122(1):71–8.

173. Mansur HS, Lobato ZP, Oréfice RL, Vasconcelos WL, Oliveira C, Machado LJ. Surface functionalization of porous glass networks: effects on bovine serum albumin and porcine insulin immobilization. Biomacromolecules. 2000;1(4):789–97.

174. Lin JJ, Wei JC, Juang TY, Tsai WC. Preparation of protein-silicate hybrids from polyamine intercalation of layered montmorillonite. Langmuir. 2007;23(4):1995–9.

175. Causserand C, Kara Y, Aimar P. Protein fractionation using selective adsorption on clay surface before filtration. J Memb Sci. 2001;186(2):165–81.

176. Alkan M, Demirbas O, Dogan M, Arslan O. Surface properties of bovine serum albumin - adsorbed oxides: Adsorption, adsorption kinetics and electrokinetic properties. Microporous Mesoporous Mater. 2006;96(1–3):331–40.

177. Tu J, Cao Z, Jing Y, Fan C, Zhang C, Liao L, et al. Halloysite nanotube nanocomposite hydrogels with tunable mechanical properties and drug release behavior. Compos Sci Technol. 2013;85:126–30.

178. Levis SR, Deasy PB. Characterisation of halloysite for use as a microtubular drug delivery system. Int J Pharm. 2002;243(1–2):125–34.

179. Ruzicka, Barbara, Zaccarelli E. A fresh look at the Laponite phase diagram. Soft Matter. 2011;7:1268–86.

180. Kegel WK, Lekkerkerker HNW. Colloidal gels: Clay goes patchy. Nat Mater. 2011;10(1):5–6.

181. Wang T, Liu D, Lian C, Zheng S, Liu X, Tong Z. Large deformation behavior and effective network chain density of swollen poly(N-isopropylacrylamide)–Laponite nanocomposite hydrogels. Soft Matter. 2012;8(3):774.

182. Chang C-W, van Spreeuwel A, Zhang C, Varghese S. PEG/clay

nanocomposite hydrogel: a mechanically robust tissue engineering scaffold. Soft Matter. 2010;6:5157.

183. Wu CJ, Gaharwar AK, Chan BK, Schmidt G. Mechanically tough Pluronic F127/Laponite nanocomposite hydrogels from covalently and physically cross-linked networks. Macromolecules. 2011;44(20):8215–24.

184. Gaharwar AK, Schexnailder PJ, Kline BP, Schmidt G. Assessment of using Laponite cross-linked poly(ethylene oxide) for controlled cell adhesion and mineralization. Acta Biomater. 2011;7(2):568–77.

185. Ghadiri M, Hau H, Chrzanowski W, Agus H, Rohanizadeh R. Laponite clay as a carrier for in situ delivery of tetracycline. RSC Adv. 2013;3(43):20193.

186. Loginov M, Lebovka N, Vorobiev E. Laponite assisted dispersion of carbon nanotubes in water. J Colloid Interface Sci. 2012;365(1):127–36.

187. Skelton S, Bostwick M, O'Connor K, Konst S, Casey S, Lee BP. Biomimetic adhesive containing nanocomposite hydrogel with enhanced materials properties. Soft Matter. 2013;9(14):3825.

188. Mahdavinia GR, Massoudi A, Baghban A, Massoumi B. Novel carrageenan-based hydrogel nanocomposites containing laponite RD and their application to remove cationic dye. Iran Polym J (English Ed. 2012;21(9):609–19.

189. Pálková H, Madejová J, Zimowska M, Serwicka EM. Laponite-derived porous clay heterostructures: II. FTIR study of the structure evolution. Microporous Mesoporous Mater. 2010;127(3):237–44.

190. Coburn JM, Kaplan DL. Engineering Biomaterial-Drug Conjugates for Local and Sustained Chemotherapeutic Delivery. Bioconjug Chem. 2015;26(7):1212–23.

191. Jung H, Kim HM, Choy Y Bin, Hwang SJ, Choy JH. Laponite-based nanohybrid for enhanced solubility and controlled release of itraconazole. Int J Pharm. 2008;349(1–2):283–90.

192. Wang S, Wu Y, Guo R, Huang Y, Wen S, Shen M, et al. Laponite nanodisks as an efficient platform for doxorubicin delivery to cancer cells. Langmuir. 2013;29(16):5030–6.

193. Li K, Wang S, Wen S, Tang Y, Li J, Shi X, et al. Enhanced in vivo antitumor efficacy of doxorubicin encapsulated within laponite nanodisks. ACS Appl Mater Interfaces. 2014;6(15):12328–34.

194. Li C, Mu C, Lin W, Ngai T. Gelatin Effects on the Physicochemical and Hemocompatible Properties of Gelatin/PAAm/Laponite Nanocomposite Hydrogels. ACS Appl Mater Interfaces. 2015;7(33):18732–41.

195. Goncalves M, Figueira P, Maciel D, Rodrigues J, Qu X, Liu C, et al. PH-sensitive Laponite/doxorubicin/alginate nanohybrids with improved anticancer efficacy. Acta Biomater. 2014;10(1):300–7.

196. Yan J, Du YZ, Chen FY, You J, Yuan H, Hu FQ. Effect of proteins with different isoelectric points on the gene transfection efficiency mediated by stearic acid grafted chitosan oligosaccharide micelles. Mol Pharm. 2013;10(7):2568–77.

197. Aitken A, Learmonth MP. Protein Determination by UV Absorption. Protein Protoc Handb. 2002;205(3):3–6.

198. Reger M, Sekine T, Okamoto T, Watanabe K, Hoffmann H. Pickering emulsions stabilized by novel clay–hydrophobin synergism. Soft Matter. 2011;7(22):11021.

199. De Lisi R, Lazzara G, Milioto S, Muratore N. Aqueous nonionic copolymer-functionalized laponite clay. A thermodynamic and spectrophotometric study to characterize its behavior toward an organic material. Langmuir. 2006;22(19):8056–62.

200. Guimarães ADMF, Ciminelli VST, Vasconcelos WL. Surface modification of synthetic clay aimed at biomolecule adsorption: synthesis and characterization. Mater Res. 2007;10(1):37–41.

201. Raneque, Rapado Manuel, Rodriguez, Rodriguez Alejandro, Covas PC. Hydrogel wound dressing preparation at laboratory scale by using electron beam and gamma radiation. Ciencias Nucl. 2013;53:24–31.

202. Palkova H, Madejova J, Zimowska M, Bielanska E, Olejniczak Z, Litynska-Dobrzynska L, et al. Laponite-derived porous clay heterostructures: I. Synthesis and physicochemical characterization. Microporous Mesoporous Mater. 2010;127(3):228–36.

203. Paul PK, Hussain SA, Bhattacharjee D, Pal M. Preparation of polystyrene-clay nanocomposite by solution intercalation technique. Bull Mater Sci. 2013;36(3):361–6.

204. Bouhekka A, Bürgi T. In situ ATR-IR spectroscopy study of adsorbed protein: Visible light denaturation of bovine serum albumin on TiO 2. Appl Surf Sci. 2012;261:369–74.

205. Huang P, Li Z, Hu H, Cui D. Synthesis and Characterization of Bovine Serum Albumin-Conjugated Copper Sulfide Nanocomposites. J Nanomater. 2010;2010:1–6.

206. Protein Secondary Structural Analysis by FTIR [Internet]. [cited 2016 Sep 1]. Available from: http://www.shimadzu.com/an/industry/pharmaceuticallifescience/proteome0205005.htm

207. Li H, Li M, Wang Y, Zhang W. Luminescent hybrid materials based on laponite clay. Chemistry. 2014;20(33):10392–6.

208. Maia J, Evangelista MB, Gil H, Ferreira L. 2 . Dextran-based materials for

biomedical applications. 2014;661(2):31–53.

209. Sankalia MG, Mashru RC, Sankalia JM, Sutariya VB. Papain entrapment in alginate beads for stability improvement and site-specific delivery: physicochemical characterization and factorial optimization using neural network modeling. AAPS PharmSciTech. 2005;6(2):E209–22.

210. Pascalau V, Popescu V, Popescu GL, Dudescu MC, Borodi G, Dinescu AM, et al. Obtaining and characterizing alginate/k-carrageenan hydrogel cross-linked with adipic dihydrazide. Adv Mater Sci Eng. 2013;2013.

211. Yanez M, Maria C De, Rincon J, Boland T. Printable Biodegradable Hydrogel with Self-Crosslinking Agents for Wound Dressings. NIP Digit Fabr. 2011;27(1):632–5.

212. Haug A LB. Solubility of Alginate at Low Ph. Acta Chem Scand. 1963;17(6):1653–62.

213. Mateen R, Hoare T. Carboxymethyl and hydrazide functionalized b-cyclodextrin derivatives: A systematic investigation of complexation behaviours with the model hydrophobic drug dexamethasone. Int J Pharm. 2014;472(1–2):315–26.

APPENDIX A

CALIBRATION CURVE OF BSA

BSA calibration curve was obtained for the samples in the range between 0.05 and 1.5 mg/ml concentration. Absorbance of the samples were measured at 280 nm via UV-VIS spectrophotometer.

A.1. BSA Calibration Curve-1

Calibration curve was obtained for the samples in 0.05 M and pH 5.5 PB.

Table 9-1 Calibration curve data for the samples in 0.05 M, pH 5.5 PB.

Concentration (mg/ml)	Absorbance 1	Absorbance 2	Absorbance 3	Average Absorbance
0.05	0.029	0.029	0.029	0.029
0.2	0.118	0.117	0.117	0.117
0.5	0.298	0.297	0.298	0.298
0.7	0.426	0.427	0.427	0.427
1	0.601	0.602	0.601	0.601
1.3	0.775	0.784	0.787	0.782
1.5	0.911	0.91	0.911	0.911

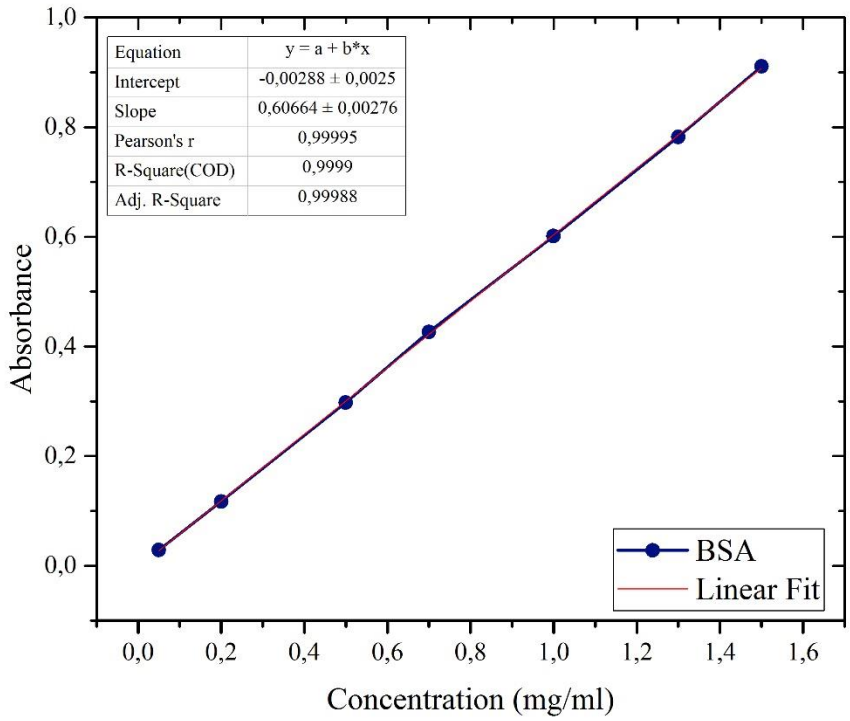

Figure 9.1 Calibration Curve of BSA in 0.05 M, pH 5.5 PB.

A.2. BSA Calibration Curve-2

Calibration curve was prepared for the samples in 0.05 M and pH 7.4 PB.

Table 9-2 Calibration curve data for the samples in 0.05 M and pH 7.4 PB.

Concentration (mg/ml)	Absorbance 1	Absorbance 2	Absorbance 3	Average Absorbance
0.05	0.029	0.029	0.030	0.029
0.2	0.120	0.122	0.115	0.119
0.5	0.304	0.303	0.304	0.304
0.7	0.427	0.427	0.428	0.427
1	0.602	0.610	0.609	0.607
1.3	0.778	0.785	0.781	0.781
1.5	0.908	0.911	0.916	0.912

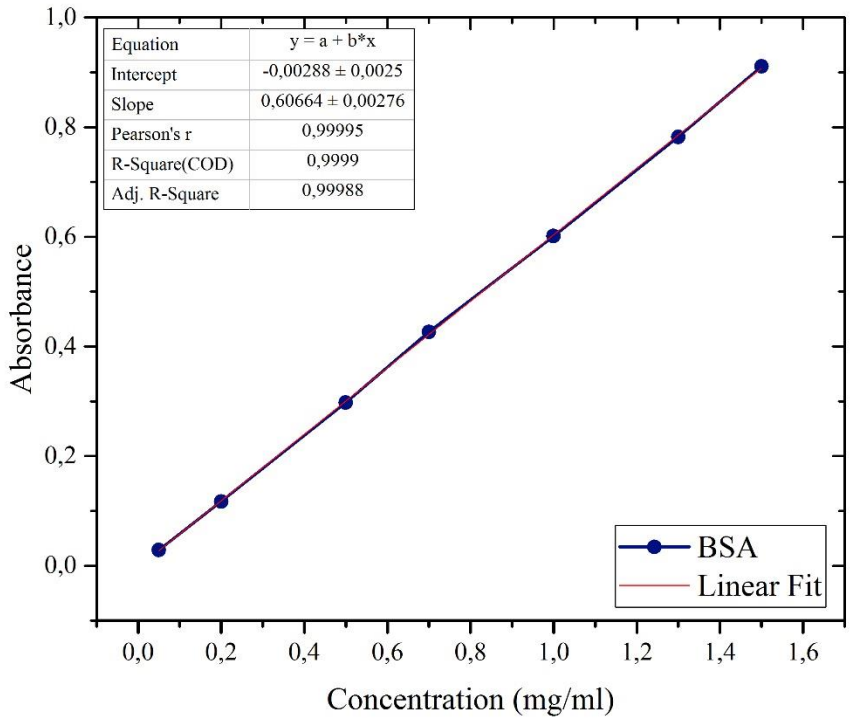

Figure 9.2 Calibration Curve of BSA in 0.05 M, pH 7.4 PB.

A.3. BSA Calibration Curve-3

Calibration curve was prepared for the samples in 0.01 M and pH 7.4 PB.

Table 9-3 Calibration curve data for the samples in 0.01 M and pH 7.4 PB.

Concentration (mg/ml)	Absorbance 1	Absorbance 2	Absorbance 4	Average Absorbance
0.05	0.030	0.031	0.030	0.0305
0.2	0.116	0.115	0.113	0.115
0.5	0.289	0.289	0.288	0.289
0.7	0.397	0.403	0.403	0.402
1	0.591	0.591	0.591	0.591
1.3	0.776	0.777	0.769	0.774
1.5	0.874	0.881	0.877	0.877

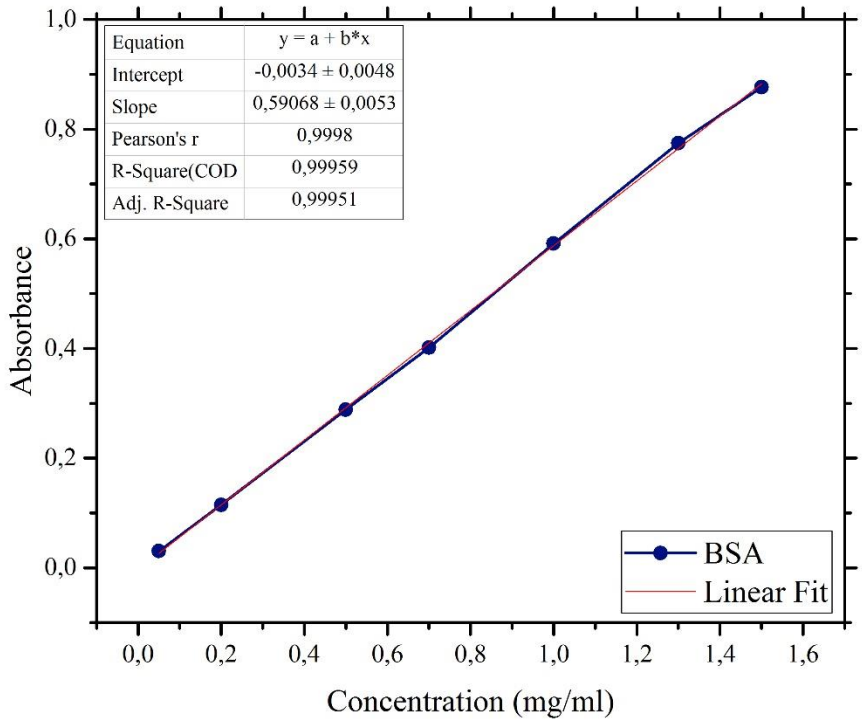

Figure 9.3. Calibration Curve of BSA in 0.01 M, pH 7.4 PB.

APPENDIX B

CARBAZATE ASSAY-TNBS ASSAY

Carbazate assay was used for the determination of aldehyde substitution degree of alginate aldehyde samples (A-A). Method was originated from Hoare *et al.* and Gil *et. al.*(94,119)

Procedure is as follows:

- 25 mg of modified polymer was dissolved in sodium acetate buffer to obtain 5 mg/ml ratio. After dissolving, 1 ml solution was taken and 0.04 g tert-butyl carbazate added to the dextran mixture. The solution was waited about 24 hours at room temperature
- End of the reaction, 25 µl sample was taken and inserted to the vial containing 9.9 ml borate buffer.
- 250 μL of 1 % w/v 2,4,6-trinitrobenesulfonic acid solution (TNBS) was added to the prepared solution containing borate buffer and waited nearly 2 hours for the interaction.
- At the end of the duration, red colour formation obtained.
- The final solution was diluted with equal volume of HCl solution (0.5 M). Afterwards, 250 μL of diluted solution was pulled and added to 9.75 ml HCl solution (0.5 M).
- The yellow final solution was obtained and its absorbance were determined via UV/VIS spectrophotometer at 334 nm.
- The same procedure was also applied for solvents without reactive species

(A-A, tBC and TNBS) and absorbance value was also measured.

- The read solvent absorbance was then subtracted from species absorbances. Thus, the calculated absorbance was belong to reacted carbazate.
- Unreacted carbazate was estimated with calibration curve. The amount of unreacted tert-Buthyl carbazate with aldehyde species presents oxidized amount.

TNBS assay was used for the determination of hydrazide substitution degree of alginate hydrazide samples (A-H). Method was also originated from aldehyde determination of the work by Hoare *et al.* and Gil *et al.*(94,119)

- The TNBS Assay for aldehyde determination described above was valid without carbazate addition for the hydrazide group detection. Modified polymer was replaced with tert buthyl carbazate and hydrazide modification was obtained with this technique.
- The read solvent absorbance was then subtracted from species absorbances. Thus, the calculated absorbance was belong to reacted hydrazide.
- Calibration curve was constituted with adipic acid dihydrazide solution. Hydrazide amount was then estimated according to the calibration curve.

Table 10-1 Absorbance values for tBC samples.

tBC Concentration (g/ml)	Absorbance 1	Absorbance 2	Absorbance 3	Average Absorbance
0.0025	0.004	0.004	0.004	0.004
0.01	0.022	0.022	0.023	0.022
0.02	0.044	0.044	0.044	0.044
0.03	0.066	0.067	0.068	0.067
0.04	0.092	0.091	0.091	0.091

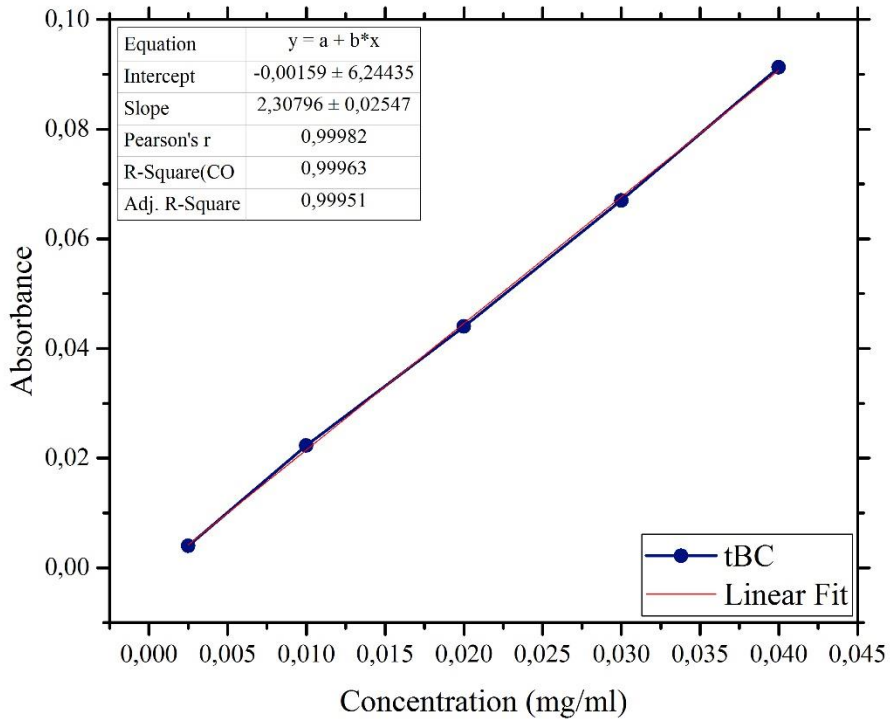

Figure 10.1 Calibration Curve for tBC.

Table 10-2 Absorbance values for ADH samples.

ADH Concentration (g/ml)	Absorbance 1	Absorbance 2	Absorbance 3	Average Absorbance
0.0025	0.009	0.011	0.013	0.011
0.01	0.034	0.035	0.038	0.036
0.02	0.066	0.066	0.071	0.068
0.03	0.092	0.094	0.091	0.092
0.04	0.128	0.128	0.128	0.128

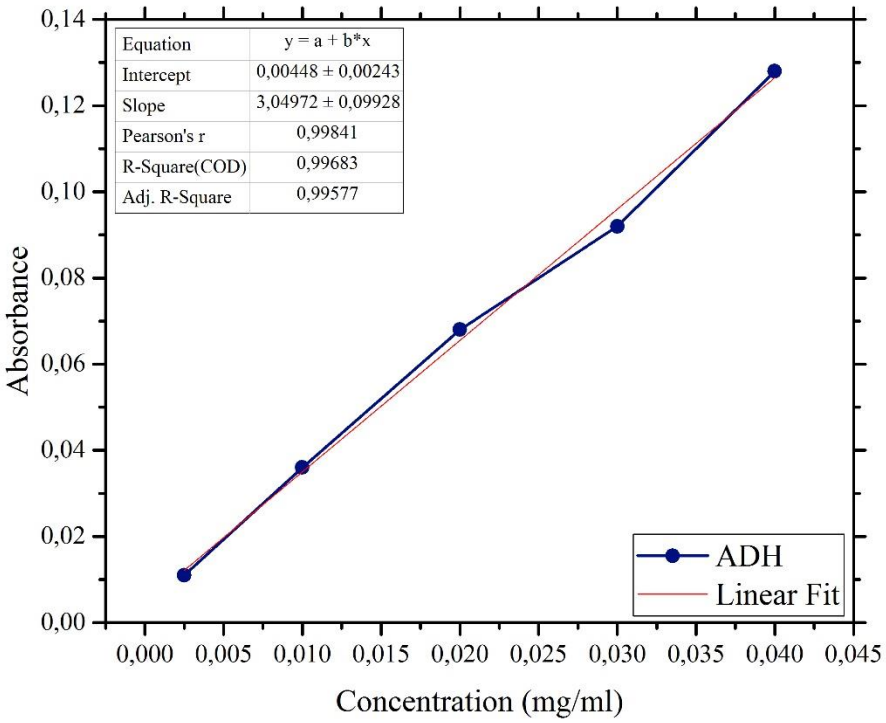

Figure 10.2 Calibration Curve for ADH

APPENDIX C

BRADFORD ASSAY

Bradford Assay was used for determination of release of model protein BSA from the hydrogel matrix. The micro assay was used for the determination of protein in the range between 1 µg and 10 µg.

- 250 µl hydrogel sample was immersed into 2.5 ml PBS in selected pH.
- The medium was pulled for protein determination assay in chosen time intervals – 2 hours, 8 hours, 24 hours, 3 days, 5 days, 10 days, and 15 days. The fresh medium was replaced after sampling for analysis.
- 50 µl solution was taken from the sampling medium and added into 450 µl PBS with respected pH.
- Bradford reagent was removed from the fridge and it was waited to reach room temperature.
- 500 µl reagent was added into solution and waited for 15 minutes.
- The UV absorbance of the samples was measured at 595 nm.
- The all samples were measured within 10 minutes.
- The same test was also applied for only buffer and absorbance value was also measured. The read buffer absorbance was then subtracted from sample absorbances.
- Absorbance of pure hydrogel was subtracted from protein containing hydrogel sample absorbance to eliminate the potential absorbance resulted from polymer. On the other part, the absorbance value of nanocomposite

containing hydrogel was eliminated from protein containing nanocomposite hydrogel. Thus, the calculated absorbance was belong to only protein samples.

- The protein amount was calculated by virtue of calibration curve.
- Each sample was measured at least 3 times and average value was calculated.

BSA samples were prepared between 25 µg/ml and 200 µg/ml in PBS to compose calibration curve graph.

- 50 µl protein solution was removed and added into 450 µl PBS with respected pH.
- 500 µl reagent was added into solution and waited for 15 minutes.
- The UV absorbance of the samples was measured at 595 nm. Each sample was measured 5 times and average value was obtained.
- The all samples were measured within 10 minutes.

Table 11-1 Absorbance values for BSA samples measured via Bradford Assay after 15 minutes.

BSA Concentration (mikg/ml)	Measured (after 15 min.) Absorbance 1	Measured (after 15 min.) Absorbance 2	Measured (after 15 min.) Absorbance 3	Measured Absorbance Zero Value (Average)
25	0.136	0.134	0.137	0.140
50	0.207	0.209	0.199	0.210
75	0.269	0.262	0.262	0.260
100	0.319	0.313	0.321	0.320
125	0.383	0.387	0.404	0.390
150	0.426	0.450	0.450	0.440
200	0.576	0.58	0.582	0.580

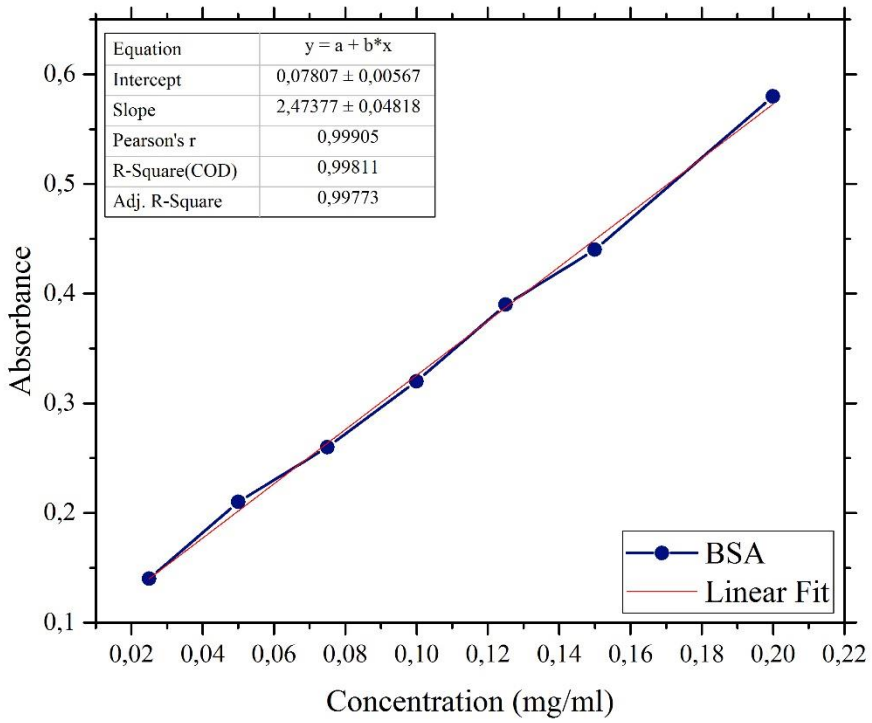

Figure 11.1 Calibration Curve for Bradford Assay.

APPENDIX D

OXIDATION OF DEXTRAN

Oxidation of dextran was performed with the same methodology described in "Oxidation of Alginate". The oxidation studies were conducted by using two types of dextran have different molecular weights - M_w: 15 000-25 000 g/mol and M_n: 100 000 g/mol. The oxidation work was prepared from the notable studies of Hoare *et al.* and Maia *et al.*(49,119,213)

Dextran was reacted with sodium periodate for the transformation of hydroxyl groups to carbonyl groups in reaction part. Since the theoretical substitution is depend on the molar ratio of sodium periodate to dextran, several reactant ratios were used. By the end of the reaction, the purification was proceed with the purpose of removing the polymers have relatively low molecular weight and unreacted substances presented in the reaction mixture. Lastly, the purified samples are freeze-dried for the completion of the modification process.

Dextran was dissolved in distilled water to acquire the required concentration given in Table 12.1. Then, the solution was putted into magnetic stirrer about an hour for obtaining homogeneous solution. On the other hand, sodium periodate were added into distilled water with the chosen amounts and putted on the magnetic stirrer. Since sodium periodate is sensitive to light, the solution was wrapped with aluminium foil for preserving the reactivity of the material.

After the both solutions became complete soluble form, the sodium periodate solution was added drop by drop into dextran solution. The reaction was proceed at room temperature in the dark with the desired time on the magnetic stirrer. After the end of the 24 hours period, ethylene glycol was added into reaction mixture in order to inactivate reactive species and stop the reaction.

The related amounts of reactive species are given Table 12.1. The molecular weight of a dextran repeating unit is determined as 162 g/mol.

Table 13-1 The materials and its amounts are used in the oxidation of dextran.

Dextran (mg)	Dextran (mg/ml)	Sodium Periodate (mg)	Dextran (mol)	Sodium Periodate (mol)	Theoretical DS
500	25	330	0.003806	0.00154	50
500	10	267	0.003806	0.00125	40
500	25	165	0.003806	0.00077	25
500	25	66	0.003806	0.0003806	10

Dialysis application was done with membrane tubing have 3.5 kD MWCO for purification of the reaction product. Firstly, the membrane tubing was immersed in a beaker filled with distilled water to dampen about 30 minutes. Afterwards, reaction product was added to into membrane tubing and clipped both ends. The membrane tubing was placed into a beaker including 2 litres of water. The water was exchanged at least 3 times in a day in the beaker. The purification application was proceed for 3 days. After the completion of the dialysis, the purified materials were transferred to the vortex tubes or borosilicate glass for drying. Samples were frozen by using with dried ice or liquid nitrogen to place in freeze dryer. The specimens were waited in the freezer dryer for 3 days. The dried samples were stored at -20 ^{o}C for further applications and tests.

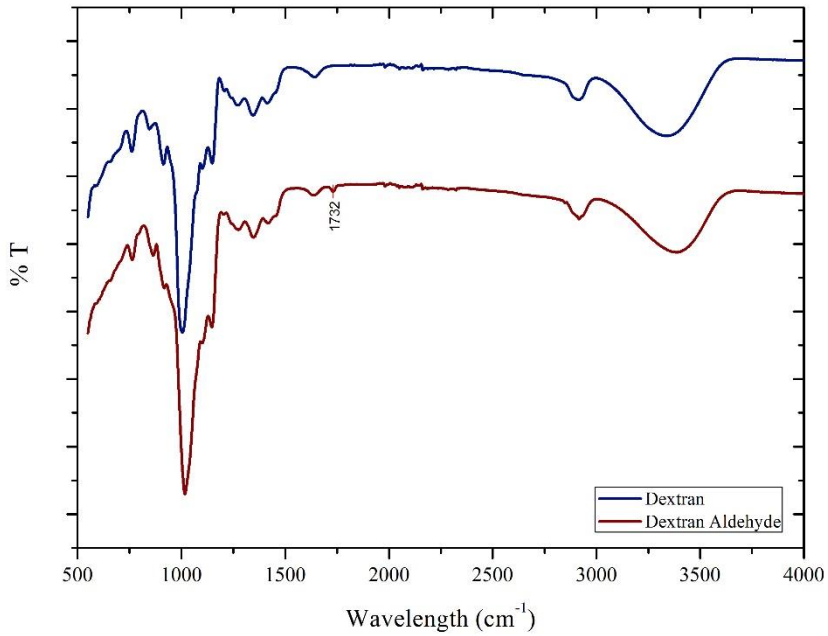

Figure 13.1 Oxidized Dextran (Low Molecular Weight)

The peak observed at 1731 cm^{-1} indicated aldehyde modification.

APPENDIX E

IMINE BASED HYDROGEL PRODUCTION

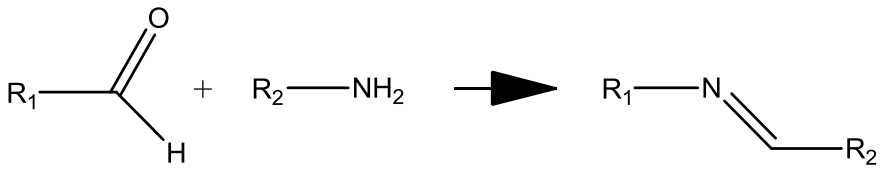

Figure 15.1 Imine bond formation

The procedure consists two main parts – oxidation of dextran and mixing chitosan with chitosan. Oxidation of dextran was described in Appendix D section.

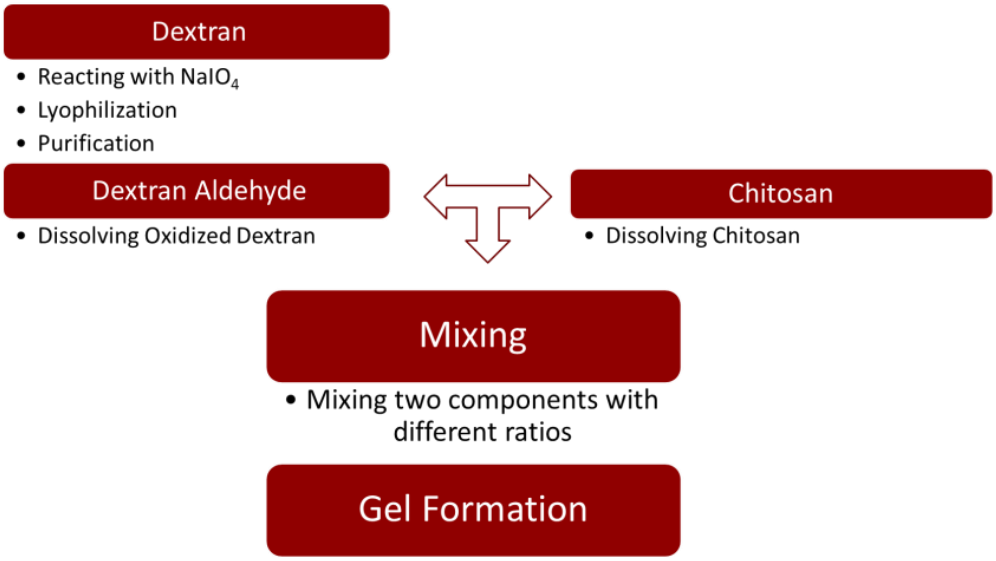

Figure 15.2 Scheme of imine bond hydrogel production

The procedure details about oxidation of dextran is given in Table 13.1.

Table 15-1. Material amounts were used in oxidation procedure.

Materials	Molecular Weight (g/mol)	Amount (mg)	Amount (ml)	Mol (mol)	Concentration (mg/ml)
Dextran	25 000	500	-	$2*10^{-5}$	10
Sodium periodate	213.89	267	-	$1.25*10^{-3}$	160
Ethylene Glycol	62.07	-	0.133	$2.39*10^{-3}$	113.2

Chitosan was dissolved in solution containing % 0.35 (v/v) acetic acid. Chitosan was prepared in % 0.83 (w/v) ratio by waited in ultrasonic bath for an hour. Dextran was dissolved in between % 0.675 and % 15 (w/v) individually.

Table 15-2 Gel formation of imine bond hydrogels

Material	Concentration (g/ml)	Total Concentration (g/ml)	Gel Formation	Duration
D-A Chitosan	7.5 0.42	7.92	+	15 min.
D-A Chitosan	7.5 0.42	7.92	+	30 min.
D-A Chitosan	5 0.42	5.42	+	30 min.
D-A Chitosan	3.75 0.42	4.17	+	2 h.
D-A Chitosan	2.5 0.42	2.92	+	3 h.
D-A Chitosan	1.25 0.42	1.67	+	3 h.
D-A Chitosan	0.63 0.42	1.05	-	> 4 h.
D-A Chitosan	0.34 0.42	0.76	-	> 4 h.

APPENDIX F

DEXTRAN ALDEHYDE AND ALGINATE BASED HYDROGEL PRODUCTION

Hydrogels containing alginate hydrazide and dextran aldehyde with different ratios are produced. Dextran aldehyde had % 40 modification degree while sodium alginate had % 5 degree of substitution.

Table 16-1. Alginate hydrazide and dextran aldehyde containing injectable hydrogel synthesis.

Material	Concentration (g/ml)	Total Concentration (g/ml)	Duration
D-A **A-H**	10.00 0.50	11.50	< 5 min.
D-A **A-H**	10.00 1.25	11.25	< 30 sec.
D-A **A-H**	5.00 1.25	6.25	< 1 min.
D-A **A-H**	2.50 1.25	3.75	< 5 min.
D-A **A-H**	10.00 1.25	11.25	< 5 min.
D-A **A-H**	0.49 4.88	5.37	< 5 min.

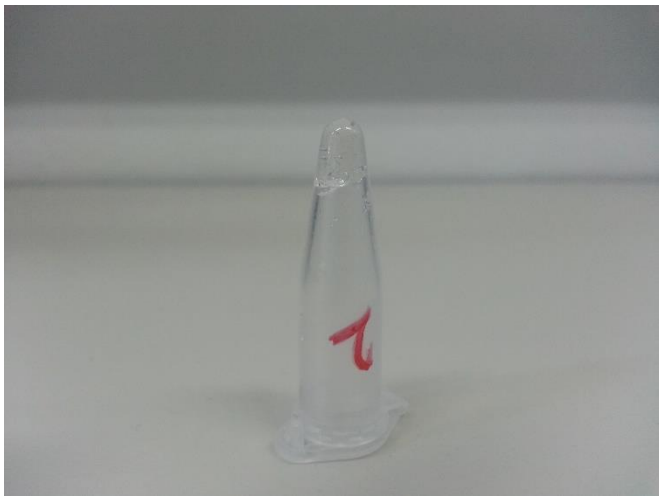

Figure 16.1 Produced hydrogel containing alginate hydrazide and dextran aldehyde.

APPENDIX G

DEXTRAN ALDEHYDE AND ADH BASED HYDROGEL PRODUCTION

Table 17-1. Dextran aldehyde and Adh based hydrogel production.

	Material	Polymer Concentration	Total Polymer Concentration	Gel Formation	Duration
Dextran Aldehyde Constant: %10 ADH: % 0.675 - %10	DA	5.00	10.00	Yes	8 hours
	ADH	5.00			
	DA	5.00	7.50	Yes	7 hours
	ADH	2.50			
	DA	5.00	6.25	Yes	6 hours
	ADH	1.25			
	DA	5.00	6.25	Yes	8 hours
	ADH	1.25			
	DA	5.00	5.34	No	> 16 hours
	ADH	0.34			
ADH Constant: %10 Dextran Aldehyde: % 0.675 - %10	DA	2.50	7.50	No	> 16 hours
	ADH	5.00			
	DA	1.25	6.25	No	> 16 hours
	ADH	5			
	DA	0.675	5.675	No	> 16 hours
	ADH	5			
	DA	0.34	5.34	No	> 16 hours
	ADH	5			
Dextran Aldehyde Constant: %20 ADH: % 0.675 - %10	DA	2.50	7.50	No	> 16 hours
	ADH	5.00			
	DA	1.25	6.25	No	> 16 hours
	ADH	5			
	DA	0.675	5.675	No	> 16 hours
	ADH	5			
	DA	0.34	5.34	No	> 16 hours
	ADH	5			

Hydrogels containing dextran aldehyde and ADH with different ratios are produced. Dextran aldehyde had % 40 modification degree.

APPENDIX H

HEMA (2-Hydroxyexthyl methacrylate) BASED HYDROGEL SYNTHESIS

HEMA (2-Hydroxylethyl methacrylate) based hydrogels were produced as pure, laponite containing and enzyme containing. In the hydrogel formation, HEMA (2-Hydroxyethyl methacrylate) was used as monomer. EGDMA was (Ethyleneglycol dimetharylate) cross linker. APS (Ammonium persulfate) was initiated the gelation with accelator-TEMED (Tetramethylene diamine). Laponite addition was done for nanocomposite hydrogel formation. Invertase was added into enzyme containing hydrogels.

The key requirements of the technique are as follows:

- HEMA was kept in % 20 (v/v) in the prepared solution.
- The amount of EGDMA was equal to % 0.5 mol of HEMA.
- Laponite was dissolved to give % 0.5 (w/v) in solution.
- APS solution had 75 mg/ml concentration.
- Invertase solution had 2 mg/ml concentration.

H.1. HEMA Based Hydrogel Production

- 2000 µl distilled water and later on 500 µl HEMA were added to the vial.

- 3.89 µl EGDMA is after added to the solution. Afterwards, 66.7 µl APS solution was added to the vial.
- After connecting pipes and fittings to the vial for nitrogen gas blowing, waited about 10-15 minutes for TEMED addition.
- 5 µl TEMED was added to the vial to accelarate the polymerization. The vial was then gently shaked for homogeneous distribution.
- Disconnected nitrogen gas approximately 15 minutes later. Wrapping the parafilm to the tube ends in order to prevent the oxygen transition to the vial.
- The prepared hydrogel was waited at room temperature at least 12 hours.

H.2. HEMA Based Nanocomposite Hydrogel Production

- 2000 µl distilled water and 0.01 g laponite were added to the vial, shake intervally and waited about 30 minutes for dissolution. After 500 µl HEMA was added to the vial.
- 3.89 µl EGDMA was added to the solution.
- 66.7 µl APS solution was added to the vial.
- After connecting pipes and fittings to the vial for nitrogen gas blowing, waited about 10-15 minutes for TEMED addition.
- 5 µl TEMED is added to the vial to accelarate the polymerization by uncovering the stopper. The vial was gently shaked for homogeneous distribution
- Disconnected nitrogen gas approximately 15 minutes later. Wrapping the parafilm to the tube ends in order to prevention the oxygen transition to the vial.
- The synthesized nanocomposite hydrogel was waited at room temperature at least 12 hours.

H.3. Enzyme Containing HEMA Based Hydrogel Production

- 2000 µl distilled water and later on 500 µl HEMA were added to the vial.
- 3.89 µl EGDMA is after added to the solution.
- 1000 µl invertase solution was later inserted to the solution.
- 66.7 µl APS solution is added to the vial.
- After connecting pipes and fittings to the vial for nitrogen gas blowing, waited about 10-15 minutes for TEMED addition.
- 5 µl TEMED was added to the vial to accelarate the polymerization by uncovering the stopper. The vial was gently shaked for homogeneous distribution.
- Disconnected nitrogen gas approximately 15 minutes later. Wrapping the parafilm to the tube ends in order to prevention the oxygen transition to the vial.
- Enzyme containing hydrogel was waited at room temperature at least 12 hours.

H.4. Enzyme Containing Nanocomposite HEMA Based Hydrogel Production

- 2000 µl distilled water and 0.01 g laponite were added to the vial, shake intervally and wait about 30 minutes for dissolution. After 500 µl HEMA was added to the vial.
- 3.89 µl EGDMA is next added to the solution. 1000 µl invertase solution is later added to the solution.
- 66.7 µl APS solution is added to the vial.
- After connecting pipes and fittings to the vial for nitrogen gas blowing, waited about 10-15 minutes for TEMED addition.
- 5 µl TEMED was added to the vial to accelarate the polymerization by uncovering the stopper. The vial is gently shaked for homogeneous distribution.
- Disconnected nitrogen gas approximately 15 minutes later. Wrapping the parafilm to the tube ends in order to prevention the oxygen transition to the vial.

• Enzyme containing nanocomposite hydrogel was waited at room temperature at least 12 hours.

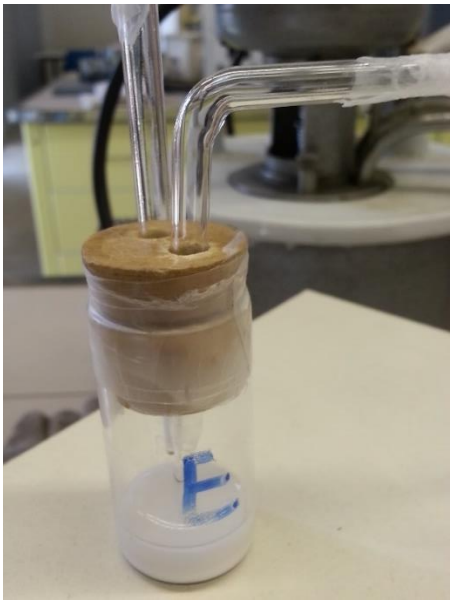

Figure 18.1 Enzyme Containing HEMA Based Hydrogel.

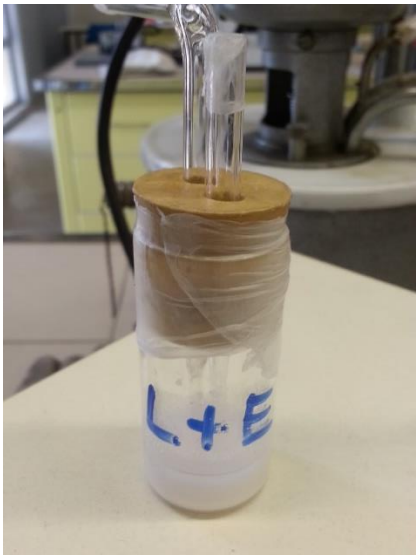

Figure 18.2 Enzyme Containing Nanocomposite HEMA Based Hydrogel.

APPENDIX I

SWELLING TEST

Effect of Laponite XLG addition was investigated on swelling.

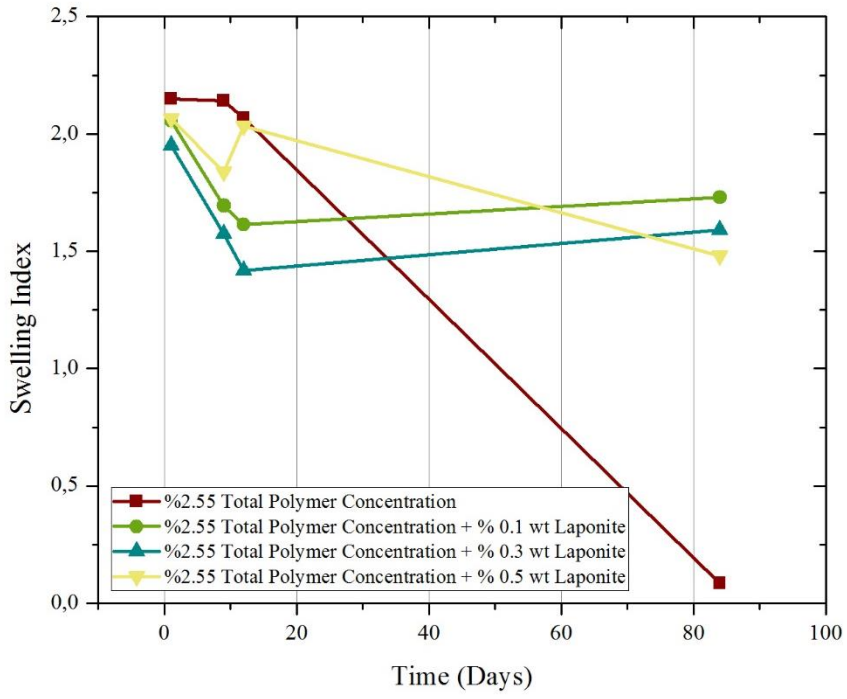

Figure 19.1 Produced hydrogels with %2.55 polymer concentration coded A50(2)-2.5